



SOLID CONTACT BIOSENSOR BASED ON MAN-TAILORED POLYMERS FOR ACETYLCHOLINE DETECTION: APPLICATION TO ACETYLCHOLINESTERASE ASSAY

Ayman H. Kamel^{[a]*}, Fatma A. Al Hamid^[b], Tamer Y. Soror^[c], Hoda R. Galal^[d]
and Fadl A. El Gendy^[c]

Keywords: Acetylcholine, acetylcholinesterase enzyme assay, molecular imprinted polymers, potentiometry, flow injection analysis.

A solid contact biosensor for Acetylcholine (ACh) based on host-guest interactions and potentiometric transduction has been designed and characterized. The biomimetic man-tailored host was synthesized using methacrylic acid as a functional monomer, ethylene glycol dimethacrylate as a crosslinker in the presence of benzoyl peroxide as an initiator. The imprinted beads were dispersed in 2-nitrophenyloctyl ether and entrapped in a poly(vinyl chloride) matrix. Slopes and detection limits are 55.2-59.6 mV decade⁻¹ and 0.65-1.31 $\mu\text{g mL}^{-1}$, respectively. Significantly, improved accuracy, precision, good reproducibility, long-term stability, selectivity and sensitivity were offered by these simple and cost-effective potentiometric biosensors. A tubular version was further developed and coupled to a flow injection system for acetylcholine determination. This simple and inexpensive flow injection analysis manifold, with a good potentiometric detector, enabled the analysis of ~ 30 samples h^{-1} without requiring pretreatment procedures. An average recovery of 98.3 % and a mean standard deviation of 1.1% were obtained. The sensors were used to follow up the decrease of a fixed concentration of ACh⁺ substrate as a function of acetylcholinesterase (AChE) activity under optimized conditions of pH and temperature. A linear relationship between the hydrolysis initial rate of ACh⁺ substrate and enzyme activity hold 0.01- 5.0 IU L⁻¹ of AChE enzyme.

* Corresponding Authors

Tel: +201000361328

E-Mail: ahkamel76@sci.asu.edu.eg

[a] Chemistry Department, Faculty of Science, Ain Shams University, 11566, Cairo, Egypt

[b] Department of Biology-College of Science and Arts, Qassim University, KSA

[c] College of Science, Qassim University, Buridah, 6644, KSA

[d] National Research Center (NRC), Dokki, Giza, 14211 Egypt

Introduction

Acetylcholine (ACh) serves an important function in the cholinergic system, where it acts as a neurotransmitter on cholinergic synapses.¹ The pharmaceutical preparation of ACh has many therapeutic utilities.² On the other hand, deficiency of ACh due to cholineacetyltransferase enzyme inhibition causes a disturbance in the transmission of nerve impulses, paralysis, and death.³ Assessment of ACh is a challenging analytical problem because it is not UV-absorbing, fluorescent, electroactive or derivatize easily. Therefore, bioassays,⁴ radiochemical methods,⁵ liquid chromatography (LC) with enzymatic reactions⁶⁻⁹ and LC with mass spectrometric detection¹⁰⁻¹³ have often been employed, despite their tedious procedures. However, the aforementioned methods have several disadvantages such as long analysis time, high cost, and specialized personnel with laboratory facilities. On the other hand, the electroanalytical techniques provide many advantages such as simple instrumentation and short analysis time. Uni-, bi-, and tri-enzyme/mediators biosensors including chemiluminometric,¹⁴ amperometric,¹⁵⁻¹⁷ conductometric¹⁸ and voltammetric¹⁹ methods have been used for monitoring AChs.

Potentiometric sensors are an important class of electrochemical sensors, which detect the relationship

between the activity of analyte species and the potential response of the two-electrode system. Compared with other analytical techniques, ion-selective electrodes (ISEs) have some unique characteristics, such as small size, ease of operation, portability and low cost. For potentiometric determination of ACh, few potentiometric membrane sensors have been developed.²⁰⁻²⁴ Some of these sensors involve the use of acetylcholine ion-pair complexes as electro-active materials that exhibit poor selectivity, limited range of linear response and long response time²⁰⁻²² and others involve macrocycle carriers.^{23,24}

Molecular imprinting is one of the most promising approaches to achieving precise molecular recognition. The challenge of synthesizing man-made molecules which are capable of molecular recognition has drawn special attention to electrochemical sensors.²⁵ The sensing and transduction principles combined with the imprinting approach are used to make the imprinting process feasible thus giving us the detailed information about the recognition phenomenon occurring on the imprinting interface.²⁶

Transducers based on potentiometric transduction comprise one of the most exciting areas of electrochemical analysis. Their appealing features, such as selectivity, sensitivity, and reproducibility, have drawn attention for the past couple of decades.²⁷⁻³¹ In this direction, the immobilization of biomolecules on the electrode surface for molecular recognition is a reasonable choice, thus gaining a great importance in the field of electrochemical sensors. The use of synthetic materials that imitate recognition characteristics of biological materials has been explored.^{31,32} Particularly, molecularly imprinted polymers (MIPs) can be thought of as viable alternates to replace natural receptors. Bulk polymerization in the presence of a template is just one among many frequently used procedures for the fabrication of MIPs.³³⁻³⁷ First, the preformed complex of the functional

monomer and template is copolymerized with an excess of the cross-linking agent in a porogenic solvent. This step results in a solid matrix of the highly cross-linked polymer. After template removal, molecular cavities featuring recognition sites are formed. These cavities are suitable for hosting the template compound used as the analyte in this step.

In this study, we have investigated the preparation of MIPs, new man-tailored hosts for ACh, based on imprinting technology. The polymers could be regarded as an artificial receptor to recognize ACh by shape recognition ability, non-covalent interactions as well as induced polarization between MIP and ACh. The newly synthesized sensors have been employed for rapid and sensitive measurements of AChE enzyme activities.

Experimental

All potentiometric measurements were made at 25 ± 0.1 °C with a Cole-Parmer pH/mV meter (USA model 59003-05). The assembly of the potentiometric cell was constructed as follows: Copper base | graphite | ACh selective membrane | buffered sample solution (PBS, 0.01 M, pH 7) || electrolyte solution, KCl | AgCl(s) | Ag. The reference electrode was a Sentek, Ag/AgCl double junction reference electrode (UK model R2/2MM) filled with 4.0 M KNO₃ in the outer compartment. The selective electrode was prepared and designed to be suitable for static and hydrodynamic measurements. The design had no internal reference solution and epoxy-graphite was used as a solid contact. The pH values of the solutions were controlled by means of a combination glass pH electrode (Schott blue line 25, Germany).

The flow injection (FI) manifold consisted of a two-channel Ismatech Ms-REGLO model peristaltic pump, polyethylene tubing (0.71 mm internal diameter) and an Omnifit injection valve (Omnifit, Cambridge, UK) with a loop sample of 100 μ L volume. An Orion (Cambridge, MA, USA) model 720/SA pH/mV meter connected to a PC through the interface ADC 16 (Pico Tech, UK) and Pico Log for windows (version 5.07) software were used for recording the potential signals.

All chemicals were of analytical grade and de-ionized water (conductivity < 0.1 μ S cm^{-1}) was employed. Acetylcholine chloride (ACh), Choline chloride (Ch), Creatinine (Creat), Potassium tetrakis (4-chlorophenyl) borate (KTPCIPB⁻), tri dodecyl ammonium chloride (TDMAC), 2-nitrophenyloctyl ether (*o*,NPOE), poly (vinyl chloride) of high molecular weight (PVC), and Ethylene glycol dimethacrylate (EGDMA) were purchased from Sigma Chemicals Co. (St. Louis, MO, USA). Methacrylic acid (MAA), Benzoyl peroxide (BPO), methanol and tetrahydrofuran (THF) were purchased from Fluka (Ronkonoma, NY). Acetylcholinesterase (type VI-S) from *Electrophorus electricus* (Electriceel, EC 3.1.1.7, 288 U mg^{-1} solid) was obtained from Sigma-Aldrich (Munich, Germany).

Polymer synthesis

Molecularly imprinted polymers with ACh were prepared by using acetylcholine (ACh, 1 mmol) as a template, MAA (4 mmol) as a functional monomer, EGDMA (20 mmol) as a

cross-linking agent and acetonitrile (15 mL) as a porogenic solvent. The template-monomer mixture and solvent were transferred to a test tube and BPO (80 mg) as an initiator was added. The dissolved oxygen in the mixture was degassed by bubbling N₂ for 10 min. The tube was sealed and heated in a block heater at 70 °C for 5 h. The control blank polymers (NIPs) were prepared using an identical procedure but in the absence of the template. The polymers were obtained as brittle solids which were broken up, grounded in a mortar. The grounded polymers were washed to remove ACh with methanol/ acetic acid (9:1 v/v) to eliminate interfering compounds arising from the synthesis (template and unreacted monomers). All polymers (MIP/MAA and NIP/MAA) were let to dry at ambient temperature, before their use as potentiometric transducers.

Binding Experiments

Binding experiments were carried out by introducing 20.0 mg of MIP and NIP washed particles in contact with 10.0 mL ACh⁺ aqueous solutions ranging 10-70 μ g mL^{-1} . The solutions were incubated overnight at static equilibrium at room temperature and the solid phase was then separated by centrifugation (3000 rpm, 15 min.). Free ACh⁺ concentrations in the supernatant were measured by HPLC with a refractive index detector using calibration graph with ACh⁺ standard solutions.³⁸ The amounts of ACh⁺ bound to the polymers were calculated by subtracting the concentration of free ACh⁺ from the initial ACh⁺ concentration. The maximum binding capacity and dissociation constant for all synthesized polymers were calculated using Scatchard equation.

ISE membranes and electrodes measurements

The ACh-selective membranes for solid contact ion selective electrodes (ISEs) contained MIP/MAA [ISE I] or NIP/MAA [ISE II] (5.2 wt. %, 30 mg), *o*,NPOE (61.4 wt. %, 350 mg), and PVC (33.3 wt. %, 190 mg). The membranes were prepared by dissolving the components (in total, 570 mg) in THF (3 mL). The membrane solutions were cast into a conductive supports of conventional or tubular shapes and left to dry overnight for evaporating and yielding transparent membranes.

The sensors were conditioned by soaking in 1.0×10^{-3} M of ACh⁺ aqueous solution for 12 h. The pH of the test solution was maintained at 7.0 by the addition of different aliquots from standard ACh⁺ solution in 25 mL of 0.01 M PBS solutions. The potential of the test solutions was measured at different concentrations of ACh⁺ in the range 1.0×10^{-7} to 1×10^{-2} M. The EMF was plotted as a function of the logarithm of ACh⁺ concentration.

Flow injection set up

Transducers for flow injection analysis were prepared by mixing 30 mg of the sensing polymer, 350 mg of the plasticizer (*o*-NPOE), 190 mg PVC and 5.0 mg KpCITPB and dissolved in ~ 3 mL THF. Successive aliquots (200 μ L) of the membrane were placed into a conductive support of graphite and epoxy resin, of conventional or tubular shape. This operation was repeated until a membrane with a thickness of approximately 0.1 mm was formed. The sensor was

conditioned by soaking in 1.0×10^{-3} M of ACh⁺ aqueous solution for 12 h and was stored in the same solution when not in use. The sensor was placed in a beaker where a double junction Ag/AgCl reference electrode was placed downstream from the detector just before the solution went to the waste. A carrier stream containing 1.0×10^{-2} M PBS solution of pH 7.0 was pumped at a constant flow rate of 3.0 mL min⁻¹. To avoid slight pulsation originating from the peristaltic pump, grounding connection was made for flow system.

Potentiometric assessment of AChE activity

A volume of 45.0 mL of the pH 7.0 PBS solution was transferred into the thermostated vessel. The sensor was immersed in the solution in conjunction with a double junction Ag/AgCl reference electrode. After potential stabilization, a 2.5 mL of 10^{-2} M of ACh⁺ working solutions was injected. When the potential stabilized again, 100 μ L aliquots containing 0.01-5.0 IU L⁻¹ of AChE enzyme was added. The potential kinetic curve was left to develop, and the maximum initial rate of potential change ($\Delta E/\Delta t$) was graphically obtained using the rate portion of the curve. The initial rate was plotted as a function of the enzyme activity and the calibration curve obtained was then used for subsequent measurements of unknown enzyme activity. A blank experiment was carried out under similar conditions in the absence of the enzyme.

Results and discussion

In this study, our aim was to establish a simple, selective and sensitive analytical system based on MIPs for recognizing acetylcholine neurotransmitter. For this purpose, we proposed an electrochemical sensor utilizing the potentiometric determination method of ACh to the MIPs by electrochemical reaction. A schematic illustration of the molecular imprinting process is shown in Figure 1.

Characterization of the MIP beads

The morphology for all prepared polymer beads was investigated and presented in the cross-sectional SEM and TEM images for the MIP/MAA and NIP/MAA (Figure 2). The non-imprinted polymers had more smooth and uniform shape than the imprinted polymers which had an irregular, rough morphology with small cavities. The regular structure of the non-imprinted polymer was due to the absence of specific binding sites in the polymers. The cavities in the MIPs were probably attributed to the imprinting effect or the introduction of ACh in the polymerization process. The specific surface area and pore volume impacted significantly on the efficiency of adsorption. The homogeneous and dense morphological structure is shown in the figure indicated that the imprinted process achieved a more highly cross-linked and porous structure. It thus provided a guarantee of a sufficient extraction performance of the MIP/MAA for ACh. Polymer surface area and porosity measurements were also carried out. BET and Langmuir surface areas for polymers were calculated and presented in Table 1. Binding experiments were performed by incubating fixed amounts of all MIPs and NIPs beads with different concentrations of ACh until equilibrium as reached and the free ACh concentrations

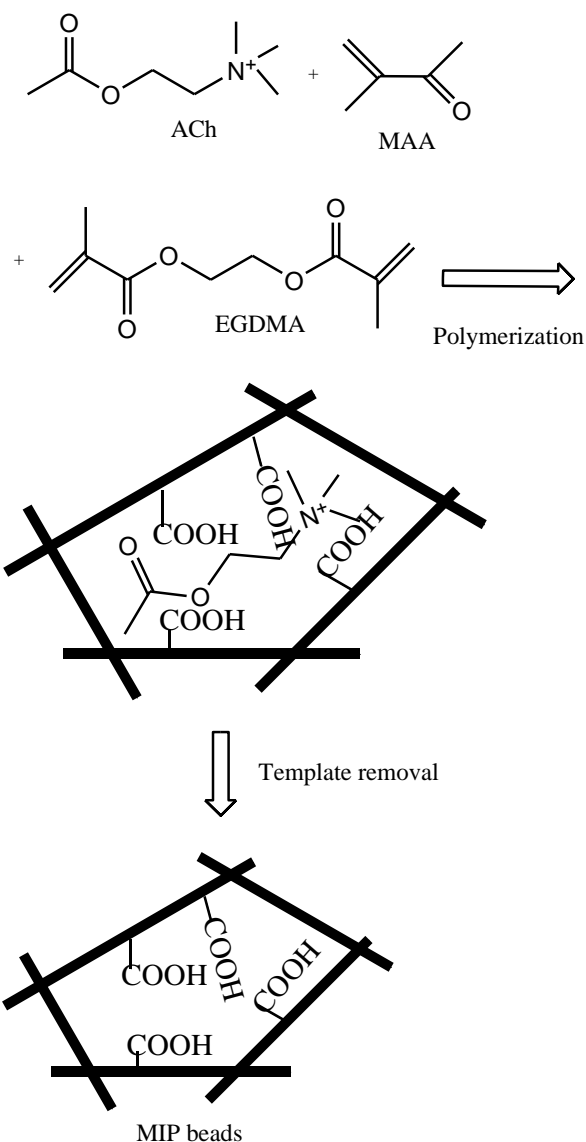


Figure 1. A schematic protocol for the molecular imprinting process.

were determined using HPLC method.³⁸ The resulting binding capacity of MIPs was calculated according to eqn. (1)

$$Q = \frac{\mu \text{ mol(ACh bound)}}{\text{g(MIP)}} = \frac{(C_i - C_f)V_s \times 1000}{M_{\text{MIP}}} \quad (1)$$

where

Q is the binding capacity of MIPs or NIPs ($\mu\text{mol g}^{-1}$),
 C_i the initial ACh concentration ($\mu\text{mol mL}^{-1}$),
 C_f the final ACh concentration ($\mu\text{mol mL}^{-1}$),
 V_s the volume of solution tested (mL) and
 M_{MIP} the mass of dried polymer (mg).

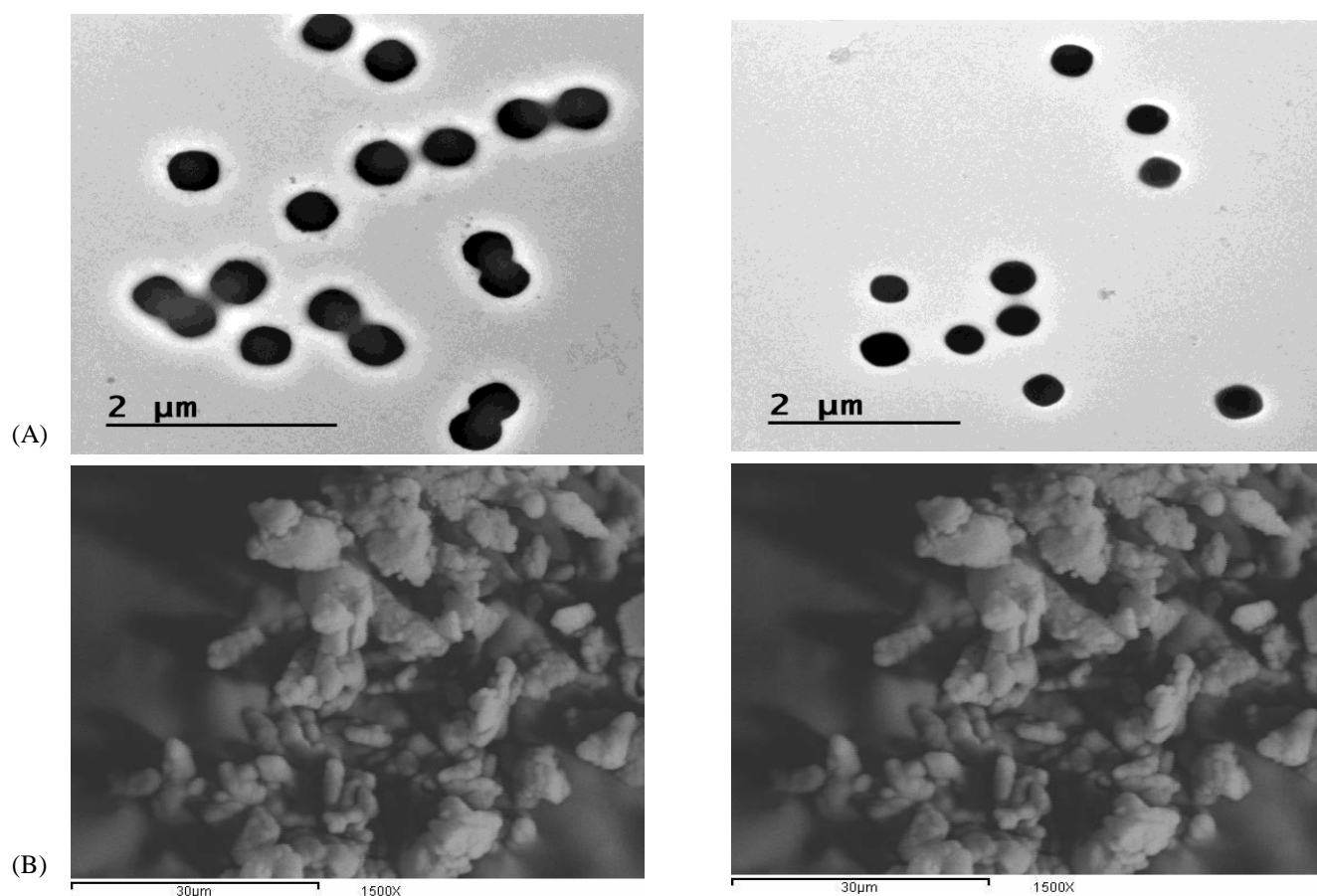


Figure 2. (A) TEM micrograph of MIP/MAA and NIP/MAA, (B) SEM micrographs of MIP/MAA and NIP/MAA under 1500 magnification.

Table 1. General characteristic of some potentiometric acetylcholine membrane sensors

Ionophore	Slope (mV decade ⁻¹)	Linear range (M)	pH range	Detection limit (M)	Interference	Ref.
Acetylcholine dipicrylaminate	54.4	5.0x10 ⁻⁵ - 1.0x10 ⁻²	Not reported	3.0x10 ⁻⁵	Choline (-1.35); Butyrylcholine (-1.02); Dopamine (-2.21); Tyrosine (-2.39); Aminobutyric acid (-2.82); Carbachol (-1.43); Amphetamine (-1.06); K ⁺ (-2.65); NH ₄ ⁺ (-3.39)	20
Cucurbit[6]uril derivative	49.1	1.0x10 ⁻⁶ - 1.0x10 ⁻³	7.2	9.7x 10 ⁻⁷	Choline (-2.51); NH ₄ ⁺ (-1.96); NMe ₄ ⁺ (-1.93); NEt ₄ ⁺ (-1.93); K ⁺ (-1.57); Na ⁺ (-1.83); Dopamine (-1.51); Ascorbic acid (-2.45)	21
Dioctyloctadecylamine	41.4	3.0x10 ⁻⁶ -	8.0	2.0x10 ⁻⁶		22
N,N-didecylaminomethylbenzene	52.9	4.5x10 ⁻⁵ - 1.0x10 ⁻⁵ - 8.0x10 ⁻³	8.0	5.0x10 ⁻⁶	Not reported	
Tetrakis(<i>p</i> -chlorophenyl)-borate			6.0	1.0 × 10 ⁻⁵ 1.0 × 10 ⁻⁵	Not reported	23
Dibenzo-18-crown-6	Not reported	Not reported	6.0	1.7 × 10 ⁻⁵		
Calix[6]arene hexaester			6.0			
β-Cyclodextrin derivative	55.6	1.0x10 ⁻⁵ - 1.0x10 ⁻²	3.0-10	2.7x10 ⁻⁶	Choline (-2.50); NH ₄ ⁺ (-3.80); Citrate (-2.53); Li ⁺ (-3.76); K ⁺ (-3.89); Caffeine (-2.30)	24
MIP/MAA+TPB ⁻	55.2	1.0x10 ⁻⁵ - 1.0 × 10 ⁻²	3.0 – 9	4.5x10 ⁻⁶	Glutamine (-1.52); Codeine (-1.37); Ephedrine (-1.45); Morphine (-1.50); Caffeine (-1.5); Quinine (-1.57); Histidine (-1.60); Choline (-1.62); Cysteine (-1.70); K ⁺ (-2.51); Ca ²⁺ (-2.54); Mg ²⁺ (-2.82); Ba ²⁺ (-2.93).	This work

Table 2. BET and Langmuir surface areas.

Polymer	Surface area, m ² g ⁻¹ (r) [*]	
	BET	Langmuir
MIP/MAA	3.7±0.3 (0.997)	4.4 ±0.5 (0.996)
NIP/MAA	2.5±0.2 (0.998)	2.8±0.3 (0.997)

^{*}r = coefficient of correlation

The adsorption data showed that the binding capacity of MIPs and NIPs increased with the increasing of the initial concentration of ACh, reaching to saturation at higher concentrations. Under the same conditions, the adsorption capacity data of MIPs were always clearly higher than those of NIPs. This indicates that the ability of MIPs to bind ACh is better than that of NIPs probably due to increased number of binding sites in MIPs thus increasing its sensing properties over NIPs.³⁹ The binding data were further processed with Scatchard analysis⁴⁰ using Eqn. (2).

$$\frac{Q}{C_f} = \frac{Q_{\max} - Q}{K_d} \quad (2)$$

where

Q is the binding capacity,
 C_f is the free analytical concentration at equilibrium ($\mu\text{mol mL}^{-1}$),
 Q_{\max} is the maximum apparent binding capacity and
 K_d is the dissociation constant at the binding site.

The equilibrium dissociation constant is calculated from the slopes and the apparent maximum number of binding sites from the y-intercepts in the linear plot of Q/C_f versus Q . Scatchard plots of both MIPs and NIPs consisted of two distinct straight lines inferring the existence of high and low-affinity populations of binding sites (Figure 3).⁴¹ The K_{d1} and $Q_{\max1}$ were 54.05 μM and 88.22 $\mu\text{mol g}^{-1}$, for the high-affinity binding sites of MIP/MAA beads. The K_{d2} and $Q_{\max2}$ 595.23 μM and 374.39 $\mu\text{mol g}^{-1}$ for the low-affinity binding sites of MIP/MAA beads. The K_{d1} and $Q_{\max1}$ were 144.92 μM and 80.34 $\mu\text{mol g}^{-1}$, for the high-affinity binding sites of NIP/MAA beads. The K_{d2} and $Q_{\max2}$ 442.47 μM and 175.21 $\mu\text{mol g}^{-1}$ for the low-affinity binding sites of NIP/MAA beads. By the evaluation of these data, it can be concluded that the adsorption of ACh onto NIPs is based on non-specific interactions because K_d and Q_{\max} quantities of NIPs are less than the values calculated for MIPs.

Sensors characteristics

The synthesized MIP's were incorporated into the PVC membrane and were tested as sensing materials in the proposed potentiometric sensors. The potential response obtained with the sensors prepared with MIP/MAA and NIP/MAA membrane was given in Figure 4. As seen from the figure, the sensors exhibited linear potentiometric response towards ACh⁺ ions over a range from 3.0×10^{-5} to 1.0×10^{-4} M, and detection limits of 1.31 and 11.7 $\mu\text{g mL}^{-1}$, for sensors based on MIP/MAA and NIP/MAA polymers, respectively.

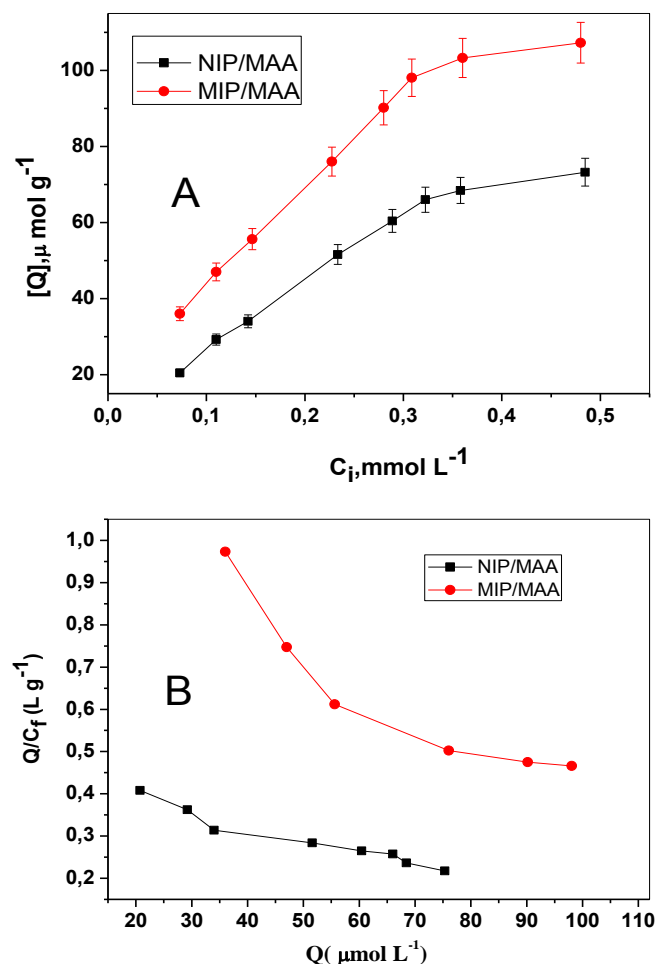


Figure 3. Binding isotherm (A) and Scatchard plot (B) for MIPs and NIPs (inset). Q is the amount of ACh bound to 20 mg of polymer; $t=25^\circ\text{C}$; $V=10.00$ mL.

All sensors exhibit near-Nernstian slopes of 59.6 ± 0.9 ($r^2=0.996$) and 39.5 ± 0.7 ($r^2=0.998$) mV decade⁻¹, respectively.

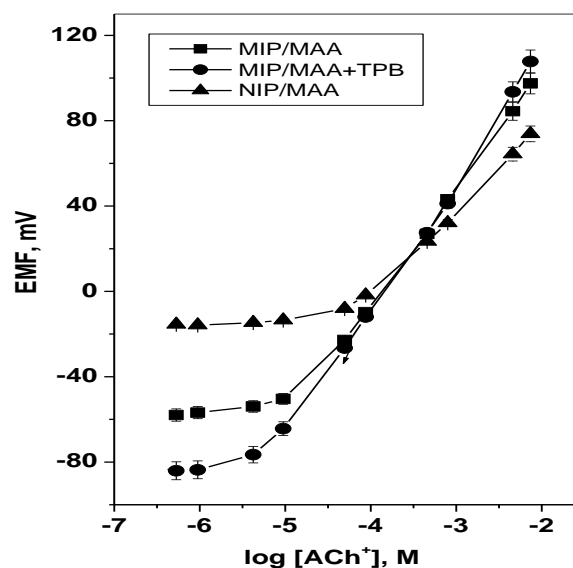


Figure 4. Potentiometric plot of acetylcholine membrane sensors in 1.0×10^{-2} M PBS solution (pH 7.0).

Table 3. Potentiometric response characteristics of ACh membrane sensors

Parameter	MIP/MAA	NIP/MAA	MIP/MAA + TPB ⁻	MIP/MAA+TDMA ⁺
Slope ^a mV decade ⁻¹	59.6 ± 0.9	39.5 ± 0.7	55.2 ± 0.8	15±0.8
Correlation coefficient (<i>r</i> ²)	0.996	0.998	0.999	0.998
Linear range, M	3.0×10 ⁻⁵ -1.0 × 10 ⁻²	1.0×10 ⁻⁴ -1.0 × 10 ⁻²	1.0×10 ⁻⁵ -1.0 × 10 ⁻²	5.0×10 ⁻³ -1.0 × 10 ⁻²
Detection limit, µg mL ⁻¹	1.31	11.7	0.65	627.8
Working range, pH	3 - 9	3 - 9	3 - 9	-
Response time, s	<10	<10	<10	-
Lifespan, week	12	12	12	-
Precision C _v w (%)	1.2	0.7	0.9	-
Between-day variability C _v b (%)	0.8	1.3	1.1	-

^a Average of six measurements

The effect of an addition of lipophilic salts or ionic additives upon the characteristics of conventional potentiometric sensors was also studied. A comparison between the membranes without ionic additive and that containing anionic additive (i.e. 30 mol % TpCIPB⁻ relative to the sensing material) showed that incorporation of TpCIPB⁻ in ACh sensors exhibited a slope of 55.2±0.8 mV decade⁻¹ with a linear dynamic range extended from 1.0 × 10⁻⁵ to 1.0 × 10⁻² M and a detection limit of 0.65 µg mL⁻¹. The incorporation of cationic site additive (i.e. 30 mol % TDMA⁺ relative to the ionophore) dramatically deteriorated the potentiometric response characteristics showing a slope of 15.0 ± 0.8 mV decade⁻¹, detection limit of 627.8 µg mL⁻¹ and linear response range begins from 5.0 × 10⁻³ M.

The stability of these transducers was monitored continuously at 1.0 × 10⁻⁴ M of ACh⁺ solution and evaluated for a period of 5 h, the potential drift noticed was ≤ 0.6 mV h⁻¹. The repeatability of the potential reading for the sensors was also examined by subsequent measurements in 5.0×10⁻⁴ M of ACh⁺ solution immediately after measuring the first set of the solution at 1.0×10⁻⁴ M of ACh⁺ solution. The standard deviations of measuring *emf* for 5 replicate measurements obtained are 0.8 mV for the solution of 1.0×10⁻⁴ M and 0.7 mV for the solution of 5.0×10⁻⁴ M. This means that the repeatability of potential response of the electrode is acceptable.

The time required to achieve a steady potential response within ±1.5 mV using the proposed sensors in 10⁻⁶ to 10⁻⁴ M ACh⁺ solutions with a rapid 10-fold increase in concentration was <10 s. Replicate calibrations for each sensor indicated low potential drift, long-term stability, and negligible change in the response of the sensors. The sensors were conditioned in 10⁻³ M ACh⁺ solution of pH 7.0 and stored in the same solution when they are not in use. With all sensors examined, the detection limits, response times, linear ranges and calibration slopes were reproducible to within ±3 % of their original values over a period of at least 12 weeks.

The influence of the pH on the potentiometric response of the proposed sensors was examined over a pH range of 2-10 for ACh⁺ standard solutions of 1.0×10⁻⁴ and 1.0×10⁻³ M. The pH of the solution was adjusted with either hydrochloric acid and/or sodium hydroxide solutions. The pH plot showed that the variation of solution pH over the range 3-9 has no significant effect on the potentiometric response for both MIP and NIP membrane based sensors. For pH<3 the sensor responses were severely influenced by H₃O⁺.

Sensors selectivity

One of the most important parameters characterizing the analytical properties of each new transducer is its selectivity over many common ions. Therefore, the potentiometric selectivity coefficients of the sensors towards different organic and cationic inorganic species commonly associated in biological samples with ACh⁺ were evaluated using the fixed solution method (FSM).⁴² Potentiometric selectivity of the sensors was related to the preferential interaction of the mimic receptors with ACh⁺ in 0.01 M PBS solution of pH 7.0 over many used common interferents. The selectivity pattern for the sensors was shown in Table 2.

Table 4. Selectivity coefficients (*K*^{Pot}_{ACh⁺,j}) of acetylcholine membrane based sensors.

Interferents, I	MIP /MAA	NIP/MAA	MIP/MAA+ TPB ⁻
Acetylcholine	0	0	0
Choline	-1.91	-1.74	-1.62
Codeine	-1.76	-1.45	-1.37
Morphine	- 1.80	-1.28	-1.50
Ephedrine	-1.67	- 1.40	-1.45
Caffeine	-1.57	- 1.29	- 1.50
Histidine	-2.03	- 1.85	-1.60
Glutamine	-1.85	- 1.54	-1.25
Quinine	-2.07	- 1.34	-1.57
Cysteine	- 2.12	-1.55	-1.70
Mg ²⁺	-2.96	-2.70	-2.82
Ca ²⁺	-2.75	-2.32	-2.54
Ba ²⁺	-3.12	-3.01	-2.93
K ⁺	-3.21	-3.00	-2.51

For MIP/MAA and NIP/MAA membrane based sensors, the selectivity order was in the order: ACh > Caffeine > Ephedrine > Codeine > Morphine > Choline > Glutamine > Quinine > Cysteine > Histidine > Ca²⁺ > Mg²⁺ > Ba²⁺ and ACh > Morphine > Caffeine > Quinine > Codeine > Ephedrine > Glutamine = Cysteine > Choline > Histidine > Ca²⁺ > Mg²⁺ > K⁺ = Ba²⁺, respectively. For MIP/MAA+TPB⁻ membrane-based sensor, the selectivity order was in the order: ACh > Glutamine > Codeine > Ephedrine > Morphine = Caffeine > Quinine > Histidine > Choline > Cysteine > K⁺ > Ca²⁺ > Mg²⁺ > Ba²⁺. Glucose, maltose, starch, talc, urea, and tween-80 at concentration level as high as 1000-fold excess over ACh⁺ have a negligible effect on the accuracy of the results. Overall, the interfering effect of doubly charged cations was lower than that of singly charged ones. Compounds of positively

charged nitrogen atoms presented more similarities to the chemical structure of the main ion and their logarithm selectivity coefficients were always below -1. This suggested that only small interference from other quaternary ammonium salts or compounds of positively charged nitrogen atoms was expected and binding to ACh^+ was the most favorable process.

Potentiometric MIP sensor in an FIA setup

A tubular-type detector incorporating an MIP/MAA+TPB-based membrane sensor was prepared and used under the hydrodynamic mode of operation for continuous monitoring of ACh. A linear relationship between ACh^+ concentrations and FIA signals was obtained over a concentration range from 1.0×10^{-4} to 1.0×10^{-2} M using 0.01 M PBS solution, pH 7 (Figure 5). The slope of the calibration plot was near-Nernstian (50.3 ± 1.9 mV decade $^{-1}$). The slightly lower sensitivity of the transducer in FI analysis may be attributed to several factors such as mass transport rate, sample dispersion and effect of contact time between sample and electrode. The limit of detection was 7.3 ± 0.3 $\mu\text{g mL}^{-1}$ and the sampling frequency was 30-32 samples hour $^{-1}$.

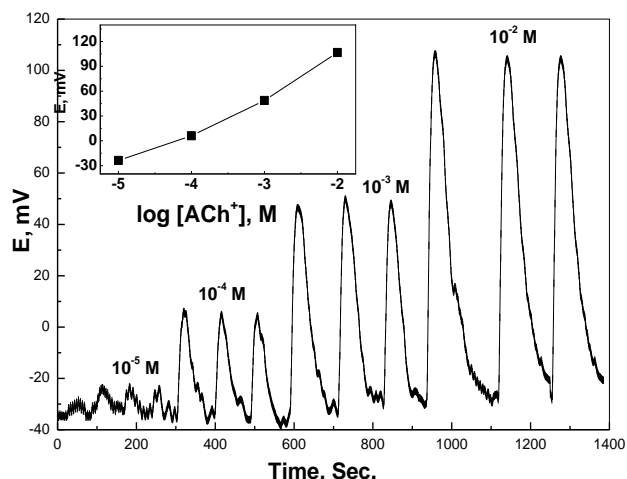


Figure 5. Typical FIA peaks produced by injection of 100 μL aqueous solutions of standard ACh into a stream of 10^{-2} M PBS solution pH 7 flowing at 3.0 mL min^{-1}

Kinetic monitoring of the acetylcholine hydrolysis

Acetylcholinesterase (AChE) terminates the transmission of impulses in the cholinergic synapses through the rapid hydrolysis of acetylcholine (ACh) to choline (Ch).⁴³

For the estimation of K_m and V_{max} of the enzymatic reaction was carried out by ACh sensor using 0.5 IU L^{-1} of the enzyme to each concentration of ACh^+ from 0.01 to 1.0 mM and monitoring the potential change. It was found that lower substrate concentrations did not significantly increase the measured initial rate. This can be attributed to the low sensitivity of the sensor at low concentration levels of ACh^+ ions. A 5.0×10^{-4} M of ACh^+ solution was used in all subsequent AChE measurements. This concentration level offered a measurable change in the reaction rate at low enzyme activity, a better linearity of calibration plot, and a fast response of the sensor. As shown in Figure 6, it provided values of 7.9×10^{-5} M and 61 mV min^{-1} for the characteristic

parameters of the enzymatic reaction, K_m , and V_{max} , respectively. This value of K_m is close to the magnitude as that obtained previously.⁴⁴

The effect of AChE concentration on the initial rate of the enzymatic reaction was also studied using an ACh concentration of 5.0×10^{-4} M, and varying the concentration of enzyme in the range of 8.0×10^{-6} to 5.0×10^{-3} U mL^{-1} .

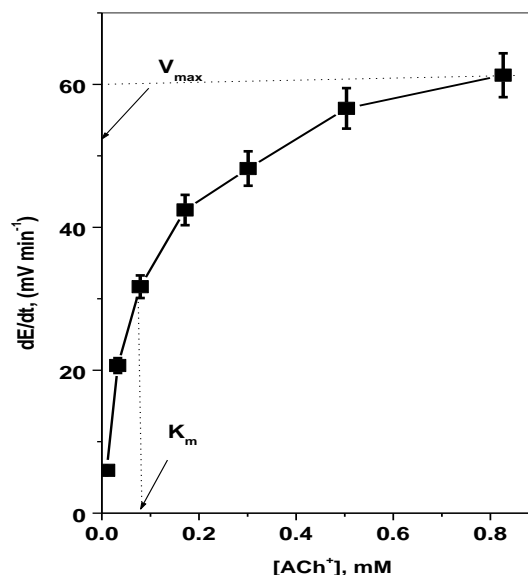


Figure 6. Michaelis-Menten plot of the hydrolysis of acetylcholine.

A linear relationship ($r = 0.9994$) was obtained in a concentration range of 1.0×10^{-5} to 5.0×10^{-3} U mL^{-1} with a detection limit of 1.0×10^{-5} U mL^{-1} .

Conclusions

The Molecular imprinting technique was employed to produce ACh host-tailored sensors for potentiometric transduction. The performance characteristics of the sensors showed stable, sensitive and selective potential responses towards ACh^+ ions over the concentration range of 3.0×10^{-5} – 1.0×10^{-2} M with a limit of detection 1.31 $\mu\text{g mL}^{-1}$ and a slope of 59.6 ± 0.9 mV decade^{-1} . The addition of an anionic additive to the membranes showed a slope of 55.2 ± 0.8 mV decade^{-1} over the concentration range of 1.0×10^{-5} – 1.0×10^{-2} M and detection limits of 0.65 $\mu\text{g mL}^{-1}$. Advantages of these sensors include the simplicity in designing, short measurement time, good precision, high accuracy, high analytical throughput, low limit of detection and good selectivity. The selectivity for acetylcholine over choline, the fast response, and low drift of the proposed sensors developed permit the assay of AChE activity via the hydrolysis of ACh^+ .

Acknowledgements

The financial support of the Deanship of Scientific Research, Qassim University, KSA, is gratefully acknowledged.

References

- ¹Mesulam, M. M., *Cholinergic neurons, pathways, diseases. In Encyclopedia of Neuroscience*, Vol. 1, Adelman G (ed.). Birkhuser: Boston, MA, **1987**, 233.
- ²Fraunfelder, F. T., Meyer, S. M. (eds). *Drug-induced Ocular Side Effects and Drug Interactions*, 2nd edn. Lea & Febiger, Philadelphia, **1982**.
- ³Coulson, F. R., Fryer, A. D., *Pharmacol. Ther.*, **2003**, 98,59.
- ⁴Khayyal, M. T., Tolba, H. M., El-Hawary, M. B., El-Wahed, S. A., *Eur. J. Pharmacol.*, **1974**, 25, 287.
- ⁵Feigenson, M. E., Saelens, J. K., *Biochem. Pharmacol.*, **1969**, 18,1479.
- ⁶Potter, P. E., Meek, J. K., Neff, N. H., *J. Neurochem.*, **1983**, 41, 188.
- ⁷Okuyama, S., Ikeda, Y., *J. Chromatogr.*, **1988**, 431, 389.
- ⁸MacDonald, R. C., *J. Neurosci. Meth.*, **1989**, 29, 73.
- ⁹Dong, Y., Wang, L., Shangguan, D., Zhao, R., Liu, G., *J. Chromatogr. B*, **2003**, 788, 193.
- ¹⁰Liberato, D. J., Yergey, A. L., Weintraub, S. T., *Biomed. Environ. Mass Spectrom.*, **1986**, 13, 171.
- ¹¹Ishimaru, H., Ikarashi, Y., Maruyama, Y., *Biol. Mass Spectrom.*, **1993**, 22, 681.
- ¹²Hows, M. E. P., Organ, A. J., Murray, S., Dawson, L. A., Foxton, R., Heidebreder, C., Hughes, Z. A., Lacroix, L., Shah, A. J., *J. Neurosci. Meth.*, **2002**, 121, 33.
- ¹³Dunphy, R., Burinsky, D. J., *J. Pharm. Biomed. Anal.*, **2003**, 31, 905.
- ¹⁴Kiba, N., Ito, S., Tachbana, M., Tani, K., Koizumi, H., *Anal. Sci.*, **2003**, 19, 1647.
- ¹⁵Bundel, D. D., Sarre, S., Eeckhaut, A.V., Smolders, I., Michotte, Y., *Sensors*, **2008**, 8, 5171.
- ¹⁶Schuvailo, S. V., Dzyadevych, A.V., A.V. Elskaya, Gautier-Sauvigne, S., Csoregi, E., Cespuglio, R., Soldatkin, A. P., *Biosens. & Bioelectron.* **2005**, 21, 87.
- ¹⁷Carballo, R., Orto, V.C.D., Rezzano, I., *Anal. Lett.*, **2007**, 40, 1962.
- ¹⁸Jaffrezic-Renault, N., Dzyadevych, S.V., *Sensors*, **2008**, 8, 2569.
- ¹⁹Periasamy, A. P., Umasankar, Y., Chen, S. M., *Sensors*, **2009**, 9, 4034.
- ²⁰Jaramillo, A., Lopez, S., Justice, J., B. *Anal. Chem. Acta*, 1983, 146, 149.
- ²¹Kima, H., Oha, J., Jeona, W. S., Selvapalam, N., Hwang, I., Koa, Y. H., Kim, K., *Supramol. Chem.*, 2012, 24, 487.
- ²²Liu, W., Yang, Y. H., Wu, Z.Y., Wang, H., Shen, G. L. Yu, R.Q., *Sens. & Actuat. B*, **2005**, 104, 186.
- ²³Poels, I., Nagels, L. J., *Anal. Chim. Acta*, **2001**, 440, 89.
- ²⁴Khaled, E., Hassan, H. N. A., Mohamed, G. G., Ragab, F. A., Seleim, A. A., *Int. J. Electrochem. Sci.*, 2010, 5, 448.
- ²⁷Kamel, A. H., Yamani, H. Z., Safwat, Galal, H. R., *Eur. Chem. Bull.*, **2016**, 5, 69.
- ²⁶Li, S., Gi, Y., Piletsky, S. A., Lunec, J., *Molecular imprinted sensors: Overview and applications*, Elsevier, **2012**.
- ²⁷Kamel, A. H., Galal, H. R., Hanna, A. A., *Int. J. Electrochem. Sci.*, **2014**, 9, 5776.
- ²⁸Kamel, A. H., Khalifa, M. E., Elgendy, F. A., Abd El-Maksoud, S. A., *Anal. Meth.*, **2014**, 6, 7814.
- ²⁹Hassan, S. S. M., Kamel, A. H., Abd El-Naby, H., *J. Chin. Chem. Soc.*, **2014**, 61, 295.
- ³⁰El-Naby, E. E., Kamel, A. H., *Mat. Sci. Eng. C*, **2015**, 54, 217.
- ³¹Kamel, A. H., Khalifa, M. E., Elgendy, F. A., Abd El-Maksoud, S. A., *Int. J. Electrochem. Sci.*, **2014**, 9, 1663.
- ³²Moreira, F. T. C., Sharma, S., Dutra, R. A. F., Noronha, J. P. C., Cass, A. E. G., Sales, M. G. F., *Microchim. Acta.*, **2015**, 182, 975.
- ³³Moreira, F. T. C., Queirós, R. B., Truta, L. A. A., Silva, T. I., Castro, R. M., Amorim, L. R., Sales, M. G. F., *J. Chem.*, **2013**, 1.
- ³⁴Kamel, A. H., Soror, T. Y., Al-Romian, F. M., *Anal. Meth.*, **2012**, 4, 3007.
- ³⁵Kamel, A. H., Al-Romian, F. M. *Int. J. Chem. Mat. Sci.*, **2013**, 1, 1.
- ³⁶Abd-Rabboh, H. S. M., Kamel, A. H., *Electroanalysis*, **2012**, 24, 1409.
- ³⁷Kamel, A. H., Galal, H. R., *Int. J. Electrochem. Sci.*, **2014**, 9, 4361.
- ³⁸Tao, F. T., Thurber, J. S., Dye, D. M., *J. Pharm. Sci.*, **1984**, 73, 1311.
- ³⁹Royani, I., Widayani, I., Abdullah, M., Khairurrijal, K., *Int. J. Electrochem. Sci.*, **2014**, 9, 5651.
- ⁴⁰Matsui, J., Miyoshi, Y., Doblhoff-Die, O., Takeuchi, T., *Anal. Chem.*, **1995**, 67, 4404.
- ⁴¹Moreira, F. T. C., Sales, M. G. F., *Sci. Eng. C. Mater. Biol. Appl.*, **2011**, 31, 1121.
- ⁴²Amemiya, S., Buhlmann, P., Pretsch, E., Bnsterholz, B., Umezawa, Y., *Anal. Chem.*, **2000**, 72, 1618.
- ⁴³Brunton, L. L., *The Pharmacological Basis of Therapeutics*, Goodman and Gilman's, 11th ed., McGraw Hill, New York, **2006**.
- ⁴⁴Cuartero, M., Ortuno, J. A., Garcia, M. S., Garcia-Canovas, F., *Anal. Biochem.*, **2012**, 421, 208.

Received: 17.07.2016.

Accepted: 21.08.2016.



NATURAL BOND ORBITAL ANALYSIS OF CYCLIC AND ACYCLIC “C-H” ACIDS

Didier Villemin^{[a]*}, Imad Eddine Charif^[b], Sidi Mohamed Mekelleche^{[b]*} and Nathalie Bar^[a]

Keywords: Meldrum's acid, barbituric acid, tetronic acid, carbon acidity donor-acceptor interactions, DFT calculations, NBO analysis.

The high acidity of Meldrum's acid, barbituric and tetronic acids in comparison to their acyclic analogues was explained by density functional theory and calculations and by natural bond orbital analysis. The present study shows that cyclic β -dicarbonyl compounds are remarkably stabilized by intramolecular donor-acceptor interactions and this effect is absent in their acyclic analogues.

* Corresponding Authors

E-Mail: villemin@ensicaen.fr

sm_mekelleche@mail.univ-tlemcen.dz

[a] Normandie Univ., France, ENSICAEN, LCMT, UMR CNRS 6507, INC3M, FR 3038, Labex EMC3, LabexSynOrg, 14050 Caen, France.

[b] Laboratory of Applied Thermodynamics and Molecular Modeling, Department of Chemistry, Faculty of Science, University of Tlemcen, BP 119, Tlemcen, 13000, Algeria.

Introduction

The high C-H acidity¹ of several precursors in multicomponent reactions² is the key for efficient acid-base synthesis. The increase of acidity in cyclic dicarbonyl compounds allows easy formation of carbon anions in Knoevenagel, Michael, or aldolisation reactions. This increase, due to the cyclic structure of compounds, was also employed in solventless reactions.² This phenomenon observed in experiment for various acids such as barbituric acid (BA), Meldrum's acid (MA), tetronic acid (TA) did not receive many explanations besides some few theoretical works on Meldrum's acid. The C-H acidity of these cyclic compounds in water ($pK_a(\text{MA}) = 4.83$, ($pK_a(\text{BA}) = 4.01$) and ($pK_a(\text{TA}) = 3.76$)⁴ are comparable to that of acetic acid ($pK_a = 4.75$). This relatively high acidity is due to the acid hydrogen bonded to carbon positioned between the two carbonyl groups. The C-H acidity of these cyclic β -dicarbonyl compounds is found to be remarkably higher than that of the related compounds with open chains, namely, diethyl malonate (DEM), malonamide (MNA) and ethyl acetoacetate (EAA) (Figure 1). The experimental pK_a values for these acyclic compounds are $pK_a(\text{DEM}) = 13.3$, $pK_a(\text{MNA}) = 12.5$ and $pK_a(\text{EAA}) = 10.7$.

Some experimental and theoretical works devoted to the spectacular high acidity of MA, BA and TA can be found in the literature.⁴ Arnett and Harrelson⁵ suggested that the high acidity of Meldrum's acid compared to dimethyl malonate, results from the restricted rotation around the ester bonds in the six-membered ring of MA. These authors also observed that the acidity decreased rapidly when going from the six-membered to the ten-membered ring. Interestingly, it has been found that the pK_a of the thirteen-membered ring is closer to that of (acyclic) methyl malonate. Wang and Houk⁶

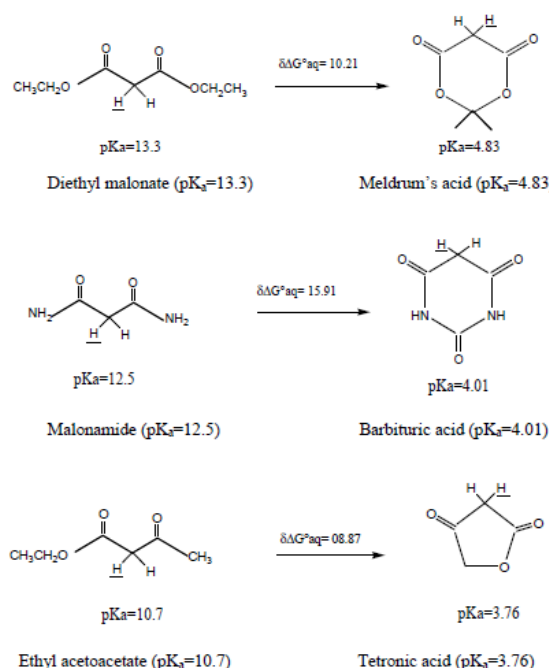


Figure 1. The relative values calculated $\delta\Delta G^{\circ}_{\text{aq}}$ of studied compounds.

suggested that the significant acidity of MA can be explained by differences in steric and electrostatic (dipole-dipole) repulsions between *E* and *Z* conformers of esters in the neutral and anionic species. Likewise, Wiberg and Laidig⁷ showed, by theoretical calculations, that the surprising high acidity of MA, displaying an ester conformation with a bis(*E*) ester conformation, can be attributed to the difference in acidity between *Z* and *E* rotamers of methyl acetate. The solvent effects on acidities of *Z* and *E* ester conformers were also studied by Evanseck et al.⁸ Their calculations showed an appreciable stabilization of the *E* conformer in comparison of the *Z* conformer by 3.0 22 kcal mol⁻¹ in water and 2.7 kcal mol⁻¹ in acetonitrile. Furthermore, the anionic form of the *E* conformer is also found to be more stable than that of the *E* conformer by 2.3 22 kcal mol⁻¹ in water and 1.5 kcal mol⁻¹ in acetonitrile. The difference in acidity observed in aqueous phase between MA and dimethyl malonate were also explained by conversion of two *Z* esters groups into two *E*

esters groups.⁸⁻⁹ Gao et al.⁹ showed that the solvent effects are rather weak and the major stabilization of the enolate anion is due to the stereoelectronic effects, called anomeric effects which represent an important factor for explaining the origin of the noteworthy acidity of the MA. Our aim in this work is to explain the origin of the remarkably high acidity of MA, BA and TA using the Natural Bond Orbital (NBO) analysis and the quantification of electron populations and intramolecular donor-acceptor interactions.¹⁰⁻¹⁴

Computational procedures

All the calculations reported in this work were carried out using the Gaussian 03W computational package.¹⁵ The geometries of the neutral and anionic (deprotonated) species are fully optimized at the B3LYP¹⁶ level of theory in combination of the standard 6-311++G(d,p) basis set. Solvent effects are taken into account using SCRF (self-consistent reaction field) calculations using PCM (polarizable continuum model).¹⁷⁻¹⁹ NBO analysis¹⁰⁻¹⁴ was performed using the NBO 3.1 program²⁰ implemented in Gaussian 03W package.

NBO analysis

Several methods have been used to analyze the contribution of localized orbitals in molecular properties.¹⁰⁻¹¹ In addition of stabilization effects, the stereoelectronic interactions also provide the manner of transmitting information between the various parts of the molecule. For example, the NBO method was employed to establish the electronic exchanges, the electronic transfer between donor-acceptor compounds and hyperconjugation interactions.^{13,21-23}

In the NBO analysis, the donor-acceptor (bond-antibond) interactions are considered by examining all possible interactions between the 'occupied' (donor) Lewis-type NBOs and the 'non occupied' (acceptor) non-Lewis NBOs. Then, their energies are estimated by second-order perturbation theory. These stabilizing interactions are referred as 'delocalization' corrections to the 0th-order natural Lewis structure. For each donor, NBO (*i*) and acceptor NBO (*j*), the stabilization energy $E^{(2)}$, which is associated with the $i \rightarrow j$ delocalization, is explicitly estimated by the following equation:

$$E_{i \rightarrow j}^{(2)} = -n_i^{(0)} \frac{\langle \varphi_i^{(0)} / F / \varphi_j^{(0)} \rangle^2}{\varepsilon_j^{(0)} - \varepsilon_i^{(0)}} \quad (1)$$

where

- n_i is the orbital occupancy,
- $\varepsilon_i, \varepsilon_j$ are NBO orbital energies and
- F is the Fock operator.

To further understanding of the electronic effects in cyclic and acyclic β -dicarbonyl compounds, NBO analysis, using B3LYP/6-311++G** geometries, has been carried out. Second order delocalization energies $E^{(2)}$, which are quantitative representation of the stabilization energies associated with the electronic delocalization, are discussed and analysed in the present work.

Results and discussions

Calculations of the free energies of deprotonation ΔG°

Energies of deprotonation at 298 K in gas,²⁴ $\Delta G^\circ_{\text{gas}}$ and in aqueous phase, $\Delta G^\circ_{\text{aq}}$, were calculated using the B3LYP/6-311++G(d, p) computational level. The results are given in table 1.

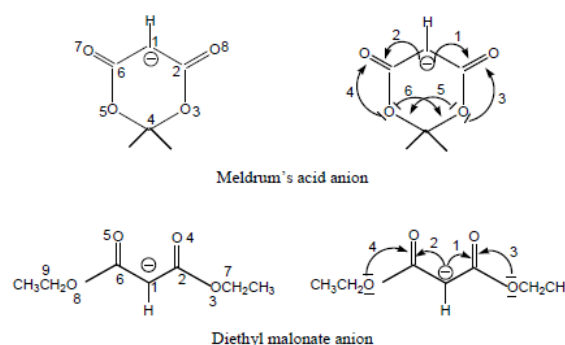
Table 1. B3LYP/6-311++G(d, p) energies of deprotonation (kcal mol⁻¹) in gas phase $\Delta G^\circ_{\text{gas}}$ and in aqueous phase $\Delta G^\circ_{\text{aq}}$ of the β -dicarbonyl compounds.

Compound	$\Delta G^\circ_{\text{gas}}$	$\Delta G^\circ_{\text{aq}}$	pK _a (exp)
Diethyl malonate	336.62	22.31	13.30
Meldrum's acid	321.34	12.10	4.83
Malonamide	340.31	27.22	12.50
Barbituric acid	316.57	11.31	4.01
Ethyl acetylacetate	331.50	19.31	10.70
Tetronic acid	319.21	10.44	3.76

The difference, $\delta \Delta G^\circ_{\text{aq}}$, between cyclic acids and their acyclic analogues are given in Figure 1. It turns out that $\Delta G^\circ_{\text{aq}}$ of all cyclic compounds are lower than those of their acyclic analogues. For instance, the free Gibbs enthalpy of MA is lower by 10.21 kcal mol⁻¹ than that of DEM, indicating the high acidity of cyclic compounds in comparison of open-chain compounds. In order to explain the difference in acidity between the cyclic β -dicarbonyl compounds and their open chain analogues, we have explored all the orbital interactions and the electronic effect of delocalization in the conjugate bases of these acids.

Case 1: Meldrum's acid / diethyl malonate

The most significant stereoelectronic interactions in the conjugate bases (anions) of the MA and DEM are illustrated in Scheme 1. The stabilization energies, expressed in terms of $E^{(2)}$, are given in Table 2. The acyclic anions are asymmetrical and their geometry is in sickle form, so both C=O are not directed in the same direction.²⁵ In the cyclic anions, there is symmetry (form W) in the Meldrum anion and barbiturate.



Scheme 1. The most significant stereoelectronic interactions of MA and DEM anions.

The acidity of these dicarbonyl compounds (cyclic and acyclic) is attributed to the hydrogen positioned between the two carbonyl groups which facilitate the deprotonation process. NBO analysis shows that the negative charge on

carbon atom C_1 of MA and DEM anions are strongly delocalized on the two carbonyl groups ($C=O$) by charge transfer $n_{C1} \rightarrow \pi^*_{C=O}$. As can be seen from the Table 2, there is a significant stabilization energy for $n_{C1} \rightarrow \pi^*_{C=O}$ delocalization in Meldrum's acid and DEM anions ($E^{(2)} = 105$ and $132.22 \text{ kcal mol}^{-1}$ respectively). The two compounds also exhibited a second donor-acceptor interactions of the type $n_O \rightarrow \pi^*_{C=O}$ between the lone pair of the ester oxygen and the unoccupied orbital π^* of the carbonyl group. The $E^{(2)}$ stabilization energies are $22.68 \text{ kcal mol}^{-1}$ (twice) for MA and 29.70 and $36.22 \text{ kcal mol}^{-1}$ in diethylmalonate (see Table 2).

Table 2. $E^{(2)}$ energies of the main donor-acceptor interactions for MA and DEM anions.

Meldrum's (MA) anion	
Interaction	$E^{(2)}$ (kcal mol ⁻¹)
1. $n_{C1} \rightarrow \pi^*_{C2=O8}$	105.06
2. $n_{C1} \rightarrow \pi^*_{C6=O7}$	105.06
3. $n_{O3}(\text{LP2}) \rightarrow \pi^*_{C2=O8}$	22.68
4. $n_{O5}(\text{LP2}) \rightarrow \pi^*_{C6=O7}$	22.68
5. $n_{O3}(\text{LP1}) \rightarrow \sigma^*_{C4-O5}$	4.00
$n_{O3}(\text{LP2}) \rightarrow \sigma^*_{C4-O5}$	8.00
6. $n_{O5}(\text{LP1}) \rightarrow \sigma^*_{C4-O3}$	4.00
$n_{O5}(\text{LP2}) \rightarrow \sigma^*_{C4-O3}$	8.00
7. $n_{O3}(\text{LP1}) \rightarrow \sigma^*_{C2-C1}$	3.77
8. $n_{O5}(\text{LP1}) \rightarrow \sigma^*_{C6-O1}$	3.77
Diethyl malonate (DEM) anion	
Interaction	$E^{(2)}$ (kcal mol ⁻¹)
1. $n_{C1} \rightarrow \pi^*_{C2=O4}$	132.35
2. $n_{C1} \rightarrow \pi^*_{C6=O5}$	132.19
3. $n_{O3}(\text{LP2}) \rightarrow \pi^*_{C2=O4}$	29.70
4. $n_{O8}(\text{LP2}) \rightarrow \pi^*_{C6=O5}$	36.22

In Table 3, we have calculated by NBO analysis the electron occupations of the orbitals including the various interactions donor-acceptor for MA and DEM anions.

The analysis of these occupations, for the two compounds, shows that orbitals $\pi^*_{C=O}$ which are "usually" vacant, have an occupation of 0.40 - 0.44 electrons and the occupation of the negative charge of carbon C_1 is lower than 2 electrons (1.35 and 1.37 electrons for MA and DEM respectively). The second lone pair occupancies of ester oxygen atoms n_O are also decreased (1.836 - 1.865 electrons) due to charge transfer interactions (See table 3). These results confirm the $E^{(2)}$ values previously found (Table 2) corresponding to $n_O \rightarrow \pi^*_{C=O}$ donor-acceptor interactions.

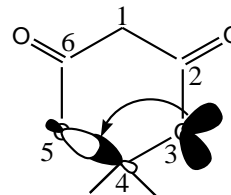
In addition to $n_C \rightarrow \pi^*_{C=O}$ and $n_O \rightarrow \pi^*_{C=O}$ interactions, MA presents other important interactions (which are absent in DEM). Indeed, for MA, there is a charge transfer of the type $n_O \rightarrow \sigma^*_{C-O}$ due to the donor-acceptor interaction between the nonbonding electron pairs of ester oxygens and antibonding orbitals of the vicinal sigma bonds. These interactions are called anomeric stabilization or anomeric effects (Scheme 2). These effects are very frequent in cyclic bilactone compounds like MA. The sum of $E^{(2)}$ energies of these interactions (orbitals of the four lone pairs of two ester oxygens and the two vicinal sigma antibonding orbitals σ^*_{C4-O5} and σ^*_{C4-O3})

are of the magnitude $21.6 \text{ kcal mol}^{-1}$ (Table 2). Gao et al.⁹ showed that the dissociation of the MA is accompanied by an increase of $E^{(2)}$ stabilization energy due to anomeric effects. The analysis of the occupancies of the antibonding orbitals indicated that anomeric effects lead to an occupancy of σ^*_{C4-O5} and σ^*_{C4-O3} orbitals by 0.10 electrons.

Table 3. Electron Occupancies of orbitals calculated by NBO method.

Compound	Orbital	Occupancy
Meldrum's (MA) anion	n_{C1}	1.350
	$\pi^*_{C2=O8}$	0.405
	$\pi^*_{C6=O7}$	0.405
	$n_{O3}(\text{LP2})$	1.856
	$n_{O5}(\text{LP2})$	1.856
	σ^*_{C4-O5}	0.100
	σ^*_{C4-O3}	0.100
Diethyl malonate (DEM) anion	n_{C1}	1.370
	$\pi^*_{C2=O4}$	0.435
	$\pi^*_{C5=O6}$	0.435
	$n_{O3}(\text{LP2})$	1.845
	$n_{O8}(\text{LP2})$	1.845

These anomeric effects present in the MA anion, which are completely absent in DEM anion, lead to a substantial stabilization of the MA conjugate base and therefore make an important contribution in increasing of the acidity of the cyclic MA compound in comparison with its corresponding acyclic compound (DEM).

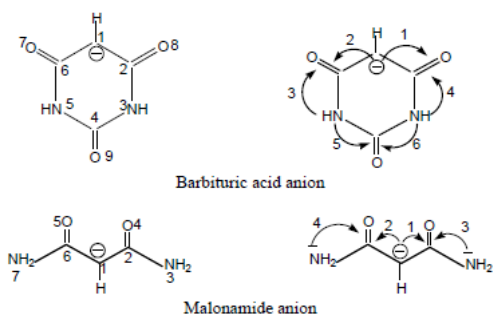


Scheme 2. Anomeric effects in MA.

Case 2: Barbituric acid/malonamide

The main interactions donor-acceptor and their corresponding stabilization $E^{(2)}$ energies for cyclic BA anion and its acyclic analogous compound, namely MNA anion are given in scheme 3 and Table 4, respectively.

NBO analysis shows that the negative charge on carbon atom C_1 of BA and MNA are strongly delocalized with the two carbonyl groups ($C=O$) via vicinal charge transfer interactions. For the BA anion, $E^{(2)} = 79.07 \text{ kcal mol}^{-1}$ for $n_{C1} \rightarrow \pi^*_{C2=O8}$ and 78.28 kcal/mol for $n_{C1} \rightarrow \pi^*_{C6=O7}$. For MNA anion, $E^{(2)} = 100.84 \text{ kcal/mol}$ for $n_{C1} \rightarrow \pi^*_{C2=O4}$ and $92.08 \text{ kcal mol}^{-1}$ for $n_{C1} \rightarrow \pi^*_{C6=O5}$ interactions. BA and MNA also exhibited a second type of donor-acceptor interactions involving the lone pair of the nitrogen atoms and the antibonding π^* orbitals of the adjacent carbonyl groups. For BA anion, $E^{(2)} = 49.60 \text{ kcal/mol}$ for $n_{N5} \rightarrow \pi^*_{C6=O7}$ interaction and $E^{(2)} = 50.39 \text{ kcal/mol}$ for $n_{N3} \rightarrow \pi^*_{C2=O8}$ interaction. For MNA anion, $E^{(2)} = 22.51 \text{ kcal/mol}$ for $n_{N3} \rightarrow \pi^*_{C2=O4}$ and $18.84 \text{ kcal mol}^{-1}$ for $n_{N7} \rightarrow \pi^*_{C6=O5}$ interactions (Table 4).



Scheme 3. The important stereoelectronic interactions of BA and MNA anions.

Table 4. $E^{(2)}$ energies of the main donor-acceptor interactions for BA and MNA anions.

Barbituric acid (BA) anion		Malonamide (MNA) anion	
Interaction	$E^{(2)}$ (kcal mol ⁻¹)	Interaction	$E^{(2)}$ (kcal mol ⁻¹)
$n_{C1} \rightarrow \pi^*_{C2=O8}$	79.07	$n_{C1} \rightarrow \pi^*_{C2=O4}$	100.84
$n_{C1} \rightarrow \pi^*_{C6=O7}$	78.29	$n_{C1} \rightarrow \pi^*_{C6=O5}$	92.08
$n_{N5} \rightarrow \pi^*_{C6=O7}$	49.60	$n_{N3} \rightarrow \pi^*_{C2=O4}$	22.51
$n_{N3} \rightarrow \pi^*_{C2=O8}$	50.39	$n_{N7} \rightarrow \pi^*_{C6=O5}$	18.84
$n_{N5} \rightarrow \pi^*_{C4=O9}$	37.42		
$n_{N3} \rightarrow \pi^*_{C4=O9}$	37.36		

The electron occupancies of the orbitals involved in donor-acceptor interactions for BA and MNA anions, calculated by NBO analysis are given in Table 5. Note that a light difference in energies (less than 1 kcal mol⁻¹) is tolerated in NBO calculations.

Table 5. Electron occupancy of orbitals calculated by NBO method.

Compound	Orbital	Occupancy
Barbituric acid (BA) anion	n_{C1}	1.379
	$\pi^*_{C2=O8}$	0.423
	$\pi^*_{C6=O7}$	0.422
	n_{N3}	1.664
	n_{N5}	1.663
	$\pi^*_{C4=O9}$	0.339
Malonamide (MNA) anion	n_{C1}	1.372
	$\pi^*_{C2=O4}$	0.413
	$\pi^*_{C6=O5}$	0.418
	n_{N3}	1.866
	n_{N5}	1.882

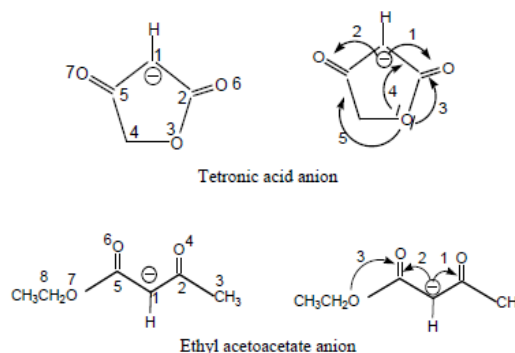
The analysis of electron occupancies shows that the two antibonding $\pi^*_{C=O}$ orbitals are not completely vacant and have an occupancy of 0.42 electrons. The negative charge on carbon atom C_1 shows occupancy less than 2 electrons (1.379 and 1.372 electrons for BA and for MNA anions, respectively). The lone pairs n_N of nitrogen atoms are also diminished to 1.663–1.866 electrons due to charge transfer of the type $n_N \rightarrow \pi^*_{C=O}$. These results confirm the calculated $E^{(2)}$ stabilizations due to donor-acceptor interactions (Table 4).

B3LYP/6-311++G** calculations of the deprotonation free energies give a difference in aqueous phase $\delta\Delta G^\circ = \Delta G^\circ(\text{BA}) - \Delta G^\circ(\text{MNA}) = 15.91$ kcal mol⁻¹ indicates the high acidity of BA

compared to MNA. This behavior can be explained by the strong delocalization between the lone pairs of nitrogen atoms and the carbonyl group $C_4=O_9$ situated between these two nitrogen atoms. These interactions, denoted designated by numbers 5 and 6 in Scheme 3 are present in BA anion but they are absent in MNA anion. These interactions give a supplementary stabilization of the cyclic anion and consequently justify the high acidity of BA. The $E^{(2)}$ energies are equal to 37.4 kcal mol⁻¹ for both $n_{N3} \rightarrow \pi^*_{C4=O9}$ and $n_{N5} \rightarrow \pi^*_{C4=O9}$ donor-acceptor interactions (Table 4). These stabilization interactions are also supported by the strong occupancy of the antibonding orbital $\pi^*_{C4=O9}$ (0.339 electrons, see Table 5).

Case 3: Tetric acid/ethyl acetoacetate

The main stereoelectronic interactions for cyclic TA and acyclic EAA anions are illustrated in Scheme 4 and the corresponding $E^{(2)}$ energies are given in Table 6.



Scheme 4. The significant stereoelectronic interactions for TA and EAA anions.

Table 6. $E^{(2)}$ energies of the main donor-acceptor interactions for TA and EAA anions.

Tetric acid (TA) anion		Ethyl acetoacetate (EAA) anion	
Interaction	$E^{(2)}$ kcal mol ⁻¹	Interaction	$E^{(2)}$ kcal mol ⁻¹
$n_{C1} \rightarrow \pi^*_{C2=O6}$	129.02	$n_{C1} \rightarrow \pi^*_{C2=O4}$	123.61
$n_{C1} \rightarrow \pi^*_{C5=O7}$	109.27	$n_{C1} \rightarrow \pi^*_{C5=O6}$	134.11
$n_{O3}(\text{LP2}) \rightarrow \pi^*_{C2=O6}$	70.21	$n_{O7}(\text{LP2}) \rightarrow \pi^*_{C5=O6}$	39.57
$n_{O3}(\text{LP1}) \rightarrow \sigma^*_{C1-C2}$	6.80		
$n_{O3}(\text{LP1}) \rightarrow \sigma^*_{C4-C5}$	1.84		

As it has been discussed above for MA/DEM and BA/MNA couples, the same of donor-acceptor interactions of the type $n_C \rightarrow \pi^*_{C=O}$ are observed for TA/EAA couple. For the TA anion, $E^{(2)} = 129.02$ kcal mol⁻¹ for $n_{C1} \rightarrow \pi^*_{C2=O6}$ and 109.27 kcal mol⁻¹ for $n_{C1} \rightarrow \pi^*_{C5=O7}$. For EAA anion, $E^{(2)} = 123.61$ kcal mol⁻¹ for $n_{C1} \rightarrow \pi^*_{C2=O4}$ 134.11 for $n_{C1} \rightarrow \pi^*_{C5=O6}$. TA and EAA anions also exhibited donor-acceptor interactions involving the lone pairs of the ester oxygen atoms and the antibonding π^* orbitals of the adjacent carbonyl group. For the TA anion, $E^{(2)} = 70.21$ kcal mol⁻¹ for $n_{O3}(\text{LP2}) \rightarrow \pi^*_{C2=O6}$ interaction. For the EAA anion, $E^{(2)} = 39.57$ kcal mol⁻¹ for $n_{O7}(\text{LP2}) \rightarrow \pi^*_{C5=O6}$ interaction (Table 6).

The analysis of electronic populations (Table 7) of the TA/EAA couple shows that the antibonding $\pi^*_{C=O}$ orbitals have an occupancy of 0.399 - 0.454 electrons. It is also noted that the occupation of the negative charge C_1 is diminished to 1.355 and 1.340 electrons in TA and EAA anions, respectively. The occupancies of the second lone pairs (LP2) of the ester oxygen atoms n_O are also reduced to 1.784 and 1.828 electrons. These results are in accordance with the calculated $E^{(2)}$ stabilizations given in Table 6.

Table 7. Electronic occupations of the orbitals calculated by NBO method.

Compound	Orbital	Occupancy
Tetronic acid (TA) anion	n_{C1}	1.355
	$\pi^*_{C2=O6}$	0.454
	$\pi^*_{C5=O7}$	0.435
	n_{O3} (LP2)	1.784
	σ^*_{C4-C5}	0.060
	σ^*_{C1-C2}	0.052
	Ethyl acetoacetate (EAA) anion	n_{C1}
$\pi^*_{C2=O4}$		0.399
$\pi^*_{C5=O6}$		0.425
n_{O7} (LP2)		1.828

As it has been observed for MA and BA anions, TA anion also presents important supplementary donor-acceptor interactions of the type $n_O \rightarrow \sigma^*$ between the lone pairs of the ester oxygen and the antibonding σ^* orbital. The sum of $E^{(2)}$ energies of $n_{O3(1)} \rightarrow \sigma^*_{C1-C2}$ and $n_{O3(1)} \rightarrow \sigma^*_{C4-C5}$ interactions is equal to 8.64 kcal mol⁻¹. The analysis of electron populations shows that the antibonding σ^*_{C1-C2} and σ^*_{C4-C5} orbitals are not empty and have an occupation of 0.052 and 0.060 electrons, respectively (see Table 7). These donor-acceptor stereo-electronic interactions, which are totally absent in the EAA anion, are the origin of the increase of the stabilization of the cyclic TA anion and consequently may justify explain the notable acidity of TA.

Conclusion

In this present work, we have presented a theoretical study based on NBO analysis in order to explain the remarkably high acidity of the acids of MA, BA and TA acids compared to their analogous open chains. We have rationalized the role of the stereoelectronic effects on the stability of the studied β -dicarbonyl anions by the quantification of the main donor-acceptor interactions using the $E^{(2)}$ stabilization energies and electron occupations. It turns out that there is several stabilizing interactions which are present in the cyclic β -dicarbonyl anions are completely absent in the corresponding acyclic compounds. These stereoelectronic charge transfer interactions play a determinant role in the stabilization of the conjugate bases of the studied cyclic acids and may explain the origin of their high acidity.

References

- Reutov, O. A., Beletskaya, I. P., Butin, K. P., *CH-acids*, Pergamon Press, London, **1978**.
- (a) Zhu, J., Bienaymé, H., *Multicomponent Reactions*, Wiley-VCH Verlag GmbH & Co. KGaA, **2005**. (b) Zhu, J., Qian, W. Q., Wang, M., *Multicomponent Reactions in Organic Synthesis*, Wiley-VCH Verlag GmbH & Co. KGaA, **2014**.
- (a) Villemin, D., Labiad, B., *Synth. Commun.*, **1990**, 20, 3207, 3213 and 3333. (b) Villemin, D., Martin, B., *Synth. Commun.*, **1995**, 25, 3135.
- (a) Rezende, M. C., *Tetrahedron*, **2001**, 57, 5923. (b) *Ionisation Constants of Organic Acids in Aqueous Solution* (IUPAC chemical data series), Pergamon Press, New York, **1979**. (c) Pearson, R. G., Dillon, R. L., *J. Am. Chem. Soc.* **1953**, 75, 2439. (d) Bordwell, F. G., *Acc. Chem. Res.*, **1988**, 21, 456.
- Arnett, E. M., Harrelson, J. A., *J. Am. Chem. Soc.*, **1987**, 109, 809.
- Wang, X., Houk, K. N., *J. Am. Chem. Soc.*, **1988**, 110, 1870.
- Wiberg, K. B., Laidig, K. E., *J. Am. Chem. Soc.*, **1988**, 110, 1872.
- Evanseck, J. D., Houk, K. N., Briggs, J. M., Jorgensen, W. L., *J. Am. Chem. Soc.*, **1994**, 116, 10630.
- Byun, K., Mo, Y., Gao, J., *J. Am. Chem. Soc.*, **2001**, 123, 3974.
- Foster, J. P., Weinhold, F., *J. Am. Chem. Soc.*, **1980**, 102, 7211.
- Reed, A. E., Weinhold, F., *J. Chem. Phys.*, **1983**, 78, 4066.
- Reed, A. E., Weinstock, R. B., Weinhold, F., *J. Chem. Phys.*, **1985**, 83, 735.
- Reed, A. E., Weinhold, F., *J. Chem. Phys.*, **1985**, 83, 1736.
- Weinhold, F., Landlis, C., *Valency and bonding: a natural bond orbital donor-acceptor perspective*, Cambridge University Press, **2005**.
- Frisch, M. J., Trucks, G. W., Schlegel, H. B., Scuseria, G. E., Robb, M. A., Cheeseman, J. R., Montgomery, J. A., Jr., Vreven, T., Kudin, K. N., Burant, J. C., Millam, J. M., Iyengar, S. S., Tomasi, J., Barone, V., Mennucci, B., Cossi, M., Scalmani, G., Rega, N., Petersson, G. A., Nakatsuji, H., Hada, M., Ehara, M., Toyota, K., Fukuda, R., Hasegawa, J., Ishida, M., Nakajima, T., Honda, Y., Kitao, O., Nakai, H., Klene, M., Li, X., Knox, J. E., Hratchian, H. P., Cross, J. B., Adamo, C., Jaramillo, J., Gomperts, R., Stratmann, R. E., Yazyev, O., Austin, A. J., Cammi, R., Pomelli, C., Ochterski, J. W., Ayala, P. Y., Morokuma, K., Voth, G. A., Salvador, P., Dannenberg, J. J., Zakrzewski, V. G., Dapprich, S., Daniels, A. D., Strain, M. C., Farkas, O., Malick, D. K., Rabuck, A. D., Raghavachari, K., Foresman, J. B., Ortiz, J. V., Cui, Q., Baboul, A. G., Clifford, S., Cioslowski, J., Stefanov, B. B., Liu, G., Liashenko, A., Piskorz, P., Komaromi, I., Martin, R. L., Fox, D. J., Keith, T., Al-Laham, M. A., Peng, C. Y., Nanayakkara, A., Challacombe, M., Gill, P. M. W., Johnson, B., Chen, W., Wong, M. W., Gonzalez, C., and Pople, J. A., *Gaussian 03, Revision C.02 and D.01*, Gaussian, Inc., Wallingford CT, **2004**.
- (a) Koch, W., Max Holthausen, C. A., *Chemist's Guide to Density Functional Theory*, Wiley, VCH, Weinheim, Germany, **2001**. (b) Becke, A. D., *J. Chem. Phys.*, **1993**, 98, 5648. (c) Becke, A. D., *Phys. Rev. A*, **1988**, 38, 3098. (d) Lee, C., Yang, W., Parr, R. G., *Phys. Rev. B*, **1988**, 37, 785.
- (a) Miertus, S., Scrocco, E., Tomasi, J., *Chem. Phys.*, **1981**, 55, 117. (b) Miertus, S., Tomasi, J., *Chem. Phys.*, **1982**, 65, 239.
- Tomasi, J., Persico, M., *Chem. Rev.*, **1994**, 94, 2027.
- (a) Barone, V., Cossi, M., Tomasi, J., *J. Chem. Phys.*, **1997**, 107, 3210. (b) Barone, V., Cossi, M., *J. Phys. Chem. A*, **1998**, 102, 1995.

- ²⁰Glendening, E. D., Reed A. E., Carpenter, J. E., Weinhold, F., *NBO Version 3.1*.
- ²¹(a) Schindler, M., Kutzelnigg, W., *J. Chem. Phys.*, **1982**, 76, 1919.
(b) Schindler, M., Kutzelnigg, W., *J. Am. Chem. Soc.*, **1983**, 105, 1360. (c) Schindler, M., Kutzelnigg, W., *Mol. Phys.*, **1983**, 48, 781.
- ²²Bohmann, J. A., Weinhold, F., Farrar, T. C., *J. Chem. Phys.*, **1997**, 107, 1173.
- ²³Peralta, J. E., Contreras, R. H., Snyder, J. P., *Chem. Commun.*, **2000**, 2025.
- ²⁴Charif, I. E., Mekelleche, S. M., Villemin, D., Mora-Diez, N., *J. Mol. Struct. (THEOCHEM)*, **2007**, 818, 1..
- ²⁵Lee, I., Han, I. S., Kim, C. K., Lee, H. W., *Bull. Korean Chem. Soc.* **2003**, 24(8), 1141.

Received: 11.07.2016.
Accepted: 29.08.2016.



NOVEL BRONSTED ACIDIC IONIC LIQUID L-PYRROLIDINE-2-CARBOXYLIC ACID SULFATE: AN EFFICIENT AND ECO-FRIENDLY CATALYST FOR SYNTHESIS OF 2,4,5-TRISUBSTITUTED-1H-IMIDAZOLES UNDER SOLVENT FREE CONDITIONS

V. W. Godse^[a], S. N. Darandale^[b], S. S. Rindhe^[c], Y. R. Parandkar^[b], R. D. Desai^[b], B. H. Zaware^[b], S. S. Jadhav^[b] and R. P. Pawar^{[a]*}

Keywords: Eco-friendly, imidazole, ionic liquid, three-component reaction.

A simple, highly efficient and eco-friendly protocol for the synthesis of bioactive 2,4,5-trisubstituted-1H-imidazoles via one-pot three component condensation of benzil, aromatic aldehydes and ammonium acetate under solvent free conditions has been achieved utilizing the novel Brønsted acidic ionic liquid, (L-pyrrolidine-2-carboxylic acid sulfate) as catalyst. The distinguishing features of this methodology are excellent yields in shorter reaction time, cleaner reaction profile, and environmentally friendly nature, use of non-toxic, easily synthesizable, inexpensive catalyst.

* Corresponding Author

Fax: +091-240-248-7284

E-Mail: rppawar@yahoo.com

[a] Department of Chemistry, Deogiri College, Aurangabad, Maharashtra, India.

[b] Department of Chemistry, NACS College, Ahmednagar, 414001, Maharashtra, India.

[c] Department of Chemistry, R K M Mahavidyalaya, Ahmednagar, 414001, Maharashtra, India.

Introduction

Heterocyclic compounds containing imidazole moiety have many pharmacological properties and play an important role in biochemical processes. Highly substituted imidazoles are the key intermediates in the synthesis of various therapeutic agents and act as a subunit in drugs such as Olmesartan, Losartan, Eprosartan (angiotensin II receptor antagonist), Metronidazole (antibiotic), Trifenagrel (platelet aggregation inhibitor), Dacarbazine (antineoplastic), Cimetidine (H₂-receptor antagonist) (Figure 1), methimazole (antithyroid), Pilocarpine (muscarinic receptor agonist), Etomidate (intravenous anesthetic) as well as plant growth regulators,¹ fluorescence labeling agents, biological imaging² and chromophores for non-linear optic systems. These moieties have been reported as antibacterial, anti-inflammatory, antihypertensive, antithrombotic, fungicidal,³ antiallergic, antiviral⁴ and herbicidal properties. On the other hand an ionic liquid catalyzed reaction have gained considerable attention because of their interesting properties like high thermal stability, non volatility, eco-friendly benign nature and reusability leading to proceed the reaction effectively with high yields in shorter reaction times.

In view of the diverse pharmacological properties of these potent compounds, many methodologies have been developed using various catalytic systems such as InF₃,⁵ In-Cl₃.3H₂O,⁶ BF₃.SiO₂,⁷ Zr(acac)₄,⁸ I₂,⁹ TBAB,¹⁰ CAN,¹¹ DABCO,¹² Yb(OTf)₃,¹³ L-proline,¹⁴ zirconium(IV)-modified

silica gel,¹⁵ p-TSA,¹⁶ Wells–Dawson heteropolyacid,¹⁷ MCM-41-SO₃H,¹⁸ p-dodecylbenzenesulfonic acid, cellulose sulfuric acid,¹⁹ silica-bonded sulfonic acid, boric acid²⁰ and ammonium metavanadate.²¹ Ionic liquid catalyzed reactions were also reported using [EMIM]OAc,²² [Et₃NH][HSO₄],²³ [HeMIM]BF₄,²⁴ [(CH₂)₄SO₃HMIM][HSO₄],²⁵ and triphenyl(propyl-3-sulphonyl)phosphonium toluenesulfonate. Recently sulphated tin oxide,²⁶ poly ethylene glycol,²⁷ and molecular iodine²⁸ were also used efficiently for this reactions. However, many of these reported methods suffer from one or several drawbacks such as low yields, prolonged reaction times, use of toxic, costly, moisture-sensitive, excess quantity of reagents, harsh reaction circumstances, special apparatus, difficult workup procedure and difficulty in recovery and reusability of the catalysts. Therefore, still there is a need to build up an efficient, eco-friendly and easy method for the synthesis of imidazole derivatives.

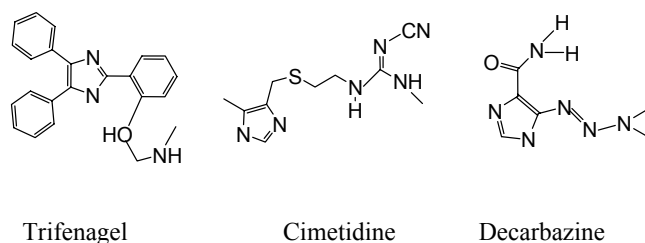


Figure 1. Physiologically highly active substituted imidazole derivatives.

With respect of our efforts to develop Brønsted acidic ionic liquid catalyzed synthetic methodologies, we report here in a simple, highly efficient and eco-friendly method for the synthesis of 2,4,5-trisubstituted-1H-imidazoles under solvent-free conditions (Scheme 1) in excellent yields utilizing an inexpensive novel Brønsted acidic ionic liquid, pyrrolidine-2-carboxylic acid sulphate (IL), as catalyst.

Table 1. Synthesis of 2,4,5-trisubstituted-1H-imidazole (**2a-i**).

S.	Aldehyde	Time	Yield (%)	Melting point (°C)	
				Observed	Reported
2a	Benzaldehyde	90	80	271 - 273	270 - 272
2b	2-Hydroxy benzaldehyde	180	85	205-206	204-207
2c	4-Nitro benzaldehyde	45	75	241-243	242-243
2d	4-Chloro benzaldehyde	30	75	260-262	261-263
2e	4-Methoxy benzaldehyde	180	75	230-232	231-233
2f	1-Naphthaldehyde	90	82	240-242	242-243
2g	4-Dimethylamino benzaldehyde	45	75	256-257	256-258
2h	2-Hydroxy 1-naphthaldehyde	90	75	188	---
2i	9-Anthraldehyde	90	80	222	---

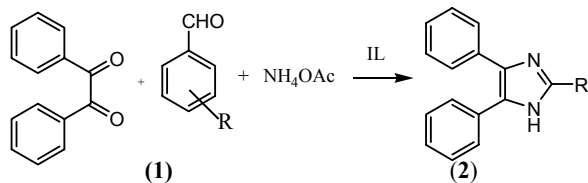
Experimental

All the reagents were purchased from Aldrich/Merck and used without further purification. Melting points were obtained by using Digital melting point apparatus EQ730 (Equiptronics) and are uncorrected. The progress of the reactions and purity of product formation were monitored by thin layer chromatography using hexane/ethyl acetate ((8/2) as eluent. The products were characterized by comparing with authentic samples and spectroscopic data (IR, ¹H NMR). IR spectra were recorded on Shimadzu IR Solution 150SUI spectrophotometer using KBr pellet, values are expressed in cm⁻¹. NMR spectra were recorded on Bruker 400 MHz spectrometer using appropriate solvent and TMS as an internal standard, chemical shift are expressed in ppm. Mass spectra were measured on a Jeol JMSD-300 spectrometer. Viscosity was measured by Buckfield CPe40.

Results and discussion

2,4,5-Trisubstituted-1H-imidazoles (**2a-i**) were synthesized by condensing benzil with various aldehydes (**1a-i**) and ammonium acetate at 100 °C using IL as a catalyst (Scheme 1). The results were reported in Table 1.

The efficiency of IL catalyst has been determined and compared with those of reported acid catalysts in the synthesis of 2-(4-chlorophenyl)-4,5-diphenyl-1H-imidazole (**2d**). The results showed that IL is more efficient as a catalyst in terms of product yields and reaction times (Table 2). All the newly synthesized compounds were characterized by their analytical and spectroscopic data (IR, ¹H NMR) and the known compounds were confirmed by comparing their m. p. with authentic samples.

**Scheme 1.** Synthesis of substituted imidazoles.

Synthesis of a pyrrolidine-2-carboxylic acid sulphate

A mixture of L-proline and conc. sulphuric acid in appropriate amount was stirred for 24 h in a round bottom flask. The viscous liquid obtained was stored in dry container.

Synthesis of 2,4,5-trisubstituted-1H-imidazoles (**4a-i**)

To a mixture of benzil (1 mmol), aromatic aldehyde (1 mmol) and ammonium acetate (3 mmol), IL in catalytic amount (0.1 mmol) was added and stirred at 100 °C for an appropriate time as indicated in table 1. After completion of the reaction, as monitored by TLC, 10 mL of water was added and stirred at room temperature for further 10 min. The separated solid was filtered, washed with excess water, dried and recrystallized from ethanol to afford pure product in good yield.

Spectral studies

L-Pyrrolidine-2-carboxylic acid sulfate catalyst.

Golden yellow colour, b. P. 272 °C. ES-MS *m/z* (%): 231 (M+H). Viscosity: 3.06 CP. IR (KBr): 3510 (OH), 3410(NH), 3005(CH₂), 1514(N-H), 1788(C=O) cm⁻¹. ¹H NMR (CDCl₃): δ = 4.32(1H, m, 8.20 Hz), 3.41-3.17(2H, m, 6.20 Hz), 2.23-2.290 (2H, m, 6.20 Hz), 2.27-2.50 (2H, m, 6.40 Hz, 8.70 Hz), 1.86-1.99(2H, m, 6.40 Hz, 6.20 Hz), 9.31(1H, acidic proton), 8.68(2H, N-H, Proton).

2,4,5-Triphenyl-1H-imidazole (**2a**)

White Solid, m.p. 271-273°C. ES-MS *m/z* (%): 297 (M+H). IR (KBr): 3149 (NH), 1610(C=N), 1537(C=C) cm⁻¹. ¹H NMR (CDCl₃): δ = 7.54 - 8.09 (m, 5H), 7.20-7.51 (m, 10H), 12.17 (s, 1H).

2-(Anthra)-4,5-diphenyl-1H-imidazole (**2i**).

Yellow solid. IR (KBr): 3005 (NH), 1602 (C=N), 1537 (C=C) cm⁻¹. ¹H NMR (CDCl₃): 7.24-7.31 (m, 2H), 7.40-7.43 (m, 4H), 7.54(m, 1H), 8.16 - 8.19 (m, 4H), 7.91-7.93(m, 4H), 12.92 (s, 1H). ES-MS *m/z* (%): 396 (M+H).

Table 2. The effect of catalyst on reaction.

S. No.	Catalyst	Time (min)	Yield (%)
1	No catalyst	600	Traces
2	P-TSA	120	68
3	Sulphamic acid	90	82
4	Sulphanilic acid	70	85
5	IL Catalyst	30	90

Conclusion

In conclusion, we have derived a simple, highly efficient and environmentally friendly protocol for the synthesis of 2,4,5-tri-substituted-1H-imidazoles by one pot three component condensation of benzil, aromatic aldehydes, and ammonium acetate utilizing inexpensive and eco-friendly Bronsted acidic ionic liquid as a catalyst.

Acknowledgements

The authors are thankful to the Principal, Deogiri College, Aurangabad, and Principal of New Arts, Commerce & Science, College, Ahmednagar for constant encouragement and providing necessary facilities. The authors are also thankful to the Director, SAIF, Punjab University, Chandigarh for providing spectral information.

References

- Freedman J., Loscalzo J., *New Therapeutic Agent in Thrombosis and Thrombolysis*, **2009**, 3rd edition, Taylor and Francis.
- Sun, Y. F., Huang, W., Lu, C.G., Cui, Y.P., *Dyes Pigments*, **2009**, *81*, 10–17.
- Pozharskii A. F., Soldalakov A. T., Katritzky A. R., In *Heterocycles in Life Society*, **1997**, vol. 179. Wiley, New York.
- Horton D. A., Bourne G. T., Sinythe M. L., *Chem. Rev.*, **2003**, *103*, 893–930.
- Reddy M. V., Jeong Y. T., *J. Fluorine Chem.* **2012**, *142*, 45–51.
- Saikat D. S., Parasa H., Dilip, K., *Tetrahedron Lett.*, **2008**, *49*, 2216–2220.
- Sadeghi B., Mirjalili B. B. F., Hashemi M. M., *Tetrahedron Lett.*, **2008**, *49*, 2575–2577.
- Khosropour A. R., *Ultrason. Sonochem.*, **2008**, *15*, 659–664.
- Mazaahir K., Poonam M., Vikas B., Rishi K. S., Abdul S. E., *J. Mol. Catal. A: Chem.*, **2007**, *265*, 177–182.
- Chary M. V., Keerthysri N. C., Srinivasu V. N. V., Lingaiah N., Srinivas K., *Catal. Commun.*, **2008**, *9*, 2013–2017.
- Rajanarendar E., Murthy K. R., Nagi Reddy M., *Indian J. Chem.*, **2011**, *50B*, 926–930.
- Murthy S. N., Madhav B., Nageswar Y. V. D., *Tetrahedron Lett.*, **2010**, *51*, 5252–5257.
- Wang L. M., Wang Y. H., Tian H., Yao Y. F., Shao J. H., Liu B., *J. Fluorine Chem.*, **2006**, *127*, 1570–1573.
- Subhasis S., Ganesh C. N., Pallavi S., Singh M. S., *Tetrahedron*, **2009**, *65*, 10155–10161.
- Sharma R. K., Sharma C., *Catal. Commun.*, **2011**, *12*, 327–331.
- Mohammad M. K., Kiumars B., Iman, K., *J. Chin. Chem. Soc.*, **2007**, *54*, 829–833.
- Ali R. K., Zahra A., Mostafa M. A., *Mol. Divers.*, **2012**, *14*, 635–641.
- Mahdavinia G. H., Amani A. M., Sepehrian H., *Chin. J. Chem.*, **2012**, *30*, 703–708.
- Shelke K. F., Sapkal S. B., Kakade G. K., Shingate B. B., Shingare M. S., *Green Chem. Lett. Rev.*, **2010**, *3*, 27–32.
- Shelke K. F., Sapkal S. B., Sonar S. S., Madje B. R., Shingate B. B., Shingare M. S., *Bull. Korean Chem. Soc.*, **2009**, *30*, 1057–1060.²¹ Niralwad K. S., Shingate B. B. and Shingare M. S., *J.Heterocycl. Chem.*, **2011**, *48*, 742–745.
- Zang H., Su Q., Mo Y., Cheng B. W., Jun, S., *Ultrason. Sonochem.*, **2010**, *17*, 749–751.
- Deng X., Zhou Z., Zhang A., Xie G., *Res. Chem. Intermed.*, **2013**, *39*, 1101–1108.
- Xia M., Lu Y.D., *J. Mol. Catal. A: Chem.*, **2007**, *265*, 205–208.
- Majid M.H., Masoumeh Z., Narges K., Mina S., Hossien A.O., Niloofar T.H., *Synth. Commun.*, **2010**, *40*, 1998–2006.
- Dake S. A., Khedkar M. B., Iramale G. S., Ukkalgaonkar S. J., Thorat V. V., Bhosale D. S., and Pawar R. P., *Synth. Commun.*, **2012**, *42*, 1509–1520.
- Nalage S. V., Kalyankar M. B., Patil V. S., Bhosale S. V., Deshmukh S. U. and Pawar R. P., *The Open Catal. J.*, **2010**, *3*, 58–61.
- Parveen A., Ahmed M. R., Shaikh K. A., Deshmukh S. P. and Pawar R. P., *Arkivoc*, **2007**, *16*, 12–18.

Received: 18.07.2016.

Accepted: 02.09.2016..



SCREENING THE FORMATION OF THE POLYCYCLIC AROMATIC HYDROCARBONS DURING COMBUSTION OF COMMON DOMESTIC FUELS

Mpho Sekese^[a], Bokang Rakolobe^[a], Pulane Ts'ooanyane^[a], Lebohang Mosenene^[a] and Mosotho J. George^{[a]*}

Keywords: Biomass fuel, cake dung, incomplete burning, polycyclic aromatic hydrocarbons, pyrolysis.

The use of biomass and other solid material as a source of energy is associated with some deleterious effects consequent to incomplete combustion associated with poor ventilation leading to production of a number of chemical compounds that are known or suspected to be a health threat. This study reports the screening of the formation of the polycyclic hydrocarbons during pyrolysis of the fuel materials, namely, coal, dung and wood, commonly used as fuel in rural areas in Lesotho, under poor aeration using a simple in-house pyrolysis unit. The method demonstrated sufficient linearity for the standards with correlation coefficient, $R^2 \geq 0.9884$ and repeatability (%RSD ≤ 15 %) of the real samples used, coal demonstrated production of naphthalene and pyrene, while from the cake dung formation of naphthalene was detected. Despite not being extensive, the results form a basis for a more rigorous study including employing more identification tools, such as mass spectrometry that enables identification and a better detection of low levels of the analytes.

* Corresponding Authors

Tel.: +266 5221 3502

Fax: +266 2234 0000

E-mail: jm.george@nul.ls or maluti2005@gmail.com

[a] Department of Chemistry and Chemical Technology,
National University of Lesotho, P.O. Roma 180, Lesotho,
Southern Africa.

INTRODUCTION

Solid biomass fuel is one of earliest energy sources since the medieval times, and it is still the most easily accessible and affordable source of energy particularly in rural areas.^{1,2} Literally any combustible material can be used as fuel to produce heat or power. However these sources of energy are not devoid of setbacks such as producing some hazardous chemical compounds associated with the fumes they produce during combustion especially in poorly ventilated rooms,³ as well as reducing the amount that is recycled back into agricultural practices as manure.⁴ Solid fuels typically are difficult to burn in simple combustion devices such as household cooking and heating stoves without substantial emissions of hazardous chemicals, principally because of the difficulty of completely pre-mixing the fuel and air during burning, which is done easily with liquid and gaseous fuels.

Consequently, a substantial fraction of the fuel carbon is converted to by-products of incomplete combustion, namely, fine particulates which are reportedly highly oxidising² and other obnoxious gases containing principally carbon monoxide, carbon dioxide and polycyclic aromatic hydrocarbons (PAHs).⁵ Of these chemicals carbon monoxide is the most dangerous as it can cause fatality within minutes if inhaled, consequently, highly sensitive detectors have been developed for detection and monitoring of carbon monoxide in places that are likely to produce them. On the other hand, PAHs, a series of six-membered ring compounds, are suspected to be carcinogenic⁶ and/or to have some endocrine activity.⁷

The major source of indoor air pollution in rural areas around the world is the burning of traditional biomass fuel such as wood, dung and agricultural wastes.⁸ Due to their poor aeration solid fuels are characterized by incomplete combustion. A study reported that household coal and biomass cooking stoves in China (similar to those in households of developing countries) diverted between 10% and 38 % of their fuel carbon into by-products of incomplete combustion.⁹ Due to this incomplete combustion, solid fuels are associated with respiratory ailments. Another study in India on 897 women, 615 of whom used biomass exclusively, demonstrated a correlation of the effect of biomass burning to prevalence of respiratory ailments, 71 % of these women presented respiratory symptoms as opposed to only 28 % of the 282 who used LPG gas exclusively.

These ailments included chest tightness or chest discomfort (43.3 % vs. 7.3 %), sore throat, cough, recurring headache, eye irritation, eye watering, dizziness, muscle pain, tingling and numbness in the extremities. Like the adults, children from biomass using families had 2-times more respiratory symptoms than age- and sex-matched children from LPG gas using families (70.3 vs. 35.9 %). The prevalence of respiratory symptoms both in adults and children was positively correlated with particulate pollutant level in indoor air.¹⁰

A different study showed that chronic exposures to biomass smoke were associated with impaired lung function. Lung function decrement was most prevalent in women who cook predominantly with dung cake and in kitchen adjacent to living areas.¹¹ Reduction of lung function was positively associated with years of exposure to biomass smoke and low socio-economic status.¹² Women who used to cook with biomass fuels had greater prevalence of metaplasia and dysplasia of airway epithelial cells, which are recognized as early cellular changes towards development of cancer, several-fold rise in micronucleus frequency in buccal and airway epithelial cells that suggest chromosomal damage in these cells.

Taken together, these findings indicate greater risk of cancer in the lungs and the airways in rural women who are inhaling smoke from burning biomass during daily household cooking. According to Zhang and Smith,⁹ global meta-analyses of epidemiologic studies indicate that indoor air pollution from solid fuel use in many developing countries is responsible for approximately 420,000 premature deaths annually, more than the approximately 300,000 attributed to urban outdoor air pollution in cities with populations of more than 100,000.¹³ Household use of solid fuels is thus estimated to be the largest single environmental risk factor and ranks sixth among all risk factors examined for ill-health.

As a typical least developed country, Lesotho, a small mountainous country wholly landlocked within South Africa still relies heavily on burning of biomass for provision of energy for domestic purposes with about 67 % usage.¹⁴ Although, there is considerable urbanisation, about 85 % of Lesotho's population of about 2.2 million, still reside in rural areas,¹⁵ while also a considerable fraction of poor urban residents still rely almost exclusively to the use solid fuels (biomass and coal) for household cooking and/or heating. Among the most widely used solid fuel in Lesotho are wood (70 %), animal dung in all its forms (25 %) and the remaining 5 % ascribed to crops residues as well as any other combustible materials,¹⁴ with coal being accessible to middle class, usually for heating rather than cooking. Of the used solid materials used for fuel, coal is the widely studied and well-documented fuel globally in terms of its benefit and disadvantages while the other materials are not as widely studied.

Usually dung is used in two forms after natural air and sun drying, normal droppings and the cake dung (compacted dung) which is usually dug in the kraals after a number of years of using that kraal to secure the animals. Due to its compactness, cake dung hardly burns into a flame. It is however preferred as it is believed to provide more heat per unit volume as compared to wood and normal dropping. Despite this benefit, cake dung is associated with obnoxious smell and produces a lot of smoke leading to soot formation on the roof and the top part of the walls of the room in which it is burned. This is possibly due to the lower porosity than the other form (normal dropping). Consequently, it is believed that this cake dung should be liable to producing more PAHs as well as other xenobiotic compounds than the other solid materials used as fuel.

PAHs are usually analysed using chromatographic techniques coupled to different detectors depending on their concentration levels.^{16,17} Being such conjugated systems PAHs have relatively high molar absorptivity as such they can easily be detected using either molecular absorption or fluorescence spectrophotometry.¹⁸ However, this still requires some sample preparation and extraction of these compounds from the matrices they are occurring in. Some of the extraction and sample preparation methods employed include the purge and trap,¹⁹ solid- and liquid-based with the solid-based techniques the most preferred for gaseous samples.²⁰ In this study we describe an application of a simple in-house built pyrolysis unit coupled to hollow-fibre supported liquid-liquid micro-extraction and gas chromatography for screening of production of PAHs during

pyrolysis of some solid materials like coal, wood, cow dung (both normal droppings and cake dung), which are commonly used as fuel source in Lesotho.

EXPERIMENTAL

All the chemicals were of analytical grade and obtained from Merck South Africa. Toluene, xylene and dodecane were used as extracting solvents, while trichlorobenzene was used as internal standard for the real samples, the choice of which was based on the lack of possibility of neither being present nor produced during pyrolysis of these materials. Different PAHs, namely, naphthalene and pyrene were used as standards for the extraction. A sample of activated charcoal was used as reference virgin sample on which the preliminary experiments were carried out. A coal sample was obtained from a local coal supplier while the cow dung samples - dry dropping sample and the compacted cake dung were collected from one small-holder farmer in a village just outside the NUL – Roma campus. All the solid samples were ground to a fine powder and were weighed appropriately before the sampling.

Apparatus

Samples were collected in a cock-stoppered Schlenk® tube leaving only the side-arm open to release the pyrolysis gases. A gas tight 100 μ L Hamilton® syringe was fitted with a 1 cm long hollow-fibre membrane (HFM) filled with sufficient organic solvent. The extracts were analysed using a Saturn 3800 gas chromatograph (Varian, USA) fitted with a 30 m x 0.53 mm x 0.25 μ m SGE-BP5 (5 % phenyl-95 % dimethyl-polysiloxane) fused glass capillary column (Texas, USA) connected to the flame ionisation detector. Grade 5.0 nitrogen was used as a carrier gas at a constant flow rate of 5 mL min⁻¹. The temperature program started with the 80 °C held 3 min, followed by 10 °C min⁻¹ ramping to 300 °C and held for 3 min. The split-splitless injection port was kept on split at the ratio of 1:10 and set at 250 °C while the detector temperature was also set at 250 °C.

Preparation of the solid samples and the sampling procedure

About 100 g of a fine activated charcoal powder was heated in the oven at a temperature of 250 °C for 30 minutes to get rid of any organic compounds that it may have adsorbed. This activated charcoal sample was spiked with a mixture of naphthalene and pyrene and mixed thoroughly to obtain a surrogate sample with the composition of about 0.1 g the PAH in 100 g of activated charcoal. Working samples were prepared from this surrogate and were used in portions of about 1 g in all the experiment except where the variation of mass was necessary, in which case the actual mass will be stated.

To test whether the experiment could succeed, about 1 g of the surrogate sample was poured gently (to reduce the amount of sample attaching on the walls) into the Schlenk tube mounted on the retort stand. Thereafter, an organic solvent-filled hollow fibre membrane was introduced through the syringe into the pyrolysis unit through the side-arm to about 1.5 cm deep so that it gets into contact with the

plum of gases from the sample as it is heated/pyrolysed. Thereafter a flame was introduced using the Bunsen burner to heat the test tube gently. After the sampling time has elapsed, the extract (2 μL of the remaining sampling organic solvent) was injected into the gas chromatograph for analysis repeated in triplicates for determination of repeatability. The pyrolysis assembly can be visualised in Supplementary material (Figure S1).

Following the success thereof, different parameters were tried for experiment to optimise the extraction of the spiked PAHs virgin charcoal samples. Only a few parameters were studied following a univariate approach, namely, the choice of solvent for the HF-LPME, effect of distance of the flame from the test tube base, the effect of varying sample size (linearity) and repeatability. Following the optimisation, the charcoal samples were replaced by the real fuel samples, coal, wood, normal and compacted (cake) dung respectively. Trichlorobenzene was spiked into the extracting solvent as an internal standard at a concentration of $0.01 \text{ g } 100 \text{ g}^{-1}$ which was later reduced accordingly so that the responses were in the same order of magnitude as the analytes from the real samples.

RESULTS AND DISCUSSIONS

Demonstration of the assembly and proof of concept

A home-made pyrolysis and sampling unit using a Schlenk tube, a Bunsen burner and a Hamilton® syringe fitted a hollow fibre membrane containing an organic solvent was used. Since the membrane gets colourless when it is impregnated with the solvent, sampling was stopped at the first sight of white colouration appearing at the tip as the solvents start to evaporate due to the hot gas coming from the heated sample.

The experiment initially suffered a lot of inconsistencies as a few times, the extracting solvent evaporated to dryness before the importance of controlled the heating rate was noted. Different trials were made moving the flame back and forth until a perfect distance was achieved both by height of the test tube relative to the flame and the distance from the flame. These were, however, not measured accurately except that the test tube should about 5 cm from the end of the visible part of the flame to ensure slow heating. A summary of the chromatographic information is summarised in Table 1. The method was further refined for the choice of solvent used for extraction, variation of sample size and composition the results of which are presented in the following sections of this report.

Effect of solvent choice on the extraction efficiency

Only three solvents with sufficient purity and high boiling temperatures were available as such solvent choice was limited to these three. Figure 1 shows the effect of different solvents on the extraction efficiency of the analytes from the spiked charcoal sample.

As can be seen, dodecane demonstrated better extraction efficiency although this was coupled with a limitation that dodecane and naphthalene were significantly overlapping leading to sometimes difficulty in integrating the naphthalene peak. On the other hand, xylene was a bit old and contaminated, consequently toluene was chosen as a best solvent. The efficiency with dodecane could be attributable to a relatively higher boiling point, hence lower volatility than the other two solvents, as such it would sample for a slightly longer period than toluene.

Investigation of the effect of varying sample size on the amount of PAHs recovered

To assess the effect of the sample size, different amounts of the charcoal sample were introduced and treated as explained. The results presented in Figure 2 demonstrated an expected increase with the increase in sample size although as the sample mass increases, there is a slight drop in extraction efficiency with an compromised precision as evidenced by an increased standard deviation denoted by the error bars. However, it seems that the extraction reaches a somewhat saturation beyond 1.5 g. This could be due to the uneven distribution of heat throughout the sample leading to different times of the analytes pyrolysis from the matrix, hence the increased variation between the analytes. Moreover, as the extracting solvent kept evaporating from the hot fumes, it could be that as the late analytes pyrolysed, the solvent was already too limited in the membrane to efficiently extract it.

Effect of varying the concentration of the analytes in the charcoal sample

To investigate the effect of varying initial concentration of the analytes in sample, the pre-spiked 'stock' sample was diluted by mixing it different amounts of the virgin charcoal sample to obtain different concentrations/compositions. Table 1 depicts the effect of varying the initial concentration on the extraction efficiency.

Table 1. Some analytical calibration data obtained using the variation of analyte composition

Parameter	Naphthalene	Pyrene
Retention time	11.583	16.002
Repeatability (% RSD)	11.3	13.9
Regression eqn.	$y = 7147x + 97$	$y = 10085x + 104$
Linearity, R^2	0.9986	0.9884
Calibration error	57	63
Error of the intercept	29	47
Est. LOD* ($\text{mg } 100 \text{ g}^{-1}$)	0.016	0.014
Est. LOD ($\mu\text{g } \text{g}^{-1}$)	0.16	0.14

*Estimated LOD calculated using equation $\text{LOD} = 3\sigma/m$ where σ represents the standard error and m represents the slope of the calibration data from varying the analyte composition.

Clearly this approach yields similar trend to the one using different mass of sample except that the linearity is more improved ($R^2 \geq 0.9884$ from 0.9132).

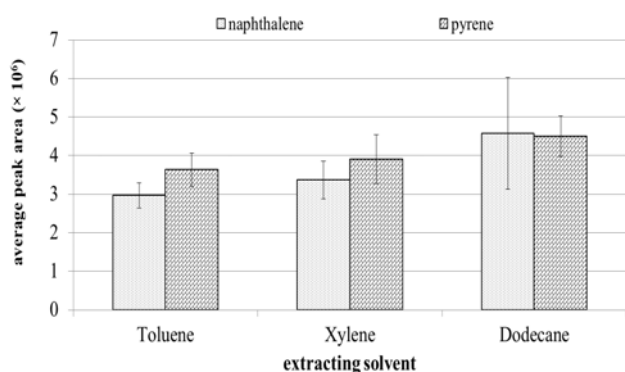


Figure 1. The effect of different organic solvents on extraction efficiency.

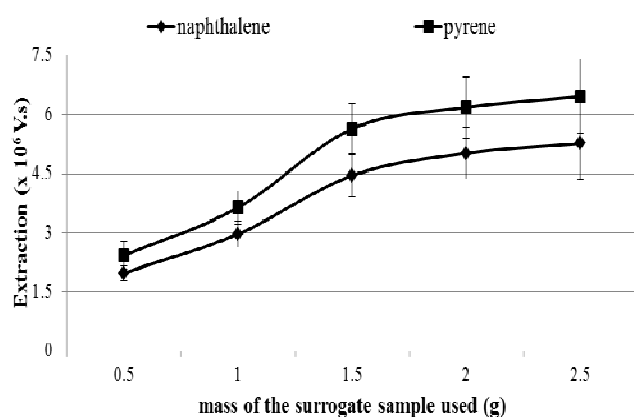


Figure 2. The effect of increasing the sample size on the recovery of the analytes.

This is possibly due to uneven distribution of heat as the sample increases, while in the latter approach, there is always the same sample mass, hence the problem of non-uniform heat distribution is minimised.

Due to the inevitable analytes loss with the fumes through the side-arm opening, the method demonstrated relatively high limits of detection (0.14 and $0.16 \mu\text{g g}^{-1}$ of sample). However, these are gratifying considering the method is yet to be fully validated. Moreover, these can be improved by using an online pyrolysis, which is not a very common instrument in resource-constrained laboratories.

Analysis of real samples

To determine the amount and presence of the PAHs in the real samples, an external standard calibration approach with 1-g samples was used whereby the intensities of the signals were read off and corresponding concentrations for the 1 g real samples calculated from the regression equations in Table 2. As can be seen from Table 2, no analyte was detectable in the normal dropping but naphthalene was detectable in both the coal and compacted dung samples. The considerably high % RSD could be attributable to poor validation of the method, which will be improved in the next

phase of the experiment as well as the fact that the amounts of the detectable analytes are at the same level as the limits of detection.

The normal droppings did not show any detectable levels of the PAHs, possibly due to the fact that droppings are highly porous which enables effective aeration during combustion, hence burning of droppings was more complete than that of the compacted dung.

Table 2. Determination of the production of the PAHs from the different fuel samples.

Sample	Amount of analyte in the sample*	
	Naphthalene	Pyrene
Coal	8.31 (11 [#])	0.67 (14 [#])
Wood	n.d.	n.d.
Cow dung dropping	n.d.	n.d.
Cake cow dung	0.78 (18)	n.d.

* $\mu\text{g g}^{-1}$ of sample; [#] % RSD for $n = 3$

Besides naphthalene, the coal sample demonstrated a production of some compounds with retention times between 12 and 14 minutes. These could be lower order PAHs such as anthracene and phenanthrene (3-membered ring) since pyrene is a 4-membered ring structure. There was another dominant peak whose peak area was about 20 times that of pyrene at the retention time of 6.988 minutes. Unfortunately this peak could not be attributed to any PAHs since the lowest in the PAHs family and hence the most volatile is naphthalene with the retention time of 11.583 minutes. However, since there were no standards against which to compare with, these compounds were not identified nor quantified.

CONCLUSION

The presence of naphthalene in the compacted sample confirms what the researchers had apprehended i.e., the potential production of PAHs during burning these materials in poorly ventilated areas. Although the levels are low, this is still a concern given that the materials are usually burnt in poorly ventilated rooms sometimes with no windows thus exposing the occupants to these compounds. Although this is only at the preliminary level, the results are gratifying since they can point towards the need of further research in the safe use of these materials, since not all households can afford the other fuel materials. Unfortunately, no similar work is available for comparison.

However, it can be concluded that the in-house constructed technique can be usable for the detection of the PAHs, with the only limitation being the detection limit of the detector used. Only one PAH – naphthalene was detected and tentatively identified in coal ($8.31 \mu\text{g g}^{-1} = 0.831 \text{ mg } 100 \text{ g}^{-1}$) and compacted cake dung ($0.78 \mu\text{g g}^{-1} = 0.078 \text{ mg } 100 \text{ g}^{-1}$) of sample. The method demonstrated sufficient linearity ($R^2 \geq 0.9884$) and a relatively low repeatability with an average standard deviation between 11 and 18 %. Since Lesotho cannot afford to electrify every household and neither can every household afford the

electricity as a sole domestic fuel source it is recommended that introduction of overhead chimneys or chulhas should be considered for proper ventilation for kitchens.

REFERENCES

- ¹Balakrishnan, K., Sankar, S., Parikh, J., Padmavathi, R., Srividya, K., Venugopal, V., Prasad, S., Pandey, V. L., *Environ. Health Perspect.*, **2002**, *110*(11), 1069.
- ²Barnes, D. F., Openshaw, K., Smith, K. R., van der Plas, R. *World Bank Techn. Paper 242*, World Bank, **1994**, 1.
- ³Mudway, I. S., Duggan, S. T., Venkataraman, C., Habib, G., Kelly, F.J., Grigg, J. *Part. Fibre Toxicol.*, **2005**, *2*(1), 6.
- ⁴Pant, K. P. *A Report to the South Asia Network of Economic Res. Inst.*, **2010**, 1.
- ⁵Raiyani C. V., Jani J. P., Desai, N. M., Shah, S. H., Shah, P. G., Kashyap, S. K. *Bull. Environ. Contam. Toxicol.*, **1993**, *50*(5), 757.
- ⁶Mastrangelo, G., Fadda, E., Marzia, V. *Environ. Health Perspect.* **1996**, *104*(11), 1166.
- ⁷Kummer. V., Mašková, J., Zralý, Z., Neča, J., Šimečková, P., Vondráček J., Machala, M. *Toxicol. Lett.*, **2008**, *180*(3), 212.
- ⁸Nigel. B., Perez-Padilla. R., Albalak, R. *Bull. World Health Organ.*, **2000**, *78* (9), 1078.
- ⁹Zhang, J., Smith, K. R. *Environ. Health Perspect.*, **2007**, *115*(6), 848.
- ¹⁰Albalak, R., Frisancho, A. R., Keeler, G. J. *Thorax*, **1999**, *54*(11), 1004.
- ¹¹Ki-Hyun. K., Jahan. S. A., Kabir, E. *J. Hazard. Mater.*, **2011**, *192*(2), 425.
- ¹²Anderson. H. R. A Chapter in *The Rising Trends in Asthma*, Wiley, Chichester, **1997**, *206*, 190.
- ¹³Cohen, A. J., Anderson, H. R., Ostro, B., Pandey, K. D., Krzyzanowski, M., Künzli, N., Gutschmidt, K., Pope III, C. A., Romieu, I., Samet, J. M., Smith, K. R., *Comp. Quantif. Health Risks*, **2004**, *2*, 1353.
- ¹⁴Tsehlo, T. B. *A Report to the United Nations Commission on Africa (UNECA)*, United Nations, Washington DC, USA, 2012.
- ¹⁵*United Nations Development Programme Lesotho*, **2006**, pp1-72. Maseru, Lesotho. Retrieved on 21 May 2016 from http://www.undp.org/content/dam/undp/documents/projects/LSO/00042547_LREBRE_00049143_Prodoc.pdf.
- ¹⁶Poster. D. L., Schantz. M. M., Sander, L. C., Wise, S. A. *Anal. Bioanal. Chem.*, **2006**, *386*(4), 859.
- ¹⁷Pandey. S. K., Kim. K. H., Brown, R. J. *Trends Anal. Chem.*, **2011**, *30*(11), 1716.
- ¹⁸Ghasemi, J. B., Zolfonoun, E. *Environ. Monit. Assess.*, **2013**, *185*(3), 2297.
- ¹⁹Wang, M., Zhang, S., Zhang, X., Zhang, J. *Anal. Lett.*, **2013**, *46*(12), 1951.
- ²⁰Hüffer, T., Osorio, X. L., Jochmann, M. A., Schilling, B., Schmidt, T. C. *Anal. Bioanal. Chem.*, **2013**, *405*(26), 8387.

Received: 07.07.2016.

Accepted: 05.09.2016.



COMPARATIVE ASSESSMENT OF THE BIOCHEMICAL COMPOSITION OF FRUIT OF THE *OXYCOCCUS* *MACROCARPUS* (AIT.) PERS. CULTIVARS INTRODUCED IN BELARUS

Zhanna Rupasova^{[a]*}, Nikolay Pavlovsky^[a], Tamara Vasilevskaya^[a], Natalia Krinitskaya^[a], Elizaweta Tishkovskaya^[a], Vladimir Titok^[a], Vladimir Reshetnikov^[a] and Yulia Pinchukova^[b]

Keywords: *Oxycoccus macrocarpus*, cranberry, cultivar, fruit, biochemical composition, organic acids, carbohydrates, bioflavonoids.

The article describes the findings of a comparative study of the sugar-acid index, content of free organic, ascorbic, and hydroxycinnamic acids, dry, tanning, and pectic substances, soluble sugars, and the main groups of bioflavonoids in fruit of six newly introduced *Oxycoccus macrocarpus* (Ait.) Pers. cultivars in Belarus — Stevens (st), Bain Favorite, Holliston, Hollister Red, Stankovich, and WSU 108. It is established that the *Hollister Red* cultivar has the highest integrated level of nutritive and vitamin value of fruit based upon the combination of properties analyzed, from 1.8 to 11 times the level observed in the other cultivars, whereas the *WSU 108* and especially the *Bain Favorite* cultivars have the lowest levels.

* Corresponding Authors

E-Mail: J.Rupasova@cbg.org.by

[a] Central Botanical Garden of the National Academy of Sciences of Belarus, 2v, Surganova Str., 220012, Minsk, Republic of Belarus

[b] Belarus State Economic University, 26, Partizanski Av., 220070, Minsk, Republic of Belarus

Gantsevichy District of the Brest Region, in the central agro-climatic region of the country with light sandy sodpodzolic soils and dried high peatbogs.

Weather conditions in the area were characterized by higher-than-normal temperature settings and relatively favorable precipitation pattern throughout the season.

Six cultivars of the *Oxycoccus macrocarpus* variety had been selected as objects of the study: Stevens(st), Bain Favorite, Holliston, Hollister Red, Stankovich, and WSU 108.

The comparative assessment of the biochemical composition of their fruit was conducted based upon a broad range of indicators associated with various classes of active substances. Fresh averaged samples of ripe fruit were used to determine the content of (i) dry matter in accordance with GOST (State Standard) 28561-90,¹⁵ (ii) ascorbic acid (Vitamin C) by the standard indophenol method,¹⁶ and (iii) titratable acids (total acidity) by the volumetric method.¹⁶ Samples of plant materials dried at a temperature of 60 °C were used to determine the content of hydroxycinnamic acids (in terms of chlorogenic acid) by the spectrophotometric method,¹⁷ soluble sugars by the accelerated semi-micro method,¹⁸ pectic substances by the calcium pectate method,¹⁶ the amount of anthocyanin pigments according to Swain and Hillis¹⁹ with a calibration curve made based upon crystalline cyanidin derived from black chokeberry fruit and purified according to Skorikova and Shaftan,²⁰ true anthocyanins and the amount of catechins (with the use of the vanillin reagent) by the photolorimetric method,^{16,21} the amount of flavonols (in terms of rutin) by the spectrophotometric method¹⁶ and tannins by Leventhal's titrimetric method.²² All analytical determinations were made with a three-time biological repeatability. The data were statistically processed using the Excel software programme. The data showed statistically significant differences from the reference (standard) cultivar Student's *t*-test at $p < 0.05$.

Introduction

Data on the biochemical composition of fruit of American/large cranberry (*Oxycoccus macrocarpus* (Ait.) Pers.) are currently widely available in international academic literature.¹⁻⁷ The 45 years' worth of studies of introduced varieties carried out by the Central Botanical Garden of the National Academy of Sciences of Belarus resulted in a significant amount of scientific data on the issue, including several major monographs.⁸⁻¹⁴

Over the past few years, new varieties of large cranberry have been added to the Botanical Garden's extensive collection. With a view to identifying the most promising cultivars for regional assignment and selection, a comparative monitoring study was conducted for these cultivars for the first time to determine the content of the most physiologically valuable compounds, based upon an integrated assessment of not only breeding and bioproductive parameters, but also nutritive and vitamin value of fruit. The study made it possible to identify the new cultivars of the introduced variety with the highest level of nutritive and vitamin value of fruit.

Experimental

Research was carried out in 2015–2016 at the Experimental Station of the Central Botanical Garden of the National Academy of Sciences of Belarus located in the

Table 1. Content of dry substances and organic acids (in dry matter) in fruit of introduced *Oxycoccus macrocarpus* cultivars.

Cultivar	Dry substances, %		Organic acids					
			titratable, %		ascorbic, mg %		hydroxycinnamic, mg %	
	$\bar{x} \pm m_x$	t_{St}	$\bar{x} \pm m_x$	t_{St}	$\bar{x} \pm m_x$	t_{St}	$\bar{x} \pm m_x$	t_{St}
<i>Stevens(st)</i>	14.0±0.2		22.5±0.1		370.5±6.9		651.0±12.2	
<i>Bain Favorite</i>	12.7±0.3	-4.0	24.4±0.1	34.9	476.2±3.9	13.3	589.0±14.1	-3.3
<i>Holliston</i>	15.7±0.1	9.2	17.2±0.1	-76.6	345.5±6.3	-2.8	667.2±13.9	0.9
<i>Hollister Red</i>	13.3±0.1	-4.0	22.4±0.1	-0.3	426.1±4.8	6.6	710.8±25.5	2.8
<i>Stankovich</i>	12.0±0.1	-9.5	25.2±0.1	46.3	568.2±2.8	26.6	549.8±14.0	-5.4
<i>WSU 108</i>	13.0±0.1	-5.8	25.3±0.1	35.9	445.1±2.5	10.2	563.7±13.9	-4.7

The identification of large cranberry cultivars with the highest integrated level of nutritive and vitamin value of fruit based upon the combination of analyzed properties was performed on the basis of the patented plant ranging method.²³

Results and discussion

The late-ripening *Stevens* cultivar previously released in Belarus as the standard was adopted as the benchmark for the biochemical screenings of the new cultivars of the *Oxycoccus macrocarpus* variety.

According to our findings (Table 1), the content of dry matter in the fruit of the cultivars of large cranberry in question varied from 12.0 % and 15.7 %. The content of free organic acids in their dry matter was within the range of 17.2 to 25.3 %, of ascorbic acid from 345.5 mg % to 568.2 mg %, of hydroxycinnamic acids from 549.8 mg % to 710.8 mg %, which was commensurable with the findings of our earlier studies of other cultivars of this *Ericaceae* variety.

Table 2. Content of soluble sugars and pectic substances in the dry matter of fruit of introduced *Oxycoccus macrocarpus* cultivars

Cultivar	Soluble sugars		Sugar-acid index		Pectic substances	
	$\bar{x} \pm m_x$	t_{St}	x^*	t_{St}	x^*	t_{St}
<i>Stevens (st)</i>	26.5±0.1		1.21		10.0	
<i>Bain Favorite</i>	26.5±0.1	0	1.1	-7.6	9.4	-5.2
<i>Holliston</i>	29.7±0.3	9.5	1.71	26.7	8.1	-14.0
<i>Hollister Red</i>	29.3±0.3	8.5	1.3	6.9	7.6	-20.8
<i>Stankovich</i>	31.5±0.5	10.0	1.3	3.4	5.2	-39.7
<i>WSU 108</i>	28.5±0.5	4.0	1.1	-3.2	6.8	-27.7

* $St = \pm m_x$

The total content of soluble sugars in the fruit of the cranberry cultivars under study varied within a comparatively narrow range of very low values of 26.5 to 31.5 % of dry matter (Table 2). Because of the high content of titratable acids indicated above, they were characterized by extremely low sugar-acid index indicators that remained within 1.1 to 1.7, which attested to their extremely sour taste.

At the same time, cranberry fruit was characterized by the relatively high parameters, comparable to those that we have determined for highbush blueberry and *Vaccinium vitis-idaea* (lingonberry, cowberry)¹³, of the accumulation of pectic substances that varied within the range of cultivars from 5.2 % to 10.0 % of dry matter (Table 2).

As is known, *Oxycoccus macrocarpus* fruit is extremely rich in bioflavonoids that have a marked P-vitamin effect.²⁴ According to our findings (Table 3), their total amount in the dry substance of the fruit of the cultivars under analysis varied within the range from 7461.0 to 11032.2 mg 100 g⁻¹. Anthocyanin pigments dominated in the bioflavonoid complex, as in all representatives of the *Ericaceae*, with total content varying from 5581.3 to 8463.0 mg 100 g⁻¹ and accounted for 74-77 % of the total. Leucoanthocyanins were the prevailing fraction in these compounds, as in the *Vaccinium*,²⁵ with content in the fruit of the cultivars under analysis between 3878.0 and 5908.0 mg /100 g⁻¹, 2.3-3.2 times the content of true anthocyanins (at 1,703.3 to 2,555.0 mg 100 g⁻¹), and the gap was the smallest in the *Bain Favorite*, *Hollister Red*, and *WSU 108* cultivars and the biggest in *Holliston*.

Catechin content in dry matter of large cranberry fruit varied between 1016.2 and 1827.6 mg 100 g⁻¹, with fluctuations of contributions of these restored compounds to the composition of the bioflavonoid complex within a range from 13 % in *WSU 108* to 18 % in *Stankovich*. Flavonols were characterized by the lowest contribution to the P-vitamin complex of cranberry fruit, varying from 7 % in *Hollister Red* to 12 % in *Bain Favorite* within the taxonomic range, with content between 771.8 and 1092.8 mg /100 g⁻¹. The content of tannins in cranberry fruit was quite high, at 2.62-3.37 % of the dry mass (Table 3).

The cultivars of large cranberry under analysis showed distinct differences from the benchmark *Stevens* cultivar when it came to the biochemical composition of fruit (Table 4). The *Bain Favorite*, *Stankovich*, and *WSU 108* cultivars showed the highest content of titratable acids, which exceeded the benchmark by 8 to 12 %. At the same time, *Hollister Red* was characterized by the accumulation of free organic acids comparable to that in *Stevens*, whereas in *Holliston*, their content was 24 % lower than in the benchmark. The fruit of all of the tested cultivars (except *Holliston*) proved to have a higher-than-benchmark content of ascorbic acid, by 15-53 %, whereas *Stankovich* showed little difference.

Table 3. Content of phenol compounds in the dry matter of fruit of introduced *Oxycoccus macrocarpus* cultivars.

Cultivar	Bioflavonoids, mg 100 g ⁻¹							
	True anthocyanins		Leucoanthocyanins		Amount of anthocyanin		Catechins	
	$\bar{x} \pm m_x$	t_{St}	$\bar{x} \pm m_x$	t_{St}	$\bar{x} \pm m_x$	t_{St}	$\bar{x} \pm m_x$	t_{St}
<i>Stevens(st)</i>	2041.7±42.1		5268.7±122.2		7310.3±80.3		1524.3±13.1	
<i>Bain Favorite</i>	1703.3±11.7	-7.8	3878.0±71.8	-9.8	5581.3±80.3	-15.2	1016.2±15.2	-25.3
<i>Holliston</i>	1761.7±30.9	-5.4	5609.3±69.1	2.8	7371.0±52.5	0.6	1456.0±52.5	-1.3
<i>Hollister Red</i>	2555.0±20.2	11.0	5908.0±32.3	5.1	8463.0±52.5	12.0	1774.5±26.3	8.5
<i>Stankovich</i>	1948.3±5.8	-2.2	5559.2±31.5	2.8	7507.5±26.3	2.8	1827.6±20.1	12.6
<i>WSU 108</i>	2070.8±35.5	0.5	4921.0±11.3	-2.8	6991.8±40.1	-3.5	1243.7±54.7	-5.0

Cultivar	Bioflavonoids, mg/100 g						Tannins,%	
	Flavonols		Flavonols / Catechins		Amount		$\bar{x} \pm m_x$	t_{St}
	$\bar{x} \pm m_x$	t_{St}	$\bar{x} \pm m_x$	t_{St}	$\bar{x} \pm m_x$	t_{St}		
<i>Stevens(st)</i>	1092.8±33.3		0.7±0.03		9927.3±103.8	59.9	3.12±0.02	
<i>Bain Favorite</i>	863.5±33.3	-4.9	0.9±0.03	3.0	7461.0±45.9	-32.7	2.62±0.02	-15.3
<i>Holliston</i>	1054.6±26.5	-0.9	0.7±0.01	0.3	9881.6±26.5	-0.7	2.99±0.01	-5.6
<i>Hollister Red</i>	794.7±7.6	-8.7	0.4±0.01	-9.3	11032.2±79.2	11.1	3.16±0.01	1.7
<i>Stankovich</i>	771.8±42.6	-5.9	0.4±0.03	-7.6	10106.9±26.5	2.8	3.37±0.02	7.7
<i>WSU 108</i>	985.8±35.0	-2.8	0.8±0.01	2.6	9221.3±125.6	-5.1	2.95±0.02	-5.2

Table 4. Relative differences (in percentage terms) between the introduced *Oxycoccus macrocarpus* cultivars and the standard *Stevens* cultivar by the content of active substances.

Indicator	<i>Bain Favorite</i>	<i>Holliston</i>	<i>Hollister Red</i>	<i>Stankovich</i>	<i>WSU 108</i>
Dry matter	-9.3	+12.1	-5.0	-14.3	-7.1
Free organic acids	+8.4	-23.6	-	+12.0	+12.4
Ascorbic acid	+28.5	-6.7	+15.0	+53.4	+20.1
Hydroxycinnamic acids	-9.5	-	+9.2	-15.5	-13.4
Soluble sugars	-	+12.1	+10.6	+18.9	+7.5
Sugar-acid index	-8.3	+41.7	+8.3	+8.3	-8.3
Pectic substances	-6.0	-19.0	-24.0	-48.0	-32.0
True anthocyanins	-16.6	-13.7	+25.1	-	-
Leucoanthocyanins	-26.4	+6.5	+12.1	+5.5	-6.6
Anthocyanin pigments	-23.7	-	+15.8	+2.7	-4.4
Catechins	-33.3	-	+16.4	+19.9	-18.4
Flavonols	-21.0	-	-27.3	-29.4	-9.8
Bioflavonoids	-24.8	-	+11.1	+1.8	-7.1
Tannins	-16.0	-4.2	-	+8.0	-5.4

However, in most of the new cultivars, the content of hydroxycinnamic acids was from 10 % to 16 % lower than in *Stevens*; it was only higher in *Hollister Red*, by 9 %, whereas *Holliston* showed no valid difference.

All of the new large cranberry cultivars, except *Bain Favorite*, were characterized by 8-19 % higher content of soluble sugars compared to the fruit of the standard *Stevens* cultivar. In *Hollister Red*, *Stankovich* and especially *Holliston*, the sugar-acid index of soluble sugars was from

8 % to 42 % higher than in *Stevens*, which results in a sweeter taste of berries compared to the benchmark (Table 4). At the same time, the same parameter in *Bain Favorite* and *WSU 108* was 8 % below the benchmark. Unlike soluble sugars, all of the tested cranberry cultivars showed 6 % to 48 % lower content of pectic substances in their fruit as against the benchmark. The most significant difference was observed in *Stankovich*. Mixed trends were observed in the nature of differences of the tested *Oxycoccus macrocarpus* cultivars from the *Stevens* benchmark in the context of

bioflavonoid content in fruit, only *Hollister Red* showed a significant difference (11 % higher), whereas *Stankovich* showed an insignificantly (within 2 %) yet reliably higher level than the benchmark. Unlike the two cultivars above, overall P-vitamin content in the *WSU 108* and especially *Bain Favorite* cultivars was lower than in *Stevens*, by 7 and 25 %, respectively, and *Holliston* showed no difference from the standard cultivar.

Also mixed were such differences in the accumulation in cranberry fruit of certain groups of bioflavonoids. Only in *Hollister Red* fruit was the content of the most valuable bioflavonoid group, true anthocyanins, higher than that in the benchmark cultivar, by 25 %, whereas the *Bain Favorite* and *Holliston* cultivars, on the contrary, showed anthocyanin content 14 % and 17 % lower, respectively, while *Stankovich* and *WSU 108* showing no significant difference. The content of leucoanthocyanins in *Holliston*, *Hollister Red*, and *Stankovich* fruit was 6 % to 12 % above that in *Stevens*, whereas in *WSU 108* and *Bain Favorite*, it was 7 % and 26 % lower, respectively (Table 4).

Because of the dominating position of leucoanthocyanins in the composition of the P-vitamin complex of cranberry fruit, similar trends in the nature of differences of the tested cultivars from *Stevens* were observed when it comes to the content of anthocyanin pigments, as well as the content of catechins, which are close to anthocyanins in their chemical nature. Only the fruit of the *Hollister Red* and *Stankovich* cultivars showed catechin content higher than that in the benchmark cultivar, by 16 and 20 %, respectively, whereas in *WSU 108* and *Bain Favorite*, catechin content was 18 and 33 % lower, respectively. The *Holliston* cultivar showed no significant difference. As for the flavonols, their content proved to be lower in all of the tested cultivars, except for *Holliston*, compared to that in *Stevens*, by 10 to 29 %. The content of tannins in the fruit of new cranberry cultivars was in most cases lower than that in the benchmark cultivar by 4 % to 16 %, and only *Stankovich* showed a higher-than-benchmark content, by 8 %.

As a result of biochemical screening of the fruit of the *Oxycoccus macrocarpus* cultivars under analysis, taxa with the highest and lowest parameters of accumulated active substances of various chemical nature were identified. *Holliston* was the leading cultivar by the content of dry matter in fruit, the *Stankovich* and *WSU 108* cultivars led in terms of the content of free organic substances, *Stankovich* was the leader by the content of ascorbic acid, *Hollister Red* in terms of hydroxycinnamic acids, *Stankovich* by the content of soluble sugars, *Holliston* by the content of sugar-acid index, *Stevens* in terms of pectic substances, *Hollister Red* in terms of bioflavonoids, including true anthocyanins and leucoanthocyanins, *Stankovich* by the content of catechins and tannins, and *Stevens* and *Holliston* in terms of flavonols.

Despite the diversity of the advantages of any given *Oxycoccus macrocarpus* cultivar in terms of the content of compounds of various chemical nature in their fruit, it is hard to identify the taxa with the highest integrated level of nutritive and vitamin value. To this end, we made use of our own, patented²³ method, based upon the juxtaposition of the relative sizes, amplitudes, and ratios of statistically valid positive and negative deviations in the cultivars in question from the reference values of analyzed characteristics of the

biochemical composition of their fruit. The scope of the combined amplitude of deviations revealed, irrespective of their sign (plus or minus), can serve as an indicator to decide on the distinctiveness of differences in each of the entities under analysis from the *Stevens* cultivar by the combination of analyzed properties, which makes it possible to rank them by the degree of these differences in the descending order. The correlation of the relative ranges of the scopes of positive and negative deviations with the reference content of active substances in fruit became an assessment criterion of the integrated level of their nutritive and vitamin value in each of the tested cranberry cultivars, based upon the premise that all of the analyzed properties are equally important for the assessment of the quality of fruit.

The data presented in table 5 that are based upon those in table 4 and characterize the direction and the significance of shifts in the biochemical composition of the fruit of the new tested *Oxycoccus macrocarpus* cultivars in reference to the *Stevens* benchmark show pronounced genotypic differences in the direction and magnitude of the said shifts. With amplitude of these differences in the cultivar range between 139.6 and 237.7 %, they appeared to be the least distinct in *Holliston*, whereas the *Bain Favorite* and *Stankovich* cultivars showed the most striking contrast. In two cranberry cultivars, *Bain Favorite* and *WSU 108*, the relative scope of negative differences from the benchmark *Stevens* cultivar in terms of the combination of analyzed properties prevailed over those positive, whereas for the rest of the cultivars, the situation was the opposite.

Table 5. Relative scopes, amplitudes, and correlations of variously oriented differences, in percentage terms, in the biochemical composition of fruit of newly introduced *Oxycoccus macrocarpus* cultivars from the standard *Stevens* cultivar.

Cultivar	Relative scale of differences, %			
	+	-	amplitude	+/-
<i>Bain Favorite</i>	36.9	194.9	231.8	0.2
<i>Holliston</i>	72.4	67.2	139.6	1.1
<i>Hollister Red</i>	123.6	56.3	179.9	2.2
<i>Stankovich</i>	130.5	107.2	237.7	1.2
<i>WSU 108</i>	40.0	112.5	152.5	0.4

The most objective account of the integrated level of nutritive and vitamin value of the fruit of each of the newly introduced *Oxycoccus macrocarpus* cultivars can be provided with the help of the multiple scale of the correlation of the relative amounts of positive and negative deviations of the combination of analyzed properties with the reference value. It turned out that only in three cranberry cultivars this scale exceeded 1.0, which attested to a higher integrated level of nutritive and vitamin value of their fruit compared to the standard *Stevens* cultivar. Below is the sequence of tested cultivars in the descending order of the degree of their advantages with reference to the benchmark cultivar, based upon the above criterion:

Hollister Red > *Stankovich* > *Holliston* > *Stevens* > *WSU 108* > *Bain Favorite*

It can be ascertained that *Hollister Red* is the breakaway leader in the group of large cranberry cultivars, whereas the least valuable cultivars in terms of the biochemical

composition of their fruit are *WSU 108* and especially *Bain Favorite*, both of which are at the end of the sequence.

Based upon the comparison of the scale of the correlation under analysis, a quantitative assessment was provided for the degree of decrease, as against the *Hollister Red*, the leader in the taxonomic range, in the integrated level of nutrient and vitamin value of the fruit of the remaining cranberry taxa. As one would expect, that degree was highest in *Bain Favorite*, which was 11 times behind the leading cultivar in terms of this feature. The gap was significantly narrower for the rest of the cultivars, between 1.8x and 5.5x.

Conclusion

As a result of the comparative examination of sugar-acid index, content of free organic, ascorbic, and hydroxycinnamic acids, dry substances, tannins, and pectic substances, soluble sugars, and main groups of bioflavonoids in fruit of six *Oxycoccus macrocarpus* cultivars, *Stevens(st)*, *Bain Favorite*, *Holliston*, *Hollister Red*, *Stankovich*, *WSU 108*, that have been newly introduced in Belarus, it has been established that the *Hollister Red* cultivar was characterized by the highest level of nutritive and vitamin value of fruit in terms of the combination of properties under analysis, which proved to be 1.8x to 11x above that in the other cultivars, whereas *WSU 108* and especially *Bain Favorite* showed the lowest levels.

References

- ¹Butkus, V., Ruzgene R., *Structural and functional rehabilitation issues*, Vilnius, Lithuania, **1980**, 27-29.
- ²Butkus, V. F., Gorbunov A. B., Cherkasov A.F., *Rastitel. Resursy*, **1983**, 19(1), 125-129.
- ³Sapers, G. M., Phillips J. G., Rudolf H. M., DiVito A. M., *J. Am. Soc. Hort. Sci.*, **1983**, 108(2), 241-246.
- ⁴Fellers, C. R., Esselen W., *Mass. Agric. Exp. Sta. Bull.*, **1955**, 481, 62.
- ⁵Howell, A. B., *Acta Hort.*, **2009**, 810, 779-784.
- ⁶Kereselidze, J., *Corr. Acad. Sci. Georgia*, **1997**, 155(3), 447-449.
- ⁷Liebster, J., *Cranberry – du Kulturpreiselbure*, **1972**, 217. München, Germany.
- ⁸Sidorovich, E. A., Kudinov M. A., Ruban N. N., Sherstenikina A. V., Rupasova Zh. A., Shapiro D. K., Gorlenko S. V., *Large cranberry in Belarus*, Minsk, Belarus, **1987**, 238.
- ⁹Rupasova, Zh. A., *Development and metabolism of large cranberry in Belarusian Polesye region*, Minsk, Belarus **1989**, 205.
- ¹⁰Rupasova, Zh. A., Vasilevskaya T. I., *Large cranberry in Belarus (biochemical composition, storage, processing)*, Minsk, Belarus, **1999**, 167.
- ¹¹Rupasova, Zh. A., Yakovlev A. P., Lishtvan I. I., *Ericaceae in conditions of Belarus. Range of Ericaceae berry crops for cultivation in peat substrates*, Lap Lambert Academic Publishing GmbH & Co. KG Saarbruecken, Germany, **2012**, 67.
- ¹²Rupasova, Zh. A., Yakovlev A. P., *Phytorecultivation of peat lands in the north of Belarus that have been withdrawn from industrial use based upon the cultivation of Ericaceae berry plants*, Minsk, Belarus, **2011**, 287.
- ¹³Rupasova, Zh. A., Reshetnikov V. N., Vasilevskaya T. I., Yakovlev A. P., Pavlovski N. B., Parfenov V. I., *Formation of the biochemical composition of Ericaceae cultivar fruit when introduced to Belarus*, Minsk, Belarus, **2011**, 307.
- ¹⁴Yakovlev, A. P., Rupasova Zh. A., Volchkov V. E., *Cultivation of large cranberry and marsh blueberry on cutover bogs in the north of Belarus (optimization of the mineral nutrition regime)*, Minsk, Belarus, **2002**, 188.
- ¹⁵*Methods for determination of the dry matter*, GOST (State Standard) 8756.2-82, **1982**, 5.
- ¹⁶Marsov, N. G. *Phytochemical studies and biological activity of cowberries, cranberries and blueberries*, Perm, Russia, **2006**, 99-101
- ¹⁷Ermakova, A. I. (Ed.), *Methods for biochemical studies of plants*, Leningrad, Russia, **1987**, 430.
- ¹⁸Pleshkov, B. P. *Practical course in plant biochemistry*, Moscow, Russia, **1985**, 110-112.
- ¹⁹Swain, T., Hillis, W. J., *Sci. Food Agric.*, **1959**, 10(1), 63-68.
- ²⁰Skorikova Y. G., Shaftan, E. A., *Proc. 3rd All-union Semin. Biol. Active (Therapeutic) Subst. Fruit and Berries*, Sverdlovsk, Russia, **1968**, 451-461.
- ²¹Andreev, V. Y., Kalinkina, G. I., Kolomiyets, N. E., Isaykina, N. V., *Pharmacy*, **2013**, 3(19), AM-21.
- ²²*State Pharmacopoeia of the USSR*, Moscow, Russia, **1987**, 286-287.
- ²³Rupasova, Zh. A., Reshetnikov, V. N., Yakovlev, A. P., *Method for ranking plant taxa: Belarus Patent No. 17648 dated 08.07.2013*. Minsk, Belarus.
- ²⁴Cesonienė, L., Daubaras R., Jasutienė I., Vencloviene J., Miliauskiene I., *Plant Foods*, **2011**, 66, 238–244.
- ²⁵Rupasova, Zh. A., Reshetnikov V. N., Ruban N. N., Ignatenko V. A., Yakovlev A. P., Pyatnica F. S., *Highbush blueberry. Assessment of adaptation capacity for introduction to Belarus*, Minsk, Belarus, **2007**, 442

Received: 22.08.2016.

Accepted: 12.09.2016.



ON ENERGY PRINCIPLES OF STRUCTURAL INTERACTIONS

G. A. Korablev^{[a]*}, V. I. Kodolov^[b], G. E. Zaikov^[c] and N. G. Petrova^[d]

Keywords: Spatial-energy parameter, wave functions, electron density, structural interactions.

The notion of spatial-energy parameter (*P*-parameter) is introduced based on the modified Lagrangian equation for relative motion of two interacting material points, which is a complex characteristic of important atomic values. Wave properties of *P*-parameter are found, its wave equation having a formal analogy with the equation of Ψ -function is given. In the systems in which the interactions proceed along the potential gradient (positive performance) the resulting potential energy is found based on the principle of adding reciprocals of the corresponding energies of subsystems. Some correlations of *P*-parameter values with Lagrangian and Hamiltonian functions are obtained.

* Corresponding Authors

E-Mail: korablevga@mail.ru.

[a] Izhevsk State Agricultural Academy

[b] Kalashnikov Izhevsk State Technical University

[c] Institute of Biochemical Physics, Russian Academy of Science

[d] Agency of Informatization and Communication, Udmurt Republic

exceeds the total of their covalent radii, “superexchange” processes of overlapping cation orbitals take place through the anion between them.

In this work similar equilibrium-exchange processes are evaluated through the notion of spatial-energy parameter, *P*-parameter.

Introduction

To obtain the dependence between energy parameters of free atoms and degree of structural interactions in simple and complex systems is one of strategic tasks in physical chemistry. Classical physics and quantum mechanics widely use Coulomb interactions and their varieties for this.

Thus in Van der Waals theory,¹ orientation and charge-dipole interactions are referred to electron-conformation interactions in bio-systems, and as a particular case in exchange-resonance transfer of energy. But biological and many cluster systems are electroneutral in structural basis. And non-Coulomb equilibrium-exchange spatial-energy interactions, i.e. non-charge electrostatic processes, are mainly important for them.

The structural interactions of summed electron densities of valence orbitals of corresponding conformation centers, processes of equilibrium flow of electron densities, take place due to overlapping of their wave functions.

Heisenberg and Dirac² proposed the exchange Hamiltonian derived assumption on direct overlapping of wave functions of interacting centers as $\bar{H} = -I_0 S_1 S_2$. where \bar{H} is spin operator of isotropic exchange interaction for pair of atoms, I_0 is the exchange constant, S_1 and S_2 are the overlapping integrals of wave functions.

In this model electrostatic interactions are modelled by effective exchange Hamiltonian acting in the space of spin functions.

In particular, such approach is applied to the analysis of structural interactions in cluster systems. It is demonstrated in Anderson's works³ that in compounds of transition elements when the distance between paramagnetic ions considerably

Results and discussion

On two principles of adding energy characteristics of interactions

The analysis of kinetics of various physical and chemical processes shows that in many cases the reciprocals of velocities, kinetic or energy characteristics of the corresponding interactions are added.

Some examples: ambipolar diffusion, resulting velocity of topochemical reaction, change in the light velocity during the transition from vacuum into the given medium, effective permeability of bio-membranes.

In particular, such supposition is confirmed by the formula of electron transport possibility (W_∞) due to the overlapping of wave functions 1 and 2 (in steady state) during electron-conformation interactions:

$$W_\infty = \frac{1}{2} \frac{W_1 W_2}{W_1 + W_2} \quad (1)$$

Eqn. (1) is used when evaluating the characteristics of diffusion processes followed by non-radiating transport of electrons in proteins.¹

From classical mechanics it is known that the relative motion of two particles with the interaction energy $U(r)$ takes place as the motion of material point with the reduced mass μ in the field of central force $U(r)$, and general translational motion as a free motion of material point with the mass (Eqns. 2 and 3). Such things take place in quantum mechanics as well.⁴

$$\frac{1}{\mu} = \frac{1}{m_1} + \frac{1}{m_2} \quad (2)$$

$$m = m_1 + m_2 \quad (3)$$

The task of two-particle interactions taking place along the bond line was solved in the times of Newton and Lagrange (Eqn. 4).

$$E = \frac{m_1 v_1^2}{2} + \frac{m_2 v_2^2}{2} + U(\bar{r}_2 - \bar{r}_1) \quad (4)$$

where E is the total energy of the system, first and second elements are the kinetic energies of the particles, third element is the potential energy between particles 1 and 2, vectors \bar{r}_2 and \bar{r}_1 characterize the distance between the particles in final and initial states.

For dynamic thermodynamic systems the first commencement of thermodynamics is as follows.

$$\delta E = d\left(U + \frac{mv^2}{2}\right) \pm \delta A m \quad (5)$$

where δE is amount of energy transferred to the system, element $d[U + (mv^2/2)]$ characterizes the changes in internal and kinetic energies of the system, $+\delta A$ is the work performed by the system and $-\delta A$ is worked performed with the system.

As the work value numerically equals the change in the potential energy, it is apparent that

$$\delta A = -\Delta U \quad (6)$$

and

$$-\delta A = +\Delta U \quad (7)$$

It is probable that not only in thermodynamic but in many other processes in the dynamics of moving particles interaction not only the value of potential energy is critical, but changes in it are as well. Therefore, similar to the equation (4), the following equations should be applicable to two-particle interactions.

$$\delta E = d\left(\frac{m_1 v_1^2}{2} + \frac{m_2 v_2^2}{2}\right) \pm \Delta U \quad (8)$$

where

$$U = U_2 - U_1 \quad (9)$$

where U_1 and U_2 are the potential energies of the system in final and initial states.

At the same time, the total energy (E) and kinetic energy ($mv^2/2$) can be calculated from their zero value, then only the last element is modified in Eqn. (4).

The character of the change in the potential energy value ΔU was analyzed by its sign for various potential fields and the results are given in Table 1. From the table it is seen that the values $-\Delta U$ and accordingly $+\delta A$ (positive work) correspond to the interactions taking place along the potential gradient, and $+\Delta U$ and $-\delta A$ (negative work) occur during the interactions against the potential gradient.

The solution of two-particle task of the interaction of two material points with masses m_1 and m_2 , obtained under the condition of the absence of external forces, corresponds to the interactions flowing along the gradient, the positive work is performed by the system (similar to the attraction process in the gravitation field).

The solution of this equation via the reduced mass (μ) is the Lagrange equation for the relative motion of the isolated system of two interacting material points with masses m_1 and m_2 , which are related to x in the following way:

$$\mu \cdot x'' = -\frac{\partial U}{\partial x} \quad (10)$$

Here U is the mutual potential energy of material points, μ is the reduced mass. At the same time, $x'' = a$ (feature of the system acceleration). For elementary portions of the interactions Δx can be taken as follows:

$$\frac{\partial U}{\partial x} \approx \frac{\Delta U}{\Delta x}$$

That is $\mu a \Delta x = \Delta U$, therefore

$$\frac{1}{1/(a\Delta x)} \frac{1}{\left(\frac{1}{m_1} + \frac{1}{m_2}\right)} \approx -\Delta U,$$

$$\frac{1}{1/(m_1 a \Delta x) + 1/(m_2 a \Delta x)} \approx -\Delta U$$

or

$$\frac{1}{\Delta U} \approx \frac{1}{\Delta U_1} + \frac{1}{\Delta U_2} \quad (11)$$

where ΔU_1 and ΔU_2 are the potential energies of material points on the elementary portion of interactions and ΔU is the resulting (mutual) potential energy of this interactions.

Table 1. Direction of the interaction processes .

No.	Systems	Potential field	Process	U	Relations of parameters		Sign of		Process direction
					ΔU	δA			
1	opposite electrical charges	electrostatic	attraction	$-k \frac{q_1 q_2}{r}$	$r_2 < r_1$	$U_2 > U_1$	-	+	along the gradient
			repulsion	$-k \frac{q_1 q_2}{r}$	$r_2 > r_1$	$U_2 < U_1$	+	-	against the gradient
2	similar electrical charges	electrostatic	attraction	$k \frac{q_1 q_2}{r}$	$r_2 < r_1$	$U_2 > U_1$	+	-	against the gradient
			repulsion	$k \frac{q_1 q_2}{r}$	$r_2 > r_1$	$U_2 > U_1$	-	+	along the gradient
3	elementary masses (m_1, m_2)	gravitational	attraction	$-\gamma \frac{m_1 m_2}{r}$	$r_2 < r_1$	$U_2 > U_1$	-	+	along the gradient
			repulsion	$-\gamma \frac{m_1 m_2}{r}$	$r_2 > r_1$	$U_2 > U_1$	+	-	against the gradient
4	spring deformation	elastic forces	compression	$k \frac{\Delta x^2}{2}$	$x_2 < x_1$	$U_2 > U_1$	+	-	against the gradient
			extension	$k \frac{\Delta x^2}{2}$	$x_2 > x_1$	$U_2 > U_1$	+	-	against the gradient
5	photoeffect	electrostatic	repulsion	$k \frac{q_1 q_2}{r}$	$r_2 > r_1$	$U_2 < U_1$	-	+	along the gradient

Thus:

1. In the systems in which the interactions proceed along the potential gradient (positive performance) the resulting potential energy is found based on the principle of adding reciprocals of the corresponding energies of subsystems.⁵ Similarly, the reduced mass for the relative motion of two-particle system is calculated.

$$\frac{1}{q^2/r_i} + \frac{1}{W_i n_i} = \frac{1}{P_E} \quad (12)$$

or

2. In the systems in which the interactions proceed against the potential gradient (negative performance) the algebraic addition of their masses as well as the corresponding energies of subsystems is performed (by an analogy with Hamiltonian).

$$\frac{1}{P_0} = \frac{1}{q^2} + \frac{1}{(Wrn)_i} \quad (13)$$

Spatial-energy parameter (P -parameter)

From the equation (11) it is seen that the resulting energy characteristic of the system of two material points interaction is found based on the principle of adding reciprocals of initial energies of interacting subsystems.

Electron with the mass m moving near the proton with the mass M is equivalent to the particle with the mass

$$\mu = mM/(m + M)^6.$$

Therefore, when modifying the equation (11), we can assume that the energy of atom valence orbitals (responsible for interatomic interactions) can be calculated⁵ by the principle of adding reciprocals of some initial energy components based on the following equations.

where W_i is the electron orbital energy,⁷ r_i is the orbital radius of i orbital,⁸ $q = Z^*/n^*$,⁹ n_i is the number of electrons of the given orbital, Z^* and n^* is the effective nuclear charge and effective main quantum number, r is the bond dimensional characteristics.

P_0 was called a spatial-energy parameter (SEP), and P_E is the effective P -parameter (effective SEP). Effective SEP has a physical sense of some averaged energy of valence electrons in the atom and is measured in energy units, electron-volts (eV).

The values of P_0 -parameter are the tabulated constants for the electrons of the given atom orbital.

For dimensionality SEP can be written down as follows:

$$[P_E] = [q^2] = [E] \cdot [r] = [h] \cdot [v] = \frac{\text{kg} \cdot \text{m}^3}{\text{s}^2} = \text{J} \cdot \text{m} \quad (15)$$

where $[E]$, $[h]$ and $[v]$ are the dimensions of energy, Planck constant and velocity, respectively. Thus P -parameter corresponds to a processes going along the potential gradient.

The introduction of P -parameter should be considered as further development of quasi-classical notions using quantum-mechanical data on atom structure to obtain the criteria of energy conditions of phase-formation. At the same time, for the systems of similarly charged (e.g. – orbitals in the given atom), homogeneous systems the principle of algebraic addition of such parameters is preserved:

$$\sum P_E = \sum (P_0/r_i) \quad (16)$$

$$\sum P_E = \frac{\sum P_0}{r} \quad (17)$$

or

$$\sum P_0 = P'_0 + P''_0 + P'''_0 + \dots \quad (18)$$

$$r \sum P_E = \sum P_0 \quad (19)$$

Here P -parameters are summed on all atom valence orbitals. To calculate the values of P_E -parameter at the given distance from the nucleus, depending on the bond type, either atomic radius (R) or ionic radius (r_i) can be used instead of r .

Regarding the reliability of such approach, the calculations demonstrated that the values of P_E -parameters are numerically equal (within 2 %) to the total energy of valence electrons (U) by the atom statistic model. Using the known correlation between the electron density (β) and interatomic potential by the atom statistic model,¹⁰ we can obtain the direct dependence of P_E -parameter on the electron density at the distance r_i from the nucleus.

The rationality of such approach is confirmed by the calculation of electron density using wave functions of Clementi and its comparison with the value of electron density calculated via the value of P_E -parameter.

Wave equation of P -parameter

To characterize atom spatial-energy properties two types of P -parameters are introduced. The relation between them is a simple one, $P_E = P_0/R$, where R is an atom-dimensional characteristic. Taking into account additional quantum characteristics of sublevels in the atom, this equation can be written down in coordinate x as follows: $\Delta P_E = \Delta P_0/\Delta x$ or $\partial P_E = \partial P_0/\partial x$, where the value ΔP equals the difference between P_0 -parameter of i^{th} orbital and PCD–countdown parameter (parameter of main state at the given set of quantum numbers).

According to the established rule⁵ of adding P -parameters of similarly charged or homogeneous systems for two orbitals in the given atom with different quantum characteristics and according to the energy conservation rule we have:

$$\Delta P''_E - \Delta P'_E = P_{E,\lambda} \quad (20)$$

where $P_{E,\lambda}$ – spatial-energy parameter of quantum transition.

Taking for the dimensional characteristic of the interaction $\Delta\lambda = \Delta x$, we have:

$$\frac{\Delta P''_0}{\Delta\lambda} - \frac{\Delta P'_0}{\Delta\lambda} = \frac{P_0}{\Delta\lambda}$$

or

$$\frac{\Delta P'_0}{\Delta\lambda} - \frac{\Delta P''_0}{\Delta\lambda} = \frac{P_{0,\lambda}}{\Delta\lambda} \quad (21)$$

Let us again divide both sides by $\Delta\lambda$ term

$$\left(\frac{\Delta P'_0}{\Delta\lambda} - \frac{\Delta P''_0}{\Delta\lambda} \right) / \Delta\lambda = - \frac{P_0}{\Delta\lambda^2} \quad (22)$$

where

$$\left(\frac{\Delta P'_0}{\Delta\lambda} - \frac{\Delta P''_0}{\Delta\lambda} \right) / \Delta\lambda \sim \frac{d^2 P_0}{d\lambda^2}$$

i.e.,

$$\frac{d^2 P_0}{d\lambda^2} + \frac{P_0}{\Delta\lambda^2} \approx 0 \quad (23)$$

Taking into account only those interactions when $2\pi\Delta x = \Delta\lambda$ (closed oscillator), we have the following equation:

$$\frac{d^2 P_0}{4\pi^2 \Delta\lambda^2} + \frac{P_0}{\Delta\lambda^2} = 0$$

or

$$\frac{d^2 P_0}{dx^2} + 4\pi^2 \frac{P_0}{\Delta\lambda^2} \approx 0 \quad (24)$$

Since

$$\Delta\lambda = \frac{h}{mv}$$

then

$$\frac{d^2 P_0}{dx^2} + 4\pi^2 \frac{P_0}{h^2} m^2 v^2 \approx 0 \quad (25)$$

or

$$\frac{d^2 P_0}{dx^2} + \frac{8\pi^2 m}{h^2} P_0 E_k = 0 \quad (26)$$

where $E_k = mv^2/2$ is the electron kinetic energy.

Schrodinger equation for the stationary state in coordinate x is as follows (Eqn. 27).

$$\frac{d^2\psi}{dx^2} + \frac{8\pi^2m}{h^2} \psi E_k = 0 \quad (27)$$

Comparing these two equations it can be seen that the P_0 -parameter numerically correlates with the value of ψ -function, $P_0 \approx \psi$, and is generally proportional to it, $P_0 \sim \psi$. Taking into account the broad practical opportunities of applying the P -parameter methodology, we can consider this criterion as the materialized analog of ψ -function.

Since the P_0 -parameters like ψ -functions have wave properties, the superposition principles should be fulfilled for them, defining the linear character of the equations of adding and changing P -parameter.

Analog comparisons of Lagrange and Hamilton functions with spatial-energy parameter

Lagrange (L) and Hamilton (H) functions are the main provisions of analytical mechanics. Lagrange function is the difference between kinetic (T) and potential (U) energies of the system:

$$L = T - U \quad (28)$$

For uniform functions of the second degree Hamilton function can be considered as the sum of potential and kinetic energies, i.e. as the total mechanical energy of the system:

$$H = T + U \quad (29)$$

From these equations and in accordance with energy conservation law we can visualize eqns. (30) and (31).

$$H + L = 2T \quad (30)$$

$$H - L = 2U \quad (31)$$

Let us try to assess the movement of an isolated system of a free atom as a relative movement of its two subsystems, nucleus and orbital.

The structure of atom is formed of oppositely charged masses of nucleus and electrons. In this system, the energy characteristics of subsystems are the orbital energy of electrons (W_i) and effective energy of atom nucleus taking screening effects into account.

In a free atom, its electrons move in Coulomb field of nucleus charge. The effective nucleus charge characterizing the potential energy of such subsystem taking screening effects into account equals q^2/r_i , where $q = Z^*/n^*$.

Here Z^* and n^* are effective nucleus charge and effective main quantum number, respectively, r_i is the orbital radius. It can be presumed that orbital energy of electrons during their motion in Coulomb field of atom nucleus is mainly defined by the value of kinetic energy of such motion.

Thus, it is assumed that $T \sim W$ and $U \sim q^2/r_i$. In such an approach the total of the values W and q^2/r_i are analogous to Hamilton function (H) i.e.,

$$W + q^2/r_i \sim H \quad (32)$$

An analogous comparison of P -parameter with Lagrange function can be carried out when investigating Lagrange equation for relative motion of isolated system of two interacting material points with masses m_1 and m_2 in coordinate x . The principle of adding reciprocals of energy values models their algebraic difference by Hamiltonian. If it is presumed that $P_E \sim L$, then Eqn. (30) becomes Eqn. (33).

$$\left(W + \frac{q^2}{r_i} \right) + P_E \approx 2W \quad (33)$$

Using the values of electron bond energy as the orbital electron energy, we calculated the values of P_E -parameters of free atoms (Table 2) by equations (12-14). When calculating the values of effective P_E -parameter, mainly the atom radius values by Belov-Bokiy or covalent radii (for non-metals) were applied as dimensional characteristics of atom (R).

At the same time, the average values of total energy, valence orbitals dividing their values by a number of valence electrons considered (N):

$$\left(\frac{q^2}{r_i} + W \right) \frac{1}{N} + P_E \approx 2W \quad (34)$$

This energy in terms of one valence electron is the analogue of Hamilton function, H .

In free atoms of Ia and IIa groups of periodic system, s -orbital is the only valence orbital, and that was considered via the introduction of the coefficient, $K = n/n^*$ where n is the main quantum number, n^* is the effective main quantum number, by the eqn. (35)

$$\left(\frac{q^2}{r_i} + W \right) \frac{1}{KN} + P_E \approx 2W \quad (35)$$

Table 2. Comparison of some basic energy atomic characteristics.

Element	Valence electrons	W (eV)	r_i (Å)	q^2 (eVÅ)	P_0 (eVÅ)	R (Å)	$P_E=P_0/R$ (eV)	N	B^*	2W (eV)
Li	2s ¹	5.3416	1.586-2	5.8892	3.475	1.55	2.2419	1	9.440	10.683
Be	2s ²	8.4157	1.040	13.159	7.512	1.13	6.6478	2	17.182	16.831
B	2p ¹	8.4315	0.776	21.105	4.9945	0.91	5.4885	3	17.365	16.863
	2s ²	13.462	0.769	23.890	11.092	0.91	12.189	3	27.032	26.924
C	2p ²	11.792	0.596	35.395	10.061	0.86	11.699/2	4	23.645	23.584
	2s ²	19.201	0.620	37.240	14.524	0.77	18.862	4	38.824	38.402
N	2p ³	15.445	0.4875	52.912	15.830	0.71	22.296/3	5	32.228	30.890
	2s ²	25.724	0.521	53.283	17.833	0.71	19.788/3	5	31.392	51.448
O	2p ¹	17.195	0.4135	71.383	6.4663	0.66	9.7979/4	6	34.087	34.390
	2s ²	33.859	0.450	72.620	21.466	0.66	32.524	6	65.064	67.718
F	2p ¹	19.864	0.3595	93.625	6.6350	0.64	10.367/5	7	42.115	39.728
	2s ²	42.792	0.396	94.641	24.961	0.64	39.002	7	79.257	85.584
Na	3s ¹	4.9552	1.713-2	10.058	4.6034	1.89	2.4357	1	10.327	9.9104
Mg	3s ¹	6.8859	1.279	17.501	5.8588	1.60	3.6618	2	13.946	13.772
Al	3p ¹	5.713	1.312	26.443	5.840	1.43	4.084	3	12.707	11.426
	3s ²	10.706	1.044	27.119	12.253	1.43	8.5685	3	20.796	21.412
Si	3p ¹	8.0848	1.068	29.377	6.6732	1.17	5.7036	4	14.600	16.170
	3s ²	14.690	0.904	38.462	15.711	1.17	13.428	4	17.737	29.380
P	3p ³	10.659	0.9175	38.199	16.594	1.30	12.765/3	3	21.686	21.318
	3s ¹	18.951	0.803	50.922	11.716	1.10	10.651	3	38.106	37.902
S	3p ¹	11.901	0.808	48.108	8.0143	1.04	7.7061	4	25.566	23.802
	3p ²	11.901	0.808	48.108	13.740	1.04	13.215/2	4	24.468	23.802
	3p ⁴	11.904	0.808	48.108	21.375	1.04	20.553/4	4	22.998	23.808

$$*B = \left(\frac{q^2}{r_i} + W \right) \frac{1}{KN} + P_E$$

Thus in Ia and IIa subgroups of short periods, $K = 1$ and then $K = 4/3.7$; $5/4$ and $6/4.2$ for 4th, 5th, and 6th periods of the system only for these subgroups. For all other cases $K = 1$. Besides, for the elements only of 1a group of periodic system, the value $2r_i$ (i.e. the orbital radius of i -orbital) was used as a dimensional characteristic in the first component of Eqn. 35.

Taking into account the remarks pointed out for the initial equation, the values of both the components of Eqn. (35) for 65 elements were calculated and compared. Some results are given in Table 2. The analysis of the data given in Table 2 reveals that the proximity of the values investigated is mostly within 5 %. Thus there is a certain analogy of equations (30) and (35), and the value of P_E -parameter can be considered as the analog of Lagrange function and value

$$\left(\frac{q^2}{r_i} + W \right) \frac{1}{KN}$$

as an analog of Hamilton function.¹¹

Structural exchange spatial-energy interactions

In the process of solid solution formation and other structural equilibrium-exchange interactions, the single electron density should be set in the points of atom-component contact. This process is accompanied by the redistribution of electron density between the valence areas of both particles and transition of the part of electrons from some external spheres into the neighbouring ones. Apparently, frame atom electrons do not take part in such exchange.

Obviously, when electron densities in free atom-components are similar, the transfer processes between boundary atoms of particles are minimal and this will be favorable for the formation of a new structure. Thus the evaluation of the degree of structural interactions in many cases means the comparative assessment of the electron density of valence electrons in free atoms (on averaged orbitals) participating in the process, which can be correlated with the help of P -parameter model.

The less the difference ($P'_o/r'_i - P''_o/r''_i$), more favorable is the formation of a new structure or solid solution from the energy point.

In this regard, the maximum total solubility, evaluated via the coefficient of structural interaction, α , is determined by the condition of minimum value of α , which represents the relative difference of effective energies of external orbitals of interacting subsystems:

$$\alpha = \frac{P'_o/r'_i - P''_o/r''_i}{(P'_o/r'_i + P''_o/r''_i)/2} 100 \% \quad (36)$$

$$\alpha = \frac{P'_C - P''_C}{P'_C + P''_C} 200 \% \quad (37)$$

where P_C – structural parameter is found by equation:

$$\frac{1}{P_C} = \frac{1}{N_1 P'_E} + \frac{1}{N_2 P''_E} + \dots \quad (38)$$

here N_1 and N_2 are the number of homogeneous atoms in subsystems.

The isomorphism degree and mutual solubility are evaluated in many (over one thousand) simple and complex systems (including nanosystems). The calculation results are in compliance with theoretical and experimental data.

Conclusions

1. The introduced spatial-energy parameter (P -parameter) can be considered as materialized analog of ψ -function.
2. The application of such methodology allows modelling of physical-chemical processes based on energy characteristics of a free atom.

References

- ¹Rubin, A. B., *Biophysics*, 1, *Theoretical biophysics*, Vysshaya shkola, Moscow, **1987**, 319.
- ²Dirac, P. A., *Quantum Mechanics*, Oxford University Press, London, **1935**.
- ³Anderson, P. W., *Magnetism*, Vol.1, Academic Press, New York, **1963**, 25.
- ⁴Blokhintsev, D. I., *Basics of quantum mechanics*, Vysshaya shkola, Moscow, **1961**, 512.
- ⁵Korablev, G. A., *Spatial-Energy Principles of Complex Structures Formation*, Brill Academic Publishers and VSP, Netherlands, **2005**, 426.
- ⁶Eyring, G., Walter, J., Kimball G., *Quantum chemistry*, M., F. L., **1948**, 528.
- ⁷Fischer, C. F., *Atomic Data*, **1972**, 4, 301-399.
- ⁸Waber, J. T., Cromer, D. T., *J. Chem. Phys.*, **1965**, 42(12), 4116-4123.
- ⁹Clementi, E., Raimondi, D. L., *J. Chem. Phys.*, **1963**, 38(11), 2686-2689.
- ¹⁰Gombash, P., *Statistic theory of an atom and its applications*, M.: I.L., 1951, 398.
- ¹¹Korablev, G. A., Kodolov, V. I., Lipanov, A. M., *Chem. Phys. Mesoscopy*, **2004**, 6(1), 5-18.

Received: 15.06.2016.

Accepted: 14.09.2016.



Abdullatif Azab

Keywords: micromeria, micromeria fruticosa, essential oil, plant extracts, medicinal activities.

The genus *micromeria* is one of the most widespread plant families in the "old world". Its subspecies, especially *Micromeria fruticosa*, have been used by humans for thousands of years. The plant(s), its extracts and its chemical ingredients are reviewed in this article for their reported medicinal/biological activities. In addition, the traditional medicine and ethnobotanical uses are briefly presented.

* Corresponding Authors

Fax: +972-49861173

E-Mail: abedazab@gal-soc.org

[a] Institute of Applied Research, The Galilee Society, P.O. Box 437, Shefa-Amr 20200, Israel

Introduction

Plants have been used by human since the very dawn of our kind. They are used as major food source, medicinal-herbal, therapeutic agents, psychoactive and cosmetics. As one of the most common in the "old world",¹ the genus *micromeria* is used by inhabitants of Mediterranean basin for thousands of years, as it is indicated by archeological documentation.² Counting the known species, subspecies and varieties of the genus *micromeria*, the total number may easily reach more than one hundred.^{1,3} But in this review we relate only to the subspecies whose chemical compositions have been reported and/or have been published for their biological/medicinal activities.

Special attention is paid to *M. fruticosa* since it is one of the most known species of the genus *micromeria* and it is one of the most traditionally used as edible and medicinal plant in the middle eastern region. In addition, it is the most investigated and reported of all *micromeria* subspecies.

The similarity of *micromeria* subspecies makes it difficult to distinguish them from each other, especially when they grow in the same habitat. But despite this, in traditional Palestinian society, some people, mostly who practiced herbal medicine, could make this distinction: *M. fruticosa* (L.) Druce was used for stomach, intestine pain and inflammation, fever, asthma and respiratory system; while *M. myrtifolia* L. was used to treat skin diseases, heart diseases, digestive system and asthma.⁴ On the other hand, ordinary people who use *micromeria* species for nutrition purposes (mainly as tea flavoring) will not make this distinction.⁵ *M. myrtifolia* was also traditionally used to treat digestive system disorders, *M. fruticosa* cured poisoning of some sulfate salts (Cu/Fe/ZnSO₄) and in Asia minor and Greece, *M. nervosa* was also commonly used.⁶ In recent years, there is a growing interest in cultivation of *M. fruticosa* and the search for optimal conditions that can yield different compositions of the plant, especially the chemical composition of its essential oil.⁷ Finally, in traditional Arab medicine, *M. myrtifolia* (infusion) is known as antiseptic and helps in menstrual pain relief.⁸

Medicinal activities of micromeria subspecies (excluding *M. fruticosa*)

A number of reports are published concerning the medicinal activities of the genus *micromeria*. A reader-easy-access-summary of these reports is presented in Table 1, followed by a brief discussion on the reported findings. After reviewing Table 1, it is clear that most cited studies obtained the essential oil from the plant species, Some analyzed these oils to find their chemical compositions, but most studies tested the whole oils for medicinal activities. One major reason for this is the growing recognition of the *synergism* between the activities of natural products. This is discussed in the next section. But at the same time, it is important to notice that some major compounds detected in these oils are major sources of the plants activities.

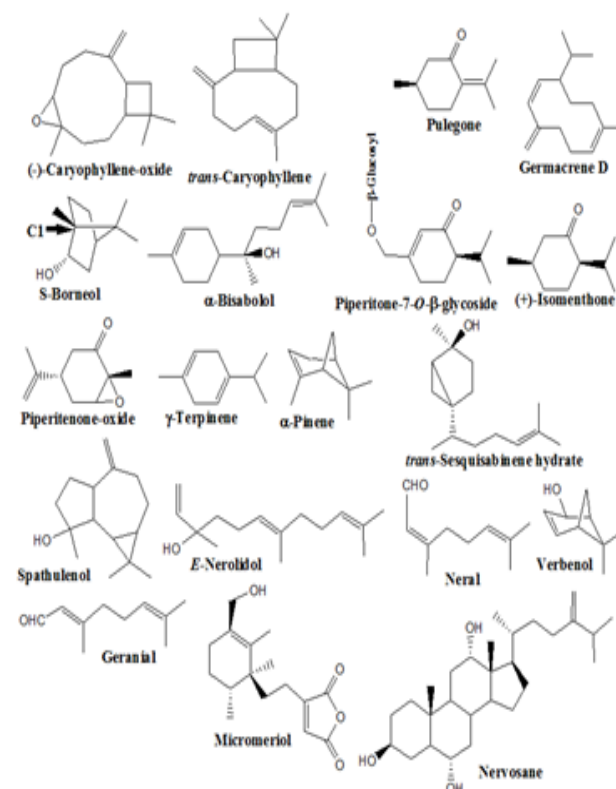


Figure 1. Structures of selected non-phenolic active compounds in *micromeria* ssp.

Table 1. Chemical compositions and medicinal activities of selected micromeria subspecies

Species ^A	Chemical Composition ^B	Medicinal Activities
<i>M. albanica</i>	⁹ Essential oil: <u>Piperitenone-oxide</u> (44%), α/β -pinene, limonene, menthone, cuminaldehyde, pulegone, piperitone, piperitone oxide ¹⁰ Flavanoids (Thymusin, major)	¹¹ Antibacterial, antifungal
<i>M. barbata</i>	¹² Ethanolic extract: <u>Chlorogenic acid</u> , Myrcetin, Hespertetin, Quercetin	¹² Antioxidant (ethanolic extract), essential oil activities: ^{13,14,15} Antimicrobial, ¹³ antioxidant, ¹⁴ sporidical
<i>M. biflora</i>	¹⁶ Essential oil: <u>trans-Caryophyllene</u> (43.7%), (-)-caryophyllene-oxide, spathulenol, α -humulene, germacrene-D, farnesene, α -myrcene, R(+)-limonene, α -pinene, ¹⁷ Essential oil: <u>Caryophyllene-oxide</u> , epi- α -cadinol, β -eudesmol, oplapanone, guaial, <i>p</i> -cymene, $\gamma/\delta/\alpha$ -cadinene ^C , ^{18,23,24} Methanol extraction, drying and fractionation with various solvents	<u>Essential oil</u> : ¹⁶ Antimicrobial, ¹⁹ Antibacterial, ²⁰ Antibacterial (dental) <u>Essential-oil/Ethanolic extract</u> : Anti-inflammatory, anti-arthritis, analgesic, antipyretic, toxic, ¹⁸ Antimicrobial: most active was n-hexane fraction, ²¹ Aqueous/methanolic extract: Antidandruff, ^{22,24} Methanolic extract: Antioxidant, ²³ Antibacterial, antifungal
<i>M. cilicica</i>	²⁵ Essential oil: <u>Pulegone</u> (65.3%), <i>cis/trans-p</i> -menthone, ²⁶ Acetone extract and its ingredients: <u>Piperitone-7-O-β-D-glucoside</u> , <u>isothymonin-4'-methyl ether</u> , ^D sudachitin, isomucronulatol, rutin, ursolic acid, saccharose	²⁵ Essential-oil, pure pulegone: antimicrobial, antibacterial, antifungal, ²⁶ Antioxidant, anticholinesterase, ³⁰ Antimicrobial
<i>M. congesta</i>	²⁷ <u>Piperitenone-oxide</u> (42.5%), pulegone, verbenone	²⁸ Essential oil: antibacterial, antioxidant
<i>M. cremnophila</i>	²⁹ Essential oil: <u>Germacrene D</u> (24%), β -caryophyllene, caryophyllene-oxide, <i>E</i> - β -farnesene, bicyclogermacrene	³⁰ Animicrobial
<i>M. cristata</i>	¹⁰ (Traces) Luteolin, apigenin, chrysoeriol, diosmetin, acacetin ³¹ Essential oil: <u>Borneol</u> (32.5%), <u>camphor</u> , caryophyllene-oxide, <i>trans</i> -verbenol, ³² Essential oil: <u>Bisabolol</u> (38.5%) ^E , verbenol, borneol, caryophyllene-oxide	³¹ Antimicrobial (essential oil and pure compounds), See also remark G
<i>M. croatica</i>	¹⁰ (Traces) Luteolin, apigenin, chrysoeriol, diosmetin, acacetin, ³³ Ethanolic extract: <u>apigenin</u> , luteolin, rosmarinic acid, chlorogenic acid	³³ Ethanolic extract: antioxidant (4 different methods), ³⁴ Methanolic extract: antioxidant, ³⁵ Ethanolic extract: hepatoprotective (CCl ₄ -induced injury)
<i>M. dalmatica</i>	¹⁰ Flavanoids: (<u>Thymonin</u> , major), ^{32,36} <u>Pulegone</u> (35.8%), piperitinone, menthone, piperitone	¹¹ Antibacterial, antifungal, ³⁷ Antibacterial (food)
<i>M. dolichodontha</i>	³⁸ Essential oil: <u>Isomenthone</u> (23.5%), pulegone, <i>cis</i> -piperitone-oxide, piperitone	³⁰ Antimicrobial
<i>M. fruticulosa</i>	³⁹ Essential oil: <u>γ-terpinene</u> (14.5%), β -caryophyllene, <i>p</i> -cymene, α -pinene β -bisabolene	³⁹ Antimicrobial
<i>M. graeca</i>	¹⁰ (Traces) Luteolin, apigenin, chrysoeriol, diosmetin, acacetin, ⁴⁰ Essential oil: <u>Caryophyllene-oxide</u> (17.0%), epi- α -bisabolol; linalool, β -chamigrene ^F , ⁴² Quinic acid (detected by H-NMR)	⁴¹ Antiphytoviral
<i>M. herpyllomorpha</i>	⁴³ Essential oil: <u>α-Pinene</u> (9.2%), borneol, <u>cubenol</u> , <i>trans</i> -Pinocarveol, dehydrosabinene	No reports
<i>M. hyssopifolia</i>	⁴³ Essential oil: <u>Borneol</u> (13.7%), α -pinene, camphor, <i>p</i> -cymene, camphene	
<i>M. inodora</i>	⁴⁴ Essential oil: <u>trans-sesquisabinene hydrate</u> (20.9 %), α -terpinyl acetate, globulol, caryophyllene oxide, β -bisabolol	⁴⁴ Antimicrobial

<i>M. juliana</i>	¹⁰ (Traces) Luteolin, apigenin, chrysoeriol, diosmetin, acacetin, ³² <u>Caryophyllene-oxide</u> (11.2%), caryophellene, germacrene D, spathulenol, ³³ Ethanol extract: <u>apigenin</u> , <u>luteolin</u> , <u>rosmarinic acid</u> , chlorogenic acid, ⁴⁶ Essential oil: <u>α-Pinene</u> (8.9%), β -pinene, β -caryophyllene, α -gurjunene, linalool, ⁴⁷ Essential oil: <u>Verbenol</u> (11.8%), thymol, caryophyllene-oxide, borneol, myrtenal ^G , ⁴⁸ Successive extractions with petroleum ether, ethyl acetate, methanol: <u>Rosmarinic acid</u> , chlorogenic acid, rutin hydrate, caffeic acid, ⁴⁹ <u>Borneol</u> (9.3%), verbenols, furanoid linalool oxide ^H	³³ Ethanol extract: antioxidant (4 different methods), ⁴⁵ Antifungal (methanolic extract), ^{47,48} Antimicrobial
<i>M. lachnophylla</i>	⁴³ Essential oil: <u>Borneol</u> (22.0%), bornyl acetate, camphene, camphor, verbenone	Not reported
<i>M. lasiophylla</i>	⁴³ Essential oil: <u>Borneol</u> (24.9%), linalool, camphor, camphene, α -pinene	Not reported
<i>M. longipedunculata</i>	⁵¹ Essential oil: <u>Spathulenol</u> (33%), piperitone-oxide, piperitone, <i>p</i> -cymene, bicyclogermacrene	Not reported
<i>M. myrtifolia</i>	⁵² Essential oil: <u>trans-Caryophyllene</u> (15.5%), caryophyllene-oxide, hexadecanoic acid, caryophylla-3,8(13)-dien-5 β -ol, germacrene D	⁵² Antioxidant ⁵³ Antifungal ⁵⁴ Cytotoxic
<i>M. nervosa</i>	⁵⁵ <u>Carvacrol</u> , ⁵⁷ Acetone extract, chromatography: <u>Micromeriol</u> , <u>Nervosane</u> , ^I β -sitosterol, oleanolic acid, ursolic acid	⁴⁵ Antifungal (methanolic extract), ⁵⁵ Antimicrobial (various extracts and carvacrol), ⁵⁶ Antimicrobial (ethanolic extract), ⁵⁷ Antioxidant, cytotoxic (micromeriol)
<i>M. nubigena</i>	⁵⁸ Essential oil: <u>Thymol</u> (36.9%), carvacrol, pulegone, caryophyllene- oxide, <u>E-phytol</u>	⁵⁸ Antimicrobial (essential oil, thymol, carvacrol)
<i>M. parviflora</i>	¹⁰ (Traces) Luteolin, apigenin, chrysoeriol, diosmetin, acacetin ⁴⁹ <u>Spathulenol</u> (29.9%)	
<i>M. persica</i>	⁵⁹ Essential oil: <u>Thymol</u> (33.1%) ^J , γ -terpinene, limonene, 1,8-cineole, <i>p</i> -cymene	⁶⁰ Methanolic extract: antioxidant, antimicrobial
<i>M. pseudocroatica</i>	¹⁰ (Traces) Luteolin, apigenin, chrysoeriol, diosmetin, acacetin, ⁶¹ Essential oil: <u>Borneol</u> (23.8%), camphor, β -caryophyllene, caryophyllene-oxide, δ -cadinene	Not reported
<i>M. thymifolia</i>	¹⁰ Flavonoids (Thymonin, major), ¹¹ Essential oil: <u>Pulegone</u> (32.8%), piperitenone, piperitone, isomenthone, limonene, ³³ Ethanol extract: <u>apigenin</u> , luteolin, rosmarinic acid, chlorogenic acid	¹¹ Antibacterial, antifungal, ³³ Ethanol extract: antioxidant (4 different methods), ⁶² Antimicrobial
<i>M. varia</i>	⁴³ Essential oil: <u>Borneol</u> (19.2%), α -pinene, <u>E-Nerolidol</u> , camphene, camphor, ⁶³ Essential oil: <u>α-Pinene</u> (27.5%), geranial, <u>trans-nerolidol</u> , β -caryophyllene-oxide, β -caryophyllene	Not reported

A) Varieties and combinations are not presented. B) Selected bioactive compounds. C) In reference 16, *M. biflora* ssp. *arabica* K. Walth was studied, while reference 17 reported the results for *M. biflora* (Buch.-Ham. Ex D. Don) Benth. D) New compounds. E) The major compounds in the essential oils of *M. cristata*,^{31,32} are from the same subspecies but from different locations, and authors of reference 32 are aware of that. F) Authors of the article in reference 40 have reported the chemical compositions of *M. graeca* from two different locations, and these compositions are notably different. On the contrary, essential oils of two samples of *M. graeca* from two Croatian islands (Vis, Komiza) show same compositions.⁴¹ G) Even though *M. cristata* and *M. Juliana* from different locations yielded different essential oil compositions (reference 47) compared with previously cited articles, in all cases, antimicrobial activities were indicated. The major compounds found in *M. cristata* essential oil are: Isoborneol (11.3%), borneol, verbenone, 10-*epi*- α -cadinol, thujan-3-ol. H) Differences in essential oils compositions from micromeria subspecies from the same localities were the basis for Kremer *et al.* to determine that the closely related *M. juliana* and *M. kernerii* are different subspecies.⁵⁰ Other evidences were also provided. I) New compounds, see Figure 1. J) Concentrations are given before and during flowering season.

The presence of mono-, di- and sesqui-terpenes is notable. Pulegone, piperitenone, piperitenone-oxide, caryophyllene and caryophyllene-oxide(s) are major examples (see Figure 1).

In *M. cristata*, the presence of Borneol and its alcoholic functional group oxidation product, camphor (ketone), is very notable.³¹ The natural enantiomeric compositions of each one of these bicyclic compounds totally prefer the C1-S-configuration (C1, indicated in Figure 1), with 100% and 99% respectively. It is worth paying attention to the fact that various locations where these species grow have great influence on the chemical composition of borneol and bisabolol (Figure 1) in *M. cristata*.^{31,32}

Each one of these compounds is widely investigated with or without connection to the genus micromeria, and some of them (piperitenone-oxide, for example) are mentioned in several research articles. However, only medicinal activities connected with micromeria are mentioned. It is interesting to notice that some research workers studied even compounds with low concentrations like the isomeric citrals, geranial and neral (Figure 1).⁶⁴ Another interesting group of compounds present in the genus micromeria and widely studied is the group of polyphenolics (Figure 2). For clear polarity and molecular mass properties, polyphenols are not present in the essential oil of the plants, but can be obtained by extraction with polar solvents (water, ethanol, methanol).

Polyphenols are known for their powerful antioxidant capacities, and they are mostly tested for this property and its related activities such as anti-inflammatory and analgesic.

Finally, it is important to point out that there are some papers that have reported chemical compositions and biological activities of micromeria as well as other taxonomic affiliation such as *M. debilis*, known also as *Satureja debilis*. This plant is recently studied and its antimicrobial⁶⁵ essential oil has very close composition [β -Pinene (19.3%), geranial, linalool, germacrene, (*E*)- β -caryophyllene; similar to those from other micromeria species, but despite this, we did not include it in Table 1.

Micromeria fruticosa: from ethnomedicine to up-to-date research

Ethnomedicine

M. fruticosa is the well-known subspecies of the genus micromeria growing on the eastern coast of the Mediterranean, and some its uses are documented in various reports.. It is believed in the Palestinian society that drinking an infusion of *M. fruticosa* leaves and stalks helps in curing different types of paralysis, nervous system disorders and it has calming effect.⁶⁶ The use for treating nervous system disorders is mentioned in traditional Palestinian medicine along with other uses: treatments of diabetes, illnesses of respiratory system, especially cough, urinary diseases, headaches and fever.⁶⁷

Sheep and goats that suffer from diarrhoea are made to drink the infused leaves of *M. fruticosa*.⁶⁸ This use is similar to one of the uses of this plants for human therapy (see below, section 3).

Chemical composition of *M. fruticosa*

The chemical composition of *M. fruticosa* (and its many subspecies) has been thoroughly studied and published. The first notable fact is that this composition varies extensively according to subspecies and season of harvesting the plant samples. This and five other compounds that have high concentration of *M. fruticosa* are reported in Table 2. A careful study of the Table 2 reveals three important facts:

1) Unlike micromeria subspecies, mentioned in Table 1, in *M. fruticosa* essential oils, borneol is not one of the five and Carvacrol is over 200% and in the fruit ripening season (October-November), compounds can change "ranks" of concentration.

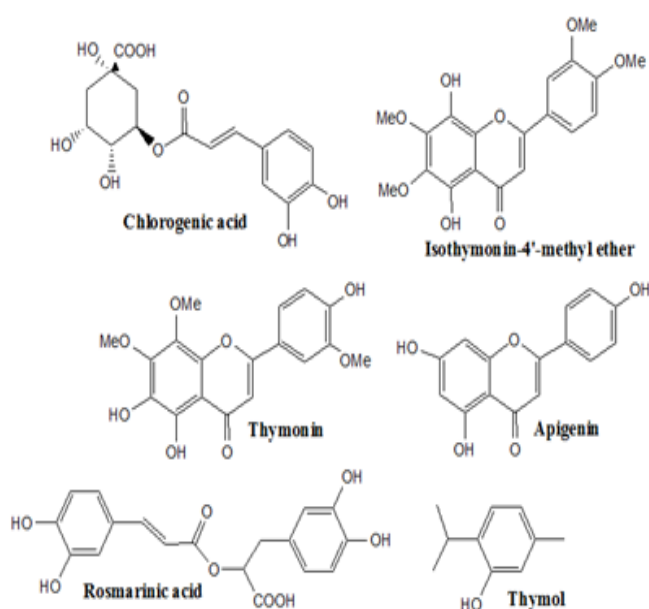


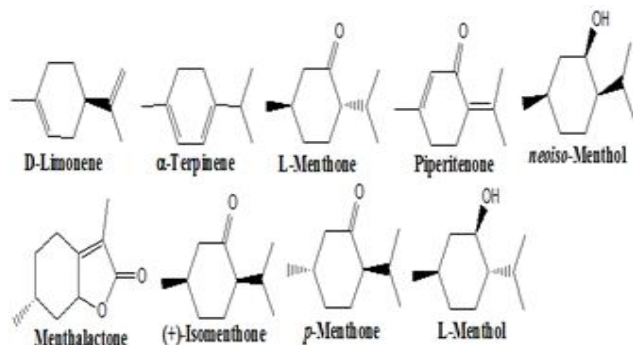
Figure 2. Structures of selected phenolic active compounds in *micromeria* ssp.

Table 2. Chemical compositions of *M. fruticosa*

Subspecies	Five compounds with highest concentration of essential oils (%)				
⁶⁹ <i>serpyllifolia</i>	pulegone 33.40	piperitenone 33.10	piperitenone oxide 4.18	spathulenol 3.15	6-allyl-2-cresol 33.07
⁷⁰ <i>giresunica</i>	pulegone 39.57	menthol 24.27	menthone 24.21	limonene 1.35	germacrene D 1.42
⁷¹ <i>serpyllifolia</i>	piperitenone 50.61	pulegone 29.19	isomenthone 3.92	α -pinene 0.79	limonene 0.68
⁷² <i>serpyllifolia</i>	linalool 30.29	pulegone 16.95	<i>p</i> -menthone 10.27	menthone 7.83	1,8-cineole 6.72
⁷² <i>brachycalyx</i>	linalool 39.92	piperitenone 31.93	pulegone 9.47	1,8-cineole 7.09	menthone 2.02
⁷³ No report July 2010	pulegone 30.41	limonene 15.64	menthalactone 10.28	menthone 7.39	menthol 5.27
⁷³ No report October 2010	menthalactone 33.89	pulegone 13.35	piperitone 13.35	guaiacol 9.97	menthone 5.13
⁷⁴ <i>serpyllifolia</i>	pulegone 58.50	<i>neoiso</i> -menthol 8.70	caryophyllene 3.90	isomenthone 3.90	α -terpinene 3.70

2) There is a clear majority of menth-sub-unit derived compounds as shown in Figure 3. See also closely related compounds shown in figure 1: pulegone, isomenthone and piperitenone-oxide (isomer).3) The variety in chemical composition and concentration of each ingredient is very wide.

Taking the example of *M. fruticosa* ssp. *Serpyllifolia*, Table 2, mentioned under the references 69, 71, 72, 74, differences are found in the five compounds with highest concentrations and the differences continue for the other compounds. Moreover, in the cited references the differences continue with materials that have lower concentrations, and sometimes, a compound reported in one reference as having significant concentration does not exist at all in other reference. In most cases, these differences are related to localities of plant collection and seasonal variety (see below). Obviously, the type of subspecies has great effect on the chemical composition, and it is clearly shown in reference 72.

**Figure 3.** Menth-sub-unit-derived major compounds in *M. fruticosa*

The seasonal effect on the chemical compositions of *M. persica*, reported in reference 59, is significant since it is related to the sampling before and during the flowering season of the plant. In reference 73 there is no indication of the subspecies of *M. fruticosa* that was analyzed, but the seasonal differences are very large.

Seasonal effect on plant composition is well reported and in some cases, it can be almost controlled. For example, the three compounds with the highest concentrations in *Satureja cuneifolia* (Syn. *Micromeria spicata* Rchb.) analyzed in Lebanon, shows seasonal fluctuations in the concentration of each compound according to the development of plants over six months (June-November 2011).⁷⁵ The change in the concentration of each compound (*p*-cymene, γ -terpinene

As can be seen in Figure 3, *M. fruticosa* contains wide variety of natural products that can be used and utilized as starting materials for organic synthesis and drug development. However, many of these compounds are structural isomers or even stereoisomers (menthone and *p*-menthone are enantiomers). Isomer purity is one of the key requirements for successful organic synthesis and many studies are published about methods of isomer separation. In Table 1 and Table 2, pulegone is reported to have high concentration in micromeria subspecies. Its (1R)(+)-pulegone isomer is separated as pure enantiomer by Cyclodex B chiral capillary column.⁷⁷ Chiral column is also used for GC-MS analysis of *cis*- and *trans*-piperitenone-oxide in *M. fruticosa* (and *Mentha longifolia*).⁷⁸ The findings of this research are interesting: Only enantiomerically pure laevo-rotatory piperitene oxides, (1*S*,2*S*,4*S*)-*trans*-piperitene-oxide and (1*S*,2*S*,4*R*)-*cis*-piperitene oxide, are detected by chiral analyses of *Micromeria fruticosa* (L.) Druce.

Table 3. Summary of the biological activities *M. fruticosa* compounds with highest concentrations.*Traditional uses, if mentioned, are indicated in brackets. Considering the variability of the chemical composition of *M. fruticosa*, efforts

Active material	Biological activities*
⁷¹ Essential oil;methanolic extract	Antimicrobial; antioxidant (Herbal tea, mint substitute, sedative, anaesthetic, antiseptic, abortifacient, antirheumatic, CNS-stimulant, treatment of heart disorders and colds)
⁷⁴ Essential oil;aqueous extract	Both: antitumor. Aqueous extract: analgesic (Treatment of abdominal pains, diarrhea, eye infections, heart disorders, elevated blood pressure, colds and wounds)
⁷⁹ Essential oil	Insecticidal, synergism with other plants essential oils (same as first row)
⁸⁰ Acetone extract	Antibacterial, acaricidal, synergism with other plants extracts (Given but not specified for single plant)
⁸¹ Essential oil	Insecticidal, synergism with other plants essential oils (same as first row)
⁸² Roots	Allelopathic: chemicals released by <u>living</u> plant's roots in soil
⁸³ Methanolic extract	Anti-inflammatory, myeloperoxidase inhibition (Abdominal pains relief, diarrhea, eye infections, heart disorders, high blood pressure, weariness, exhaustion, colds and open wounds)
⁸⁴ Essential oil	Anti microbial. Clear synergistic effect with standard antibiotics
⁸⁵ Aqueous extract	Anti-inflammatory, gastroprotective (Anti-inflammatory, wound healing, treatment abdominal pain and diarrhea)
⁸⁶ Essential oil	Anti-biofilm formation (streptococcus mutans), antimutagenic, antioxidant (Treatment of <i>stomach pain</i> , colic, uterine disorders, diarrhoea respiratory ailments, <i>coughs</i> , and colds)
⁸⁷ Ethanol extract	Animicrobial, antioxidant (Treatment of abdominal pains, diarrhea, colds, wounds and skin infections)

were made to control the concentrations of some biologically active compounds in the plant. One of these studies found clearly that artificial modification of growth conditions, mainly light hours, has negligible effect on the chemical composition of the plants, especially the monoterpene content.⁷⁶ On the contrary, the same study found that the stage of maturation has the largest effect on monoterpene content of the leaves of *M. fruticosa*. For example, the content of pulegone can be as high as 80% of the essential oil in summer time (August), and drops drastically in the winter.

The occurrence of the *cis*- and *trans*-piperitone-oxides is dependent on the population of the species. In all cases (1*S*,2*S*,4*S*)-*trans*-piperitone-oxide is detected together with (4*S*)-piperitone, while (1*S*,2*S*,4*R*)-*cis*-piperitone-oxide is detected together with (4*R*)-piperitone.

Biological activities of *M. fruticosa*

Many of the reported findings about the biological activities of *M. fruticosa* are similar to those of other subspecies. But since *M. fruticosa* is thoroughly studied, some reports present interesting results that were not reported for other subspecies (see **Table 3** below). Most articles that report findings of modern research of the biological activities of the plant, give some information about the traditional medical uses of folk medicines. Whether this linkage is evident or not, the results of modern researches are of high significance for modern medicine and drug discovery. This statement is supported

by the large number of natural products found in *M. fruticosa* and on the diverse biological activities that the plant and its ingredients have. The findings of modern researches are summarized in **Table 3** and the traditional uses of the plant, ~~hat were~~ mentioned in each reference, if any, is presented

D) Future inspirations

Plant based therapy has served humans since pre-historical era. In modern times, the study of medicinal plants and natural products has gone through intensive attention, and sometimes much less than that. The 2015 medicine Nobel prize is awarded to three scientists based on their pioneering achievements. These are based on drug discovery from natural products. This spirit and momentum of this excellence can and should inspire us, and the members of the micromeria family can provide us with many starting points.

Acknowledgement

The author is grateful to Prof. Hassan Azaizeh for his helpful remarks.

References

- ¹Bräuchler, C., Ryding, O., Heubl, G., *Willdenowia*, **2008**, *38*, 363.
- ²Naghibi, F., Mosaddegh, M., Motamed, S. M., Ghorbani, A., *Iran. J. Pharm. Res.*, **2005**, *2*, 63.
- ³Puppo, P., Meimberg, H., *Phytotaxa*, **2015**, *230*, 1.
- ⁴Said, O., Khalil, K., Fulder, S., Azaizeh, H., *J. Ethnopharmacol.*, **2002**, *83*, 251.
- ⁵Ali-Shtayeh, M. S., Jamous, R. M., Al-Shafie', J. H., Elgharabah, W. A., Kherfan, F. A., Qarariah, K. H., Khdaif, I. S., Soos, I. M., Musleh, A. A., Isa, B. A., Herzallah, H. M., Khlaif, R. B., Aiash, S. M., Swaiti, G. M., Abuzahra, M. A., Haj-Ali, M. M., Saifi, N. A., Azem, H. K., Nasrallah, H. A., *J. Ethnobiol. Ethnomed.*, **2008**, *4*, doi:10.1186/1746-4269-4-13.
- ⁶Saad, B., Said, O., *Greco-Arab and Islamic Herbal Medicine*. John Wiley & Sons, Inc., Hoboken, New Jersey. **2011**.
- ⁷Arslan, M., *Farmacia*, **2012**, *60*, 925.
- ⁸Khalifa, A. B. *Herbs: Nature's Pharmacy*, V1, 1st ed.; Arab Cultural Center: Casablanca, Morocco, 2004; pp. 286-288. (Arabic).
- ⁹Stojanovic, G., Palic, I., Ursic-Jankovic, J., *J. Essent. Oil Res.*, **1999**, *11*, 785.
- ¹⁰Tomas-Barberan, F. A., Gil, M. I., Marin, P. D., Tomas-Lorente, F., *Biochem. Syst. Ecol.* **1991**, *19*, 697.
- ¹¹Marinkovic, B., Marin, P. D., Knezevic-Vukcevic, J., Sokovic, D., Brkic, D., *Phytother. Res.*, **2002**, *16*, 336.
- ¹²Ghanem, N., El Hamaoui, B., El-Achi, N., Bakkour, Y., Alwan, S., Houmaisi, F., El-Nakat, J. H., El-Omar, F., *Int. J. Pharm. Chem.*, **2014**, *4*, 142.
- ¹³Bakkour, Y., Alwan, S., Soufi, H., El-Ashi, N., Tabcheh, M., El Omar, F., *J. Nat. Prod.*, **2012**, *5*, 116.
- ¹⁴Alwan, S., Soufi, H., Zreika, S., Sukarieh, I., *Int. J. Res. Med. Health Sci.*, **2015**, *5*, 29.
- ¹⁵Alwan, S., El Omari, K., Soufi, H., Zreika, S., Sukarieh, I., Chihib, N-E., Jama, C., Hamze, M., *J. Essent. Oil. Bear. Pl.*, **2016**, *19*, 321.
- ¹⁶Al-Rehaily, A. J., *Pak. J. Biol. Sci.* **2006**, *9*, 2726.
- ¹⁷Chandra, M., Prakash, O., Bachheti, R. K., Kumar, M., Pant, A. K., *J. Med. Plants Res.*, **2013**, *7*, 2338.¹⁸Khan, T., Mukhtarullah, Khan, M. S., Zabihullah, Inamullah, Irfanullah, Asghar, M., Khattak, S., Momin, F., Ahmad, I., Irshad, M., Ali Shah, S. W., *Int. J. Microbiol.*, **2015**, *1*, 1.
- ¹⁹Kumar, A., Gupta, R., Mishra, R. K., Shukla, A. C., Dikshit, A., *Natl. Acad. Sci. Lett.*, **2012**, *35*, 253.
- ²⁰Mishra, R. K., Kumar, A., Shukla, A. C., Tiwari, P., Dikshit, A., *J. Ecobiotechnol.*, **2010**, *2*, 22.
- ²¹Anitha, A., Sreedevi, P., Arunkumar, D., *Global J. Pharmacol.*, **2013**, *7*, 429.
- ²²Ambreen, M., Ahmad, M., *Sci. Int. (Lahore)*, 2015, *27*, 6087.
- ²³Zeb, M. A., Wahab, A., Ullah, N., Jabbar, A., Pandey, S., Muhammad, T., *Int. J. Med. Biomed. Sci.*, **2015**, *1*, 28.
- ²⁴Uddin, G., Rauf, A., Bina Shaheen Siddiqui, B. S., Khan, H., Barkatullah, Ullah, R., *Pak. J. Pharm. Sci.*, **2016**, *29*, 929.
- ²⁵Duru, A. E., Öztürk, M., Ugur, A., Ceykan, Ö., *J. Ethnopharmacol.*, **2004**, *94*, 43.
- ²⁶Ozturk, M., Kolak, U., Topcu, G., Oksuz, S., Choudhary, M. I., *Food Chem.*, **2011**, *126*, 31.
- ²⁷Kirimer, N., Özek, T., Baser, K. H. C., *J. Essent. Oil Res.*, **1991**, *3*, 387.
- ²⁸Herken, E. N., Celik, A., Aslan, M., Aydinlik, N., *J. Med. Food*, **2012**, *15*, 835.
- ²⁹Baser, K. H. C., Demircakmak, B., *J. Essent. Oil Res.*, **1997**, *9*, 725.
- ³⁰Dulger, B., *Asian J. Chem.*, **2008**, *20*, 6518.
- ³¹Tabanca, N., Kirimer, N., Demirci, B., Demirci, F., Baser, H., C., *J. Agric. Food Chem.* **2001**, *49*, 4300.
- ³²Kostadinova, E., Alipieva, K., Stefova, M., Stafilov, T., Antonova, D., Evstatieva, L., Matevski, V., Kulevanova, S., Stefkov, G., Bankova, V., *Maced. J. Chem. Chem. En.*, **2007**, *26*, 3.
- ³³Vladimir-Knežević, S., Blažeković, B., Štefan, M. B., Alegro, A., Kőszegi, T., Petrik, J., *Molecules*, **2011**, *16*, 1454.
- ³⁴Samec, D., Gruz, J., Durgo, K., Kremer, D., Kosalec, I., Zulj, L. V., Martinez, S., Salopek-Sondia, B., Piljac-Zegarac, J., *Nat. Prod. Res.* **2015**, *29*, 1770.
- ³⁵Vladimir-Knežević, S., Cvijanović, O., Blažeković, B., Kindl, M., Bival Štefan, M., Domitrović, R., *BMC Complement. Altern. Med.*, **2015**, 12 Pages, DOI: 10.1186/s12906-015-0763-8
- ³⁶Karousou, R., Hanlidou, E., Lazari, D., *Chem. Biodives.* **2012**, *9*, 2775.
- ³⁷Bukvicki, D., Stojkovic, D., Sokovic, M., Nikolic, M., Vannini, L., Montanari, C., Marin, P. D., *LWT-Food Sci. Technol.*, **2015**, *63*, 262.
- ³⁸Baser, K. H. C., Kirimer, N., Duman, H., *Flavour Fragr. J.*, **1997**, *12*, 289.
- ³⁹Formisano, C., Mignola, E., Rigano, D., Senatore, F., Bellone, G., Bruno, M., Rosselli, S., *Flavour Fragr. J.* **2007**, *22*, 289.
- ⁴⁰Tzakou, O., Couladis, M., *Flavour Fragr. J.*, **2001**, *16*, 107.
- ⁴¹Vuko, E., Dunkić, V., Bezić, N., Ruscic, M., Kremer, D., *Nat. Prod. Commun.* **2012**, *7*, 1227.
- ⁴²Scognamiglio, M., D'Abrosca, B., Esposito, A., Fiorentino, A., *J. Anal. Methods Chem.*, **2015**, Article ID 258570, 9 pages, <http://dx.doi.org/10.1155/2015/258570>
- ⁴³Perez-Alonso, M. J., Velasco-Negueruela, A., Gil-Pinilla, M., Perez De Paz, P. L., Vallejo, C. G., Esteban, J. L., *Biochem. Syst. Ecol.*, **1996**, *24*, 571.
- ⁴⁴Benomari, F. Z., Djabou, N., Medbouhi, A., Khadir, A., Bendahou, M., Selles, C., Desjobert, J-M., Costa, J., Muselli, A., *Chem. Biodives.*, **2016**, In press, doi: 10.1002/cbdv.201600098
- ⁴⁵Abou-Jawdah, Y., Warden, R., Sobh, H., Salameh, A., *Phytopathol. Mediterr.*, **2004**, *43*, 377.
- ⁴⁶Mastelić, J., Jerković, I., Kuštrak, D., *J. Essent. Oil Res.*, **2005**, *17*, 516.
- ⁴⁷Stojanović, G., Palić, I., Ursić-Janković, J., *Flavour Fragr. J.*, **2006**, *21*, 77.
- ⁴⁸Askun, T., Tekwu, E. M., Satil, F., Modanlioglu, S., Aydeniz, H., *BMC Complement. Altern. Med.*, **2013**, 11 Pages, <http://www.biomedcentral.com/1472-6882/13/365>.
- ⁴⁹Palić, I., Ursić-Janković, J.,⁴⁷Stojanović, G., *J. Essent. Oil Res.*, **2010**, *22*, 40.

- ⁵⁰Kremer, D., Dunkić, V., Rusčić, M., Matevski, V., Ballian, D., Bogunić, F., Eleftheriadou, E., Stesević, D., Kosalec, I., Bezić, N., Stabentheiner, E., *Phytochemistry*, **2014**, 98, 128.
- ⁵¹Kremer, D., Dunkić, V., Stesević, D., Kosalec, I., Ballian, D., Bogunić, F., Bezić, N., Stabentheiner, E., *Cent. Eur. J. Biol.*, **2014**, 9, 559.
- ⁵²Formisano, C., Oliviero, F., Rigano, D., Saab, A. M., Senatore, F., *Ind. Crops Prod.*, **2014**, 62, 405.
- ⁵³Ozcan, M., *Acta Aliment. Hung.*, **1999**, 28, 355.
- ⁵⁴Al-Samarraei, K. W., Al-Naimv. E. H., Al-Lihaibi. R. K., Al-Ani, R. S., *Iraqi J. Market Res. Consumer Protect.*, **2011**, 3, 131.
<http://repository.uobaghdad.edu.iq/ArticleShow.aspx?ID=1237>.
- ⁵⁵Ali-Shtayeh, M. S., Al-Nuri, M. A., Yaghmour, R., M.-R., Faidi, Y. R., *J. Ethnopharmacol.*, **1997**, 58, 143.
- ⁵⁶Khalil, A., Dababneh, B. F., Al-Gabbiesh, A. H., *J. Food. Agric. Environ.*, **2009**, 7, 103.
- ⁵⁷Abdelwahab, M. F., Hussein, M. H., Kadry, H. H., *Bull. Fac. Pharm. (Cairo Univ.) [ZDB]*, **2015**, 53, 185.
- ⁵⁸El-Seedi, H. R., Khattab, A., Gaara, A. H. M., Mohamed, T. K., Hassan, N. A., El-kattan, A. E., *J. Essent. Oil Res.*, **2008**, 20, 452.
- ⁵⁹Sefidkon, F., Kalvandi, R., *Flavour Fragr. J.*, **2005**, 20, 539.
- ⁶⁰Sonboli, A., *Research Journal of Pharmacognosy*, **2015**, 2, 27.
http://rjpharmacognosy.ir/article_10997_483102615727a5fa10e3785a8c6cc582.pdf.
- ⁶¹Kremer, D., Müller, I. D., Stabentheiner, E., Vitali, D., Koprčanec, M., Rusčić, M., Kosalec, I., Bezić, N., Dunkić, V., *Nat. Prod. Commun.*, **2012**, 7, 1667.
- ⁶²Marin, M. A., Novaković, M. M., Tesević, V. V., Kolarević, S. M., Vuković-Gaćić, B. S., *J. BioSci. Biotechnol.* **2015**, 4, 29.
- ⁶³Pedro, L. G., Figueiredo, A. C., Barroso, J. G., Fontinha, S. S., Looman, A., Scheffer, J. J. C., *Flavour Fragr. J.*, **1995**, 10, 199.
- ⁶⁴Li, K-P., Jiang, J-M., Chen, C-Z., Lao, B-T., *Physical Testing and Chemical Analysis (Part B: Chemical Analysis)*, **2011**, 829.
http://en.cnki.com.cn/Article_en/CJFDTotal-LHJH201107031.htm
- ⁶⁵Gherib, M., Bekhechi, C., Paoli, M., Bekkara, F. A., Bighelli, A., Casanova, J., Tomi, F., *J. Essent. Oil Res.*, **2016**, 28, 383.
- ⁶⁶Abu-Rabia, A., *Chin. Med.*, **2012**, 3, 157.
- ⁶⁷Ali-Shtayeh, M. S., Jamous, R. M., *Traditional Arabic Palestinian Herbal Medicine, TAPHM.*, BERC, Nablus, Palestine, **2008**.
- ⁶⁸Landau, S. Y., Muklada, A., Abu-Rabia, A., Kaadan, S., Azaizeh, H., *Small Ruminant Res.*, **2014**, 119, 161.
- ⁶⁹Kirimer, N., Özek, T., Baser, K. H. C., *J. Essent. Oil Res.*, **1993**, 5, 199.
- ⁷⁰Baser, K. H. C., Kirimer, N., Özek, T., Tümen, G., Karer, F., *J. Essent. Oil Res.*, **1996**, 8, 699.
- ⁷¹Güllüce, M., Sökmen, M., Sahin, F., Sökmen, A., Adigüzel, A., Özer, H., *J. Sci. Food Agric.*, **2004**, 84, 735.
- ⁷²Telci, I., Ceylan, M., *Chem. Nat. Compd.*, **2007**, 43, 629.
- ⁷³Al-Hamwi, M., Bakkour, Y., Abou-Ela, M., El-Lakany, A., Tabcheh, M., El-Omar, F., *J. Nat. Prod.*, **2011**, 4, 147.
- ⁷⁴Shehab, N. G., Abu-Gharbieh, E., *Pak. J. Pharm. Sci.*, **2012**, 25, 687.
- ⁷⁵El Beyrouthy, M., Cazier, F., Arnold, N. A., Aboukais, A., *J. Essent. Oil Res. Pl.*, **2015**, 18, 908.
- ⁷⁶Dudai, N., Larkov, O., Ravid, U., Putievsky, E., Lewinsohn, E., *Ann. Bot.*, **2001**, 88, 349.
- ⁷⁷Ravid, U., Putievsky, E., Katzir, E., *Flavour Fragr. J.*, **1994**, 9, 205.
- ⁷⁸Larkov, O., Matasyoh, J. C., Dudai, N., Lewinsohn, E., Alfred A. Mayer, A.A., Ravid, U., *Flavour Fragr. J.*, **2007**, 22, 328.
- ⁷⁹Aslan, I., Calmasur, O., Sahin, F., Caglar, O., *J. Plant Dis. Protect.*, **2005**, 112, 257.
- ⁸⁰Sagdic, O., Yasar, S., Kisioglu, A. N., *Ann. Microbiol.*, **2005**, 55, 67.
- ⁸¹Calmasur, O., Aslan, I., Sahin, F., *Ind. Crops Prod.*, **2006**, 23, 140.
- ⁸²Dudai, N., Chaimovitsh, D., Larkov, O., Fischer, R., Blaicher, Y., Mayer, A. M., *Plant Soil*, **2009**, 314, 311.
- ⁸³Abu-Gharbieh, E. F., Bustanji, Y. K., Mohammad, M. K., *J. Pharm. Res.*, **2010**, 3, 2492.
- ⁸⁴Toroglu, S., *J. Env. Biol.*, **2011**, 32, 23.
- ⁸⁵Abu-Gharbieh, E., Shehab, N. G., Khan, S. A., *Pak. J. Pharm. Sci.*, **2013**, 26, 799.
- ⁸⁶Boran, R., Ugur, A., *Journal of Selcuk University Natural and Applied Science*, **2015**, 4, 25.
<http://www.josunas.org/login/index.php/josunas/article/view/581>.
- ⁸⁷Al-Hamwi, M., Abou-Ela, M., El-Lakany, A., El-Achi, N., Ghanem, N., El Hamaoui, B., Bakkour, Y., El-Omar, F., *Int. J. Chem. Sci.*, **2015**, 13, 325.

Received: 09.08.2016.

Accepted: 15.09.2016.



CORROSION PROTECTION OF CARBON STEEL IN SEAWATER BY ALUMINA NANOPARTICLES WITH POLY(ACRYLIC ACID) AS CHARGING AGENT

Haider Abdulkareem Yousif Almashhdani^{[a]*} and Khulood Abid Al-Saadie^[b]

Keywords: Alumina, carbon steel, AFM, nanoparticle, polyacrylic acid, corrosion.

Nanostructured Al₂O₃ in 60-80 nm diameter has been deposited on carbon steel substrates, by cathodic electrophoretic deposition (EPD), in ethanol with poly(acrylic acid) (PAA) as charging agent, as a protective coating against corrosion for carbon steel (C.S.) in seawater environment. Potentiodynamic polarization measurements performed on the Al₂O₃ coated carbon steel coated by Al₂O₃ in 3.5 % NaCl at temperature range 298-328 K and the result showed that using PAA charging agent lead to increase the corrosion resistance.

*Corresponding Authors

Email: H_R200690@yahoo.com

[a] Al-Rasheed University College, Department of Dentistry, Baghdad, Iraq

[b] University of Baghdad, College of Science, Department of Chemistry, Baghdad, Iraq

Introduction

Corrosion is a natural phenomenon and is accompanied by the flow of electrical current involving the reversion from metallic to compound state. So it becomes clear that corrosion cannot be fully prevented instead it can be controlled to a greater extent. Many researchers have used various methods in corrosion prevention investigations, such as coated metal surfaces by nanoparticles.

The use of particles in nano scale could also change the microstructure of the electrodeposits leading to a more compact structure and thus to improved corrosion resistance.^{1,2} Nanoparticle coatings possess good thermal and electrical properties and they are resistant to oxidation, corrosion, erosion and wear in high temperature environments.³ These properties are very important factors in the applications such as pipelines, castings and automotive industry.

Electrophoretic deposition (EPD) is one of the liquid coating methods,⁴⁻⁶ which elaborates stable suspensions of Al₂O₃ particles in an appropriate liquid. Both sparse Al₂O₃ particles and dense particle coating layers on metal surface have been invented. Generally, EPD consists of two processes, i.e. the movement of charged particles in suspension in an electric field between two electrodes and the particle deposition on one of the electrodes to be protected. The mechanism of the formation of a deposit during EPD is reviewed and discussed in several theoretical papers and reviews.⁷⁻⁹

The insufficiency of surface charge and excessive weight potentially can be overcome through the use of polymeric charging agents, EPD with ethanol as suspension medium and poly(acrylic acid) (PAA) as polymeric charging agent give

good protection. Further, these polymeric charging agents play an important role as binders to improve adhesion between deposited particles and substrate.^{9,10}

The aim of the present work was to examine the efficiency of Al₂O₃ nanoparticles (NPs) to protection of carbon steel (C.S.) using absolute ethanol as suspension medium and a PAA polymeric charging agent.

Experimental

Materials

The steel used in this study is a carbon steel (C45) with a chemical composition (in wt %) of 0.42 % C, 0.40 % Si, 0.50 % Mn, 0.045 % S, 0.40 % Cr, 0.045 % P, 0.40 % Ni, 0.01 % Mo and the remainder is iron (Fe). The carbon steel samples were pre-treated prior to the experiments by grinding with emery paper SiC (120, 600 and 1200); rinse with distilled water, degreased in acetone, washed again with distilled water and then dried at room temperature before used synthesized seawater. The seawater solution was prepared by dissolved 35 g NaCl in 1L distilled water. Al₂O₃ Nanoparticles were used in diameter range (20-30nm, Hongwu nanometer, purity 99.9%) and iodine was used in 99.8% purity (Aldrich).

Preparation of emulsion solution

Emulsion solution was prepared by adding 1 % Al₂O₃ NPs powder to ethanol as solvent¹⁶ (adding 1.5 g NPs to 150 mL ethanol). To study the effect of adding different percentages of PAA (0.1, 0.25, 0.5 and 1%) in emulsion solution (0.1, 0.25, 0.5 and 1g) of PAA was added to 100 mL ethanol respectively.

To homogenize the solution, an ultrasonic (50 W) stirrer was used to mixed the solution for 30 min. The solutions were applied for coating C.S. pieces by using EPD technique method. Sometime few iodine crystals were added to increase conductivity.¹¹

Electrophoresis deposition of emulsion solution (coating samples)

To deposit emulsion solution on a piece of C.S. surfaces, deposition cell device was used. The electrodes were connected to a D.C power supply, it can be used in anodic or cathodic deposition by reversing electrodes of the power supply.¹² The deposition cell device composed of the following components: A beaker of 250 mL capacity and the cover contains two slit with distance between them equal to 1 cm. Power supply used to supply constant direct current D.C voltage was varied between 0 and 20 V. An electrical circuit was connected by ammeter, respectively, to measure the current generated between the poles. Stainless steel rod used as inert electrode in deposition process cell.¹³ A piece of carbon steel catch by tong made of stainless steel fixed with 1cm distance between it and inert electrode.

The deposition on C.S. specimens were carried for 3, 4, 5 and 6 minutes, then all specimens thermally dried at 150 °C for 2 min.

Electrochemical measurements

The electrochemical measurements were carried out using Mlab (Germany, 2000) potentiostat and controlled by a computer and MLabSci software which were used for data acquisition and analysis under static condition. The corrosion cell used had three electrodes, the reference electrode was a silver- silver chloride, platinum electrode was used as auxiliary electrode with 1 cm² surface area and the working electrode was carbon steel. All potentials given in this study were referred to this reference electrode. The working electrode was immersed in test solution for 15 min to establish steady state open circuit potential (E_{ocp}), then electrochemical measurements were performed in potential range (± 200) mV. All electrochemical tests have been performed in aerated solutions at 208-328 K.

Results and discussion

Effect of time

The deposition on C.S. specimens were carried for (3, 4, 5 and 6) minutes, to study the effect of time on the deposition on C.S. specimens and chose the optimization time for deposition to get high protection efficiency. The perfect time for coated C.S. by Al₂O₃ NPs using EPD technique was 6 min, which gave percentage of protection efficiency (PE %) as 83.9 % at 298 K as shown in Figure 1.

Polarization curve

Figure 2 shows the polarization curves for the corrosion of carbon steel coated with Al₂O₃ NPs in absence and presence of various amounts of PAA. It could be observed that both the cathodic and anodic reactions were suppressed with the addition of different amounts of PAA, which suggests that coating by Al₂O₃ in the absence PAA lead the polarization curve shifting to more positive value (less active) reach to -730.0 mV at 328 K but when PAA was added in different

concentration, the value of corrosion potential shifted to more active value but don't reach to the corrosion potentials of uncoated C.S.

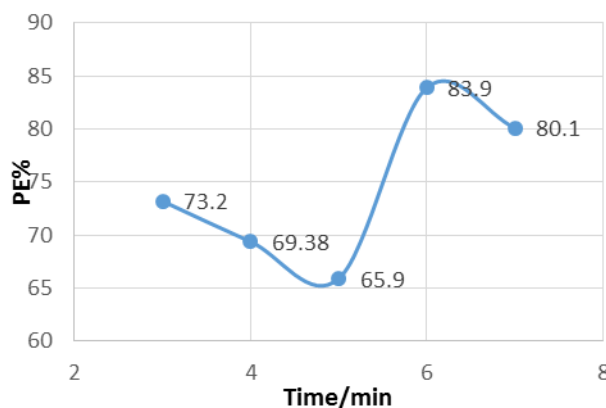


Figure 1. Relationship between PE% and coating time for coated C.S. by Al₂O₃ NPs at 298K.

PE % of all types of coating estimated by comparison with the measurements of the uncoated surface of carbon steel alloy using Eqn. (1).

$$PE \% = \frac{(i_{\text{corr uncoated}}) - (i_{\text{corr coated}})}{(i_{\text{corr uncoated}})} \times 100 \quad (1)$$

where $i_{\text{corr uncoated}}$ and $i_{\text{corr coated}}$ are corrosion current densities for uncoated and coated specimen, respectively.

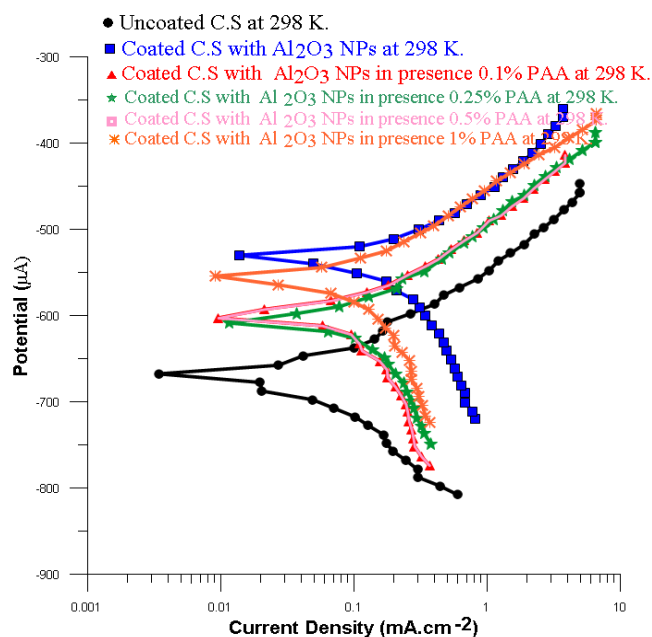


Figure 2. Polarization curves for C.S. in 3.5 % NaCl for uncoated and coated C.S. with Al₂O₃ NPs in absence and presence of PAA.

Effect of PAA

The thickness of coat layer on C.S. surface can be measured using eqn. (2)

$$\rho = \frac{Wt}{V} \quad (2)$$

where ρ is the density of NPs, Wt is weight of the coat and V is volume of the coat.

$$V = r^2 \times 3.14 \times d \quad (3)$$

where r is the radius of C.S. piece and d is thickness of the coat.

The effect of adding different PAA concentration in the Al₂O₃ NPs suspension solution, were investigated. PAA lead to decrease the thickness of Al₂O₃ layers from 14.424 μm in the absence PAA to thickness ranging between 11.1 and 11.8 μm in presence of different concentration of PAA, as shown in Figure 3.

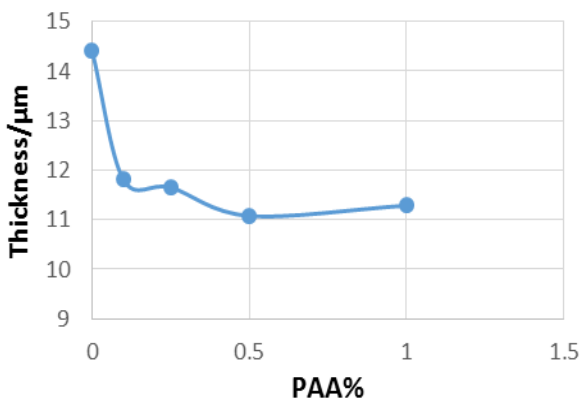


Figure 3. Relation between thickness and PPA % after 6 min coating time with Al₂O₃.

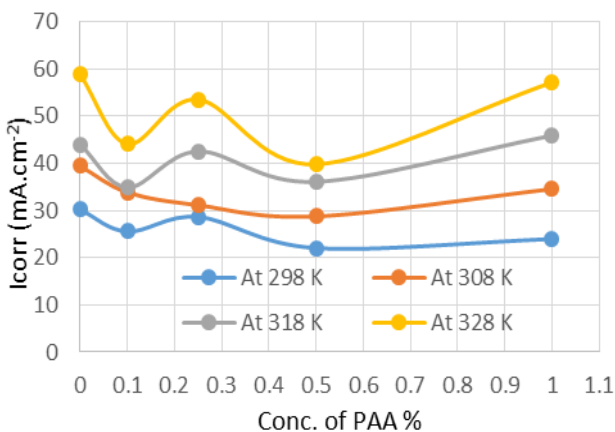


Figure 4. Effect of adding different PAA % to Al₂O₃ NPs coating suspension on i_{corr} .

Adding 0.5 % of PAA for the suspension of Al₂O₃ coating lead to the lowest i_{corr} value in temperature range of 298- 328 K, as shown in Figure 4. So the best PE % was obtained in presence of 0.5 % PAA at 298 K. So 0.5 % PAA is the right concentration for addition to suspension solution of coating which give PE % ranging between 87–85 % in the temperatures range of 298- 328 K, as shown in Figure 5.

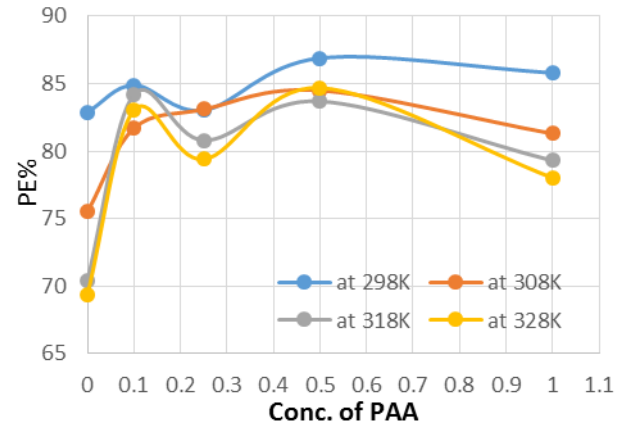


Figure 5. Effect of adding different PAA % to Al₂O₃ NPs coating suspension on PE %.

Surface Morphology

The morphologic analysis by AFM for layers of Al₂O₃ NPs without PAA and for Al₂O₃ NPs with 0.5 % PAA was done.

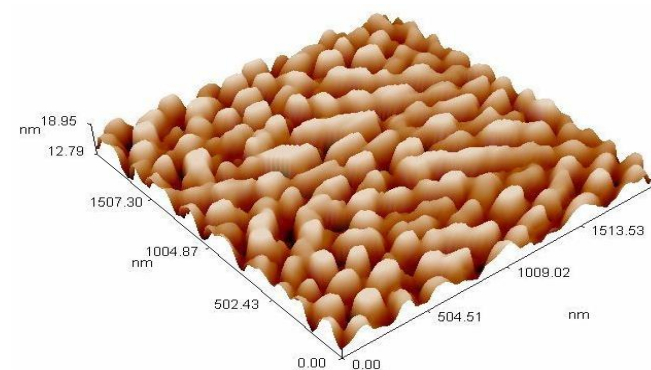
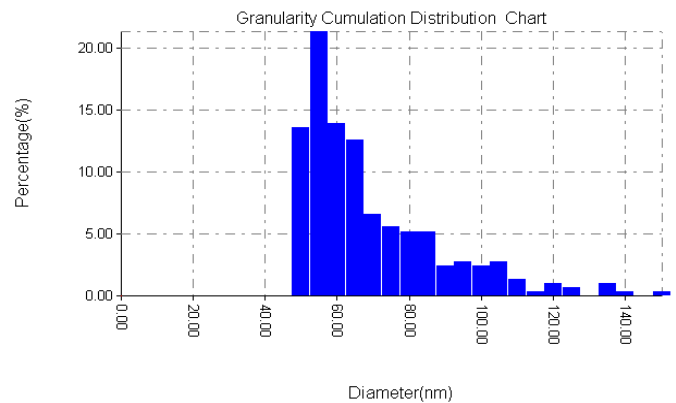


Figure 6. Granularity Cumulation Distribution and 3D views of AFM image of Al₂O₃ without PAA applied on carbon steel.

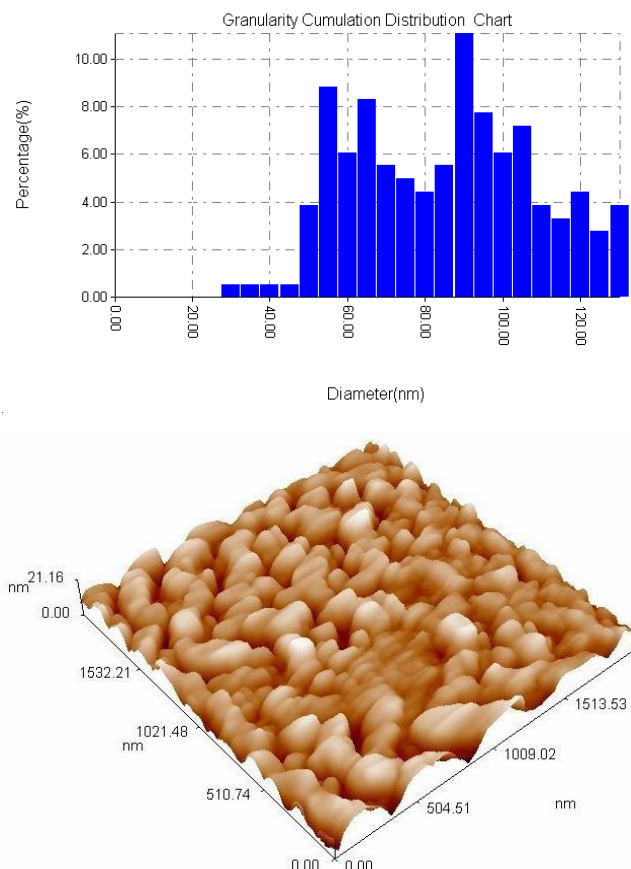


Figure 7. Granularity Cumulation Distribution and 3D views of AFM image of Al₂O₃ with PAA applied on carbon steel.

Since we started with alumina particles of 20-30 nm in diameter, AFM images shows little largest average particles sizes for the Al₂O₃ NPs without PAA and Al₂O₃ NPs with 0.5 % PAA, as shown Figures 6 and 7 respectively, and it reached around 66 nm and 82 nm respectively.

FT-IR Spectroscopy

Fourier transformation infrared spectra for Al₂O₃ NPs deposition on C.S. in presence PAA and the pure PAA show a multi peak band at 3304-3350 cm⁻¹ which indicates the presence of the OH group or N-H, which was not shown in the spectrum of pure PAA, also it shows a peak at 1735-1793 cm⁻¹ due to the presence of the carbonyl group for ketone. In this spectrum, there are bands at 1176 and 1172 cm⁻¹ indicating the presence of C=H groups.

Table 1. Wave number of FT-IR adsorption for pure PAA. and PAA/Al₂O₃ coat in C.S..

Pure PAA	Al ₂ O ₃ NPs deposition in presence PAA	Assignment
Wave number, cm ⁻¹	Wave number (cm ⁻¹)	
-	3401,13	OH stretch
3143	3350	OH stretch
1436	1458	C-O stretch
1176	1172	C=N stretch
1735	1739	C=O stretch

Surface porosity

Surface porosity percentage fraction was estimated by potentiostatic polarization. In this case, the porosity percentage (*P* %) can be calculated using the following equation:

$$P\% = \frac{R_{p,\text{uncoated}}}{R_{p,\text{coated}}} 10^{-\left(\frac{\Delta E_{\text{corr}}}{\beta_a}\right)} \times 10 \quad (4)$$

where $R_{p,\text{uncoated}}$ and $R_{p,\text{coated}}$ are the polarization resistances of the uncoated C.S. and the coating C.S. by NPs, respectively, ΔE_{corr} is the corrosion potential difference between them, and β_a is the anodic Tafel coefficient of the uncoated C.S..

In general, adding PAA increase surface porosity percentage (*P* %) for coated C.S. by Al₂O₃ NPs at all concentration of PAA, 1 % PAA lead to higher *P*% which reach to 32.5 % at 328 K, as shown in Figure 8.

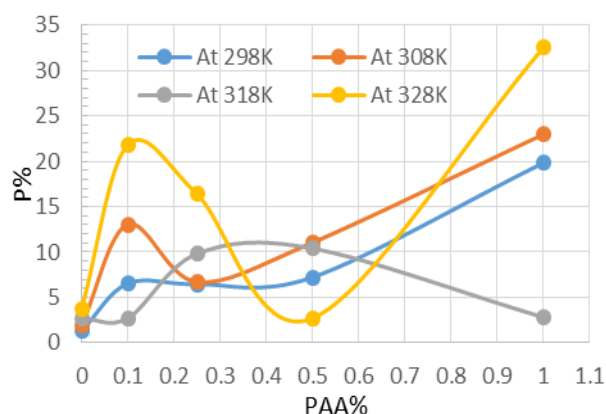


Figure 8. Variation of porosity percentage *P*% with PAA % at different temperatures.

Kinetic studies

The corrosion reaction can be regarded as an Arrhenius modified Arrhenius equation.¹⁷

$$\log i_{\text{corr}} = \log A - E_a/2.303RT \quad (5)$$

where i_{corr} is the corrosion current density, E_a is the apparent activation energy of the corrosion reaction, R is the gas constant, T is the absolute temperature and A is the Arrhenius pre-exponential factor. Figure 9 presents the Arrhenius plots of the natural logarithm of the current density vs. $1/T$, for C.S. samples uncoated and coated C.S. by Al₂O₃ in presence and absence of different concentrations of PAA, in artificial seawater.

Values E_a and A for the corrosion reaction in the absence and presence of different concentrations of the PAA are calculated by a linear regression method and given in Table 2.

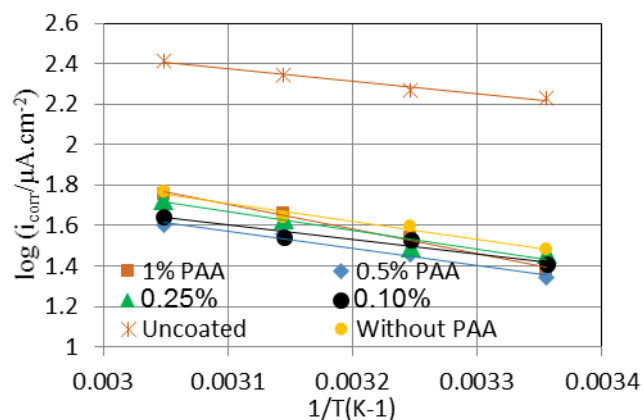


Figure 9. $\log i_{\text{corr}}$ vs $1/T$ for coated C.S. with Al₂O₃ NPs in absence and presence of different PAA % in 3.5 % NaCl.

It is found that the activation energy is increased after coating C.S. by Al₂O₃ in absence and presence PAA, and a higher value was obtained when C.S. coated with Al₂O₃ in presence 1 % PAA which reach to 23.54 kJ mol⁻¹. But Value of A increase slightly when C.S. is coated.

Table 2. Kinetic parametera for C.S. coated with Al₂O₃ in absence and presence of different PAA % in 3.5 % NaCl.

	Conc.	E_a kJ mol ⁻¹	A Molecules cm ⁻² s ⁻¹
Coated by Al ₂ O ₃	Uncoated	12.33	1.32 x 10 ²⁸
	Without PAA	20.10	3.271 x 10 ²⁸
	(0.1%) PAA	12.33	3.79 x 10 ²⁸
	(0.25%) PAA	17.69	2.02 x 10 ²⁸
	(0.5%) PAA	16.30	9.9 x 10 ²⁷
	(1%) PAA	23.54	1.9 x 10 ²⁹

E_a increases with coated C.S. by Al₂O₃ in absence and presence PAA, it is obvious that thin layer of coat is playing a role in increasing the activation energy value, thereby indicating a more efficient inhibiting effect. According to eqn. (5) low values of A and high values E_a lead to lower corrosion rates. For the present study, there is some lower in the E_a values in presence of (0.1-0.5 %) PAA. Therefore, the decrease in the carbon steel corrosion rate is controlled by the pre-exponential factor A.

Thermodynamic studies

The values of thermodynamic parameters are presented in table 3 where the value of ΔG calculated from its dependence on corrosion potential (Eqn. 6).

$$\Delta G = -nFE_{\text{corr}} \quad (6)$$

The entropy (ΔS) and enthalpy (ΔH) are obtained from the slope and intercept respectively, of the plot of ΔG vs $T\Delta S$ (Figure 10). The value of ΔG indicates that the coated C.S. functions by a chemical process on the surface of the metal. Generally, the values of ΔG up to -20 kJ mol⁻¹ are consistent

with electrostatic interaction between charged molecules and a charged metal (physical process), while those more negative than -40 kJ mol⁻¹ involve charge sharing or transfer from the inhibitor molecules to the metal surface, to form a co-ordinate type of bond (chemical process).¹⁴

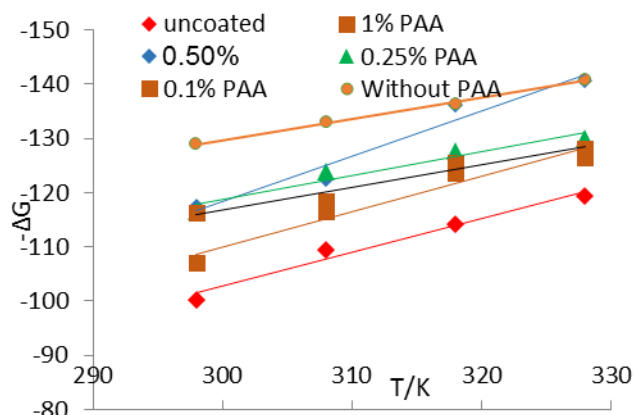


Figure 10. Plot of $-\Delta G$ vs T for coated C.S. with Al₂O₃ NPs in absence and presence of different PAA % in 3.5 % NaCl.

Table 3. Thermodynamic parameter for the coated C.S..

	Conc.	$-\Delta G_{\text{avg}}$ kJ mol ⁻¹	$-\Delta H_{\text{avg}}$ kJ mol ⁻¹	$-\Delta S$ J K ⁻¹ mol ⁻¹
Coated by Al ₂ O ₃	Uncoated	110.86	304.55	618.6
	Without PAA	136.66	257.06	390.8
	(0.1%) PAA	122.17	254.22	421.9
	(0.25%) PAA	124.52	262.61	441.2
	(0.5%) PAA	129.24	389.53	831.6
	(1%) PAA	118.40	323.26	654.5

The negative sign of the ΔG obtained indicates that the process is spontaneous, while the negative sign of ΔS indicates that a process is accompanied by a decrease in entropy.¹⁵

Conclusion

Coating C.S. with alumina nanoparticles act as a good protecting thin layer to save it from corrosion, which give PE% reach to 82 %. The rate of corrosion increased with increasing temperatures ranged from 298 to 328 K. Adding PAA in suspension solution of coating act as stabilizer agent, which were adsorbed onto the surfaces of ceramic particles which, could generate steric and electrostatic stabilization and prevent particles agglomeration. PAA additives increase the PE % which reaches up to 87 % with 0.5 % of PAA. The surface porosity percentage, P %, generally increase with increasing temperature, and adding increasing amounts PAA increase the P % as P % depended on R_p and E_{corr} . The activation energy for the corrosion of coated C.S. is increased. The corrosion is a spontaneous and exothermic reaction (values of both ΔG and ΔH are negative). The AFM images of layer particles detection that Particles size increase after coated by different NPs in all cases.

References

- ¹Arman, S. R., *Compos. Sci. Technol.*, **2011**, 471, 203.
- ²Vaezi, M. R., Sadrnezhad, S. K., Nikzad, L., *Colloids Surf., A*, **2008**, 315, 176.
- ³Saji, V. S., Joice T., *Curr. Sci.*, **2007**, 92, 51-55.
- ⁴Ishihara, T., Sato, K., Takita, Y., *J. Am. Ceram. Soc.*, **1996**, 79, 913-919.
- ⁵Xu, Z., Rajaram, G., Sankar, J., Pai, D., *Surf. Coat. Technol.*, **2006**, 201, 4484-4488.
- ⁶Vander, B. O., and Vandeperre, L. J., *Ann. Rev. Mater. Sci.*, **1999**, 29, 327-352.
- ⁷Sarkar, P., Nicholson, P. S., *J. Am. Ceram. Soc.*, **1996**, 79, 1987-2002.
- ⁸Corni, I., Ryan, M. P., Boccaccini, A. R., *J. Eur. Ceram. Soc.*, **2008**, 28, 1353-1367.
- ⁹Besra, L., Liu, M., *Prog. Mater. Sci.*, **2007**, 52, 1-61.
- ¹⁰Zhitomirsky, I., *Adv. Colloid Interface Sci.*, **2002**, 97, 277-315.
- ¹¹Dor, S., Ruhle, S., Ofir, A., Adler, M., Grinis, L., Zaban, A., *J. Phys. Chem.*, **1999**, 113, 3895-3898.
- ¹²Lessing, P., Erickson, A., Kunerth D., *J. Mater. Sci.*, **2000**, 35, 2913-2925.
- ¹³Kok-Te, L., Sorrell, C., *J. Aust. Ceram. Soc.*, **2013**, 49(2), 104-112.
- ¹⁴Srimati, M., Rajalakshmi, R., Subhashini, S., *Arab. J. Chem.*, **2010**, 1.
- ¹⁵Vashi R., Champaneri, V., *Trans. SAEST*, **1997**, 32, 5-14.
- ¹⁶Fredric, B., Alain, F., *J. Am. Ceram. Soc.*, **1999**, 82, 2001-2010.
- ¹⁷Mugulescu, I., Radovici, O., *2nd International Congress on Metallic Corrosion*, London, 10-15, April, Butterworths, London, **1961**, 202-205.

Received: 18.18.2016.

Accepted: 16.09.2016.